UNIVERSITEIT VAN PRETORIA
UNIVERSITY OF PRETORIA
YUNIBESITHI YA PRETORIA

University of Pretoric

Intercalation of fatty acids into layered double hydroxides

by

Nontete Suzan Nhlapo

Submitted in partial fulfilment of the requirements for the degree

Magister Scientiae

In the Department of Chemistry
Faculty of Natural and Agricultural Sciences
University of Pretoria
Pretoria

Supervised by: Prof. Walter W. Focke

October 2008

ABSTRACT

Surfactant-mediated intercalation of aliphatic fatty acids into a commercial, layered double hydroxide (LDH) with the approximate composition of $[Mg_{0.689}Al_{0.311}(OH_2)]$ $(CO_3)_{0.156}\cdot nH_2O$ was explored. The reactions were conducted at elevated temperatures with the LDH powder suspended in a fatty acid oil-water emulsion. The acidic fatty acid, e.g. stearic acid, reacts with the basic carbonate anions from LDH-CO_3. In the process, CO_2 is released as a gas and the fatty acids are intercalated as a bilayer. A high concentration of anionic or non-ionic surfactants, i.e. sodium dodecylsulphate or Tween 60, facilitates the intercalation process by emulsifying the molten fatty acids and dispersing the LDH particles.

The presence of carboxylate anions in the interlayer region was confirmed by the carboxylate absorption peaks observed in the region 1700–1000 cm^{-1} on Fourier-transform infrared spectroscopy (FT-IR). Several bands were observed, i.e. ionised and non-ionised. An increase in the d-spacing of the d_{003} plane of the brucite-like LDH layers was observed on X-ray diffraction (XRD) analysis of all the LDH intercalates. The d-spacing increased linearly with the length of the carboxylic acid chain. Sharp reflection peaks were obtained on XRD, showing the high crystallinity of the LDH intercalates. The thermal decomposition of these materials was explored on thermogravimetric or differential thermogravimetric analysis (TGA/DTA) and temperature-scanned XRD. The mole ratio of Mg to Al was obtained by XRF and the morphology by scanning electron microscopy (SEM).

The present method works well with long-chain aliphatic fatty acids at temperatures above or at the melting point of the desired acid. Temperature proved to be the most important parameter to control during the preparation process, i.e. at low temperatures incomplete reactions were obtained. The method is convenient, economical and environmentally friendly. It employs the readily available carbonate form of LDH as a starting reagent, water is used as medium rather than organic solvents, there are no high-temperature calcinations, and an inert atmosphere is not required.

Keywords: Layered double hydroxides, fatty acids, surfactants

ACKNOWLEDGEMENTS

First and foremost, I would like to thank God Almighty for his grace, loving kindness, help and protection all times. "Trust in the Lord with all your heart, do not lean on your own understanding, for he is good, his mercy is everlasting, and his truth endures to all generations" (Psalm 100:5).

This study would not have been possible without the contributions of the following:

Prof. W.W. Focke, my advisor, supervisor and promoter – thank you for your constant support, valuable suggestions, encouragement and guidance throughout the study.

Financial assistance from the National Research Foundation (NRF) and the University of Pretoria, gratefully acknowledged.

My family: my mom and dad (Masephoso and Dan), my brothers (Simon, Phike and Mfokazana), my sisters (Nozika, Nomthemba and Nonhlupheko) and my Uncle Chris who motivated, encouraged and supported me in difficult times. Thank you for being there for me.

My friends and colleagues at the Institute of Applied Materials (IAM): Lumbi Moyo, Bhekani Magagula, Pedro Massinga, Kolela Ilunga, Herminio Muiambo, Darren Swanepoel, Mpolokeng Makhanya and Muzi Makhaye. Thank you very much for your inputs.

I also wish to thank Mila Maksa, Dr Sabine Verryn and Dave Lillies for the analyses – your patience and guidance are highly appreciated.

DECLARATION

I, the undersigned, declare that the dissertation which I hereby submit for the degree MSc at the University of Pretoria is my own work, and has not previously been submitted by me for degree purposes or examination at this or any other tertiary institution.

.....

Nontete Suzan Nhlapo

TABLE OF CONTENTS

LIST OF FIGURES

LIST OF TABLES

LIST OF SCHEMES

LIST OF ABBREVIATIONS

AEC	anionic exchange capacity
DSC	differential scanning calorimetry
DTA	differential thermal analysis
DTG	differential thermogravimetry
FT-IR	Fourier transform infrared spectroscopy
LDH	layered double hydroxide
LDO	layered double oxide
NTA	nitrilotriacetate
PXRD	powder X-ray diffraction
SDBS	sodium dodecylbenzenesulphate
SDS	sodium dodecylsulphate
SEM	scanning electron microscopy/micrograph
SOBS	sodium octylbenzenesulphonate
SOS	sodium octylsulphate
TG	thermogravimetry
TGA	thermogravimetric analysis
XRD	X-ray diffraction
XRF	X-ray fluorescence

1 INTRODUCTION AND AIM OF STUDY

1.1 Dissertation Outline

Layered double hydroxides (LDH) have recently received considerable attention in a wide variety of industries, as well as in research. Much research has been done on the preparation of inorganic and organic anion intercalated LDH. However, most of the reported preparations had some limitations. The present study reports on a simple and environmentally friendly method for the preparation of fatty acid intercalated LDH.

Chapter 1 starts with a review of the history of clay minerals. A brief survey of the main problems encountered when preparing LDH intercalated materials using the previously reported methods is given. The aims and objectives of this study are also presented.

Chapter 2 gives a detailed review of the literature. The structure and composition of LDH and the preparation of LDH intercalates with various organic and inorganic anions are presented. Methods for preparing LDH intercalates that are investigated include direct anion exchange, rehydration, thermal melt reaction methods and coprecipitation. The techniques used to characterise LDH and LDH intercalates, carboxylic acids and the surfactants are briefly reviewed. Potential applications of LDH intercalates are also considered in this chapter.

Chapter 3 describes the experimental work carried out in this study. The main purpose of this study was to prepare various fatty acids intercalated LDH with the aid of a surfactant. The reagents and suppliers, the intercalation procedure followed, the methods used to further purify the LDH intercalates obtained, as well as a description of all the instrumentation used to carry out the analysis are presented in this chapter.

Chapter 4 presents the results and discussion. This chapter starts with the results obtained for elemental analysis, followed by the thermal decomposition of the

selected precursors and of the LDH intercalates obtained. In the case of the Fourier transform-infrared spectroscopy (FT-IR) results, the observed bands and their assignments are discussed in detail. This provides information on the presence and the state of the fatty acids in the interlayer region of the brucite-like LDH layers. The X-ray diffraction (XRD) results are used to determine the type of intercalation via the dependence of the interlayer spacing on the length of the carboxylic chain. The effect of reaction temperature, reagent stoichiometry and surfactant on intercalation is explored. The thermal behaviour of the LDH intercalates obtained is studied using differential scanning calorimetry (DSC) and hot stage microscopy. The phase changes of the intercalates are considered by means of the change in the X-ray diffraction spectra as a function of temperature during the heating and cooling of the LDH-stearate and laurate intercalates. The particle morphology is presented by means of SEM images and compared with that of the LDH-CO_3 precursor.

Finally, the conclusions are presented in Chapter 4 which also summarises the work carried out in the present study. The literature references are given in Chapter 5. Raw data are given in the Appendices.

1.2 Clay Minerals

Clay minerals are two-dimensional structural minerals found in nature, with particle sizes of less than 2 μm (Zammarano *et al.,* 2006). They are made up of different chemical compositions and characterised by a common platey morphology (Bergaya, 2008). Clays are divided into two main groups, i.e. cationic (smectites) and anionic (hydrotalcite-like minerals) clays (Vaccari, 1998). The difference between anionic and cationic clays is in the layer charge, i.e. layers are either negatively (cationic) or positively (anionic) charged (Zammarano *et al.,* 2006). The interlayer region of clays consists of cations or anions to compensate for the layer charge. The free space also contains water molecules (Cavani *et al.,* 1991). Clays vary in nature and in the number of exchangeable ions. The physical and chemical properties of these minerals are dependent on the nature and

particle size (Frost *et al.,* 2002). Clays are characterised by their ability to exchange ions from a solution (Vaccari, 1998).

Smectite clays are obtained mainly from natural rocks containing quartz and calcite (Vaccari, 1998). They are characterised by their swelling behaviour in water, a typical example being montmorillonite. However, other cationic clays exhibit non-swelling behaviour, e.g. mica (Bergaya, 2008). Smectite clay consists of an octahedral sheet of $MO_4(OH)_2$ bonded to a tetrahedral sheet of MO_4 (Rajamathi *et al.,* 2001). Mg, Al and Fe cations occupy the octahedral sites, while Si occupies the tetrahedral sites. The net negative charge is a result of the isomorphic substitution of Si cations by Al and/or Mg cations. The neutrality is maintained by the presence of the interlayer cation (Vaccari*,* 1998). Bujdák (2006) states that the orientation of cations and the arrangement of clay minerals is affected by the density of the surface charge.

The individual clay layers are composed of two, three or four sheets arranged to form hexagonal networks (Bergaya, 2008). Clays have excellent properties such as low cost, non-toxicity, flexibility and ion-exchange ability (Vaccari, 1999). Organic modification of clay is performed to change the properties from hydrophobic to hydrophillic (Vaccari, 1998). Smectite clays are characterised by a lower charge density on the octahedral sheet which makes exchange reactions easier (Auerbach *et al.*, 2004, p 10). The low charge density also results in weaker interactions between the interlayer region and the clay layers, making the exfoliation process easier (Auerbach *et al.*, 2004. p 92).

1.3 Historical Background

Early reports on clay minerals date back to 1940–1950 in relation to catalysis (Vaccari*,* 1998). The research started with the hydrated aluminosilicate minerals called zeolites in 1938 (Bergaya, 2008). Zeolites were modified by exchanging the interlayer cations for use as catalysts or catalyst supports. Since zeolites have small particle sizes, it was difficult to use these minerals for all the desired applications (Bergaya, 2008). Modification of clay minerals started with bentonite

in 1942 at the University of Chicago (Vaccari, 1998; Bergaya, 2008). Modified bentonite found applications as catalysts, catalyst supports, adsorbents and as an ion exchanger (Bergaya, 2008). Cationic clays then became important minerals for a wide variety of applications in polymers, pharmaceuticals and biologicals, and in nanotechnology (Fischer, 2003; Evans and Duan, 2006).

Natural anionic clay mineral is known as hydrotalcite. Hydrotalcite is a hydrated mineral containing magnesium, aluminium and carbonate with the general formula $Mg_6Al_2(OH)_{16}CO_3.4H_2O$ (Reichle, 1986b). Natural hydrotalcite was first discovered in 1848 in Sweden as a white-coloured mineral that can be easily crushed into powder (Cavani *et al.,* 1991). Hydrotalcite is found naturally as deposits from ground water or as a weathering product of primary oxides (Frost *et al.,* 2003a and 2003b). Unlike cationic clays, hydrotalcite is rare in nature, and it is found in small quantities in a limited number of geographic areas such as Norway and the Urals area of Russia (Cavani *et al.,* 1991).

Hydrotalcite was discovered at the same time as its two polytypes: pyröaurite and sjögrenite (Belloto *et al.,* 1996). At the time, they were referred to as 'mixed hydroxyl-carbonates of magnesium and iron', while others referred to them as 'mixed hydroxides' (Brindley and Kikkawa, 1979). However, there are some known naturally occurring minerals with structural compositions similar to that of hydrotalcite (Frost *et al.,* 2003b) (see Table 1). The only notable difference between these minerals is in the cationic composition and interlayer anions (Cavani *et al.,* 1991). The difference between hydrotalcite and manasseite is in the unit cell: hydrotalcite has a rhombohedral unit cell, whereas manasseite has a hexagonal unit cell (Belloto *et al.,* 1996).

Table 1: Naturally occurring minerals similar to hydrotalcite (adapted from Frost *et al.,* 2003b and Auerbach, 2004)

Mineral	Composition	Unit cell
Hydrotalcite	$Mg_6Al_2(OH)_{16}CO_3.4H_2O$	Rhomohedral, 3R
Manasseite	$Mg_6Al_2(OH)_{16}CO_3.4H_2O$	Hexagonal, 2H
Desautelsite	$Mg_6Mn_2(OH)_{16}CO_3.4H_2O$	Rhombohedral, 3R
Pyröaurite	$Mg_6Fe_2(OH)_{16}CO_3.4.5H_2O$	Rhombohedral, 3R
Sjögrenite	$Mg_6Fe_2(OH)_{16}CO_3.4.5H_2O$	Hexagonal, 2H
Stitchtite	$Mg_6Cr_2(OH)_{16}CO_3.4H_2O$	Rhombohedral , 3R
Babertonite	$Mg_6Cr_2(OH)_{16}CO_3.4H_2O$	Hexagonal, 2H
Reveesite	$Ni_6Fe_2(OH)_{16}CO_3.4H_2O$	Rhombohedral, 3R
Takovite	$Ni_6Al_2(OH)_{16}CO_3.4H_2O$	Rhombohedral, 3R

The synthetic hydrotalcite is referred to as layered double hydroxide, abbreviated to LDH (Reichle, 1986a). The name LDH was derived from an early work by Feitknecht. The first LDH was prepared in 1942 by Feitknecht using the coprecipitation method. This was achieved by mixing the dilute metal salts with the basic solution. The product was named *Doppelschichtstrukturen,* meaning double sheet structure. In his hypothesis, Feitknecht assumed that LDH has a structure with intercalated hydroxide layers (Cavani *et al.,* 1991). Allmann, Taylor and co-workers later corrected Feitknecht's hypothesis based on the study of single-crystal XRD (Allmann, 1968; Cavani *et al.,* 1991). The study proved that the cations are found in the layers, while the anions and water molecules are located in the interlayers (Cavani *et al.,* 1991).

The first patent on LDH was published by Miyata (1970). Following this publication, Miyata and co-workers (1973, 1975, 1977, 1980 and 1983) prepared a reasonable amount of LDH containing organic and inorganic anions. The chemical and physical properties of LDH intercalates were examined for use in catalysis. Feitknecht's method was adopted by Reichle (1985 and 1986a) to study the thermal decomposition of LDH. Later, other preparation methods were discovered and LDH was prepared with a wide variety of compositions for a wide variety of

applications (Meyn *et al.*, 1990; Dimotakis and Pinnavaia, 1990; Newman and Jones, 1998).

1.4 Problem Statement

Naturally hydrotalcite is found as a mixture of spinnels and/or other minerals such as muscovite and heavy metals such as lead (Frost *et al.,* 2002). This might be due to the existence of non-equilibrium conditions during the formation of the hydrotalcite deposit. Currently, there are no known methods for purifying or separating natural hydrotalcite. This makes it difficult for these minerals to be used in the desired applications. An alternative route is to prepare LDH on a laboratory scale. The main advantage of preparing LDH in this way is that it can be prepared with the desired combination of divalent and trivalent cations for specific purposes (Reichle, 1985 and 1986b). There are several methods of preparing LDH intercalates (Carlino, 1997). The reported methods include coprecipitation, ion-exchange, rehydration and the thermal melt or melt reaction method (Williams and O'Hare, 2006).

The reported methods require prolonged periods of synthesis, an inert atmosphere and high temperatures for calcination. In ion-exchange the common problem is contamination with the anion from the precursor or the solvent and sometimes incomplete reactions (Jackrupca and Dutta, 1995). In coprecipitation the intercalates show $M(OH)_2$ and $M(OH)_3$ mixed phases or precursor contamination from mixed salts solutions. In some cases amorphous intercalates are reported.

A common problem with all these methods is avoiding CO_2 contamination from the atmosphere. This problem is encountered mainly in the preparation of LDH with anions other than carbonates (Chibwe and Jones, 1989). Iyi *et al.* (2004) reported the decarbonation of Al-rich LDH using NaCl-HCl solutions. The degassed water is used only for washing the samples. This process is reported to be dependent on the Mg:Al ratio and the NaCl-HCl concentration.

A solution to some of these problems was also devised (Zhang *et al.,* 2004). In the method the LDH-CO_3 was dissolved in an excess of aqueous carboxylic acid and the required pure product was obtained by precipitation involving addition of the mixture to a basic solution. Presumably, this approach is limited to water-soluble acids, e.g. hydroxy-carboxylic acids such as citric, tartaric and malic acids.

1.5 Aims and Objectives

The modification of layered double hydroxides (LDH) offers many advantages in a wide variety of applications. In polymers, organo-modified LDH is used to improve the physical and chemical properties of polymeric materials (Fischer, 2003; Khan and O'Hare, 2002). The anion-exchange capacity plays a major role in the preparation of polymer clay nanocomposites (Hibino and Jones, 2001). This is achieved by modifying the surface polarity of the clay. Clay modification is usually achieved by intercalating the desired compound in between the layers of the host, depending on the final properties of the required nanocomposite (Leroux and Besse, 2001). The interlayer anions can be exchanged with the desired ones. In the pharmaceutical and medical industries, pharmaceutical drugs and biologically active compounds are intercalated for purposes such as controlled drug release (Choy, 2004 and 2007; Ambrogi *et al.*, 2002; Evans and Duan, 2006). LDH has attracted considerable attention as flame retardants, ion exchangers, catalysts and catalysts supports, and as PVC stabilisers (Evans and Duan, 2006).

The aim of the present work was to find a simple and economical way to prepare fatty-acid intercalated LDH using readily available chemicals, without employing an inert atmosphere and high-temperature calcinations. Fatty acids were used because of their ability to weaken the interactions between the adjacent clay layers. This results in the neutralisation of the brucite-like LDH layers. Fatty acids have the ability to replace the interlayer carbonate with carboxylate anions, resulting in the formation of a mono- or bilayer intercalated LDH structure through hydrophobic interactions. In this study water was used as a medium rather than an organic solvent. Surfactants were used due to their ability to interact with the

surface to form micelles, leaving the LDH layers free to capture the desired carboxylate anions. The surfactants kept the LDH particles in suspension and also ensured better dispersion.

2 LITERATURE REVIEW

2.1 LDH Structure and Composition

The structure of LDH is derived from that of the naturally occurring mineral brucite ($Mg(OH)_2$). It consists of two-dimensional structural sheets (Cavani *et al.,* 1991). The structure of brucite consists of Mg^{2+} ions co-ordinated six-fold to hydroxyl groups. Similarly, each cation in LDH is surrounded by six hydroxyl groups. These hydroxides share the edges to form an infinite sheet (Carrado and Kostapapas, 1988). The LDH structure results from a partial replacement of divalent cations (Mg^{2+}) by trivalent cations (Al^{3+}) in octahedral sites (Hickey *et al.,* 2000). This substitution results in a net positive charge on the LDH layer. Lopez *et al.* (1997) claim that the formation of basic centres in hydrotalcite appears in the bridge oxygens between two magnesium atoms. These basic centres are due to the defects in oxygen linked to fully co-ordinated magnesium (Lopez *et al.,* 1997).

The interlayer region of LDH contains anions that neutralise the excess positive charge on the brucite-like layers. The galleries also contain water molecules (Cavani *et al.,* 1991; Rajamathi *et al.,* 2001) that are free to move by breaking and forming new bonds (Cavani *et al.,* 1991). The LDH structure contains different types of water molecule, i.e. hydrogen bonded to the interlayer anions and hydrogen bonded to the –OH groups on the surface of the brucite-like layers (Cavani *et al.,* 1991; Yun and Pinnavaia, 1995; Van der Pol *et al.*, 1994). The ionic mobility of the anion is dependent on the interlayer water content. The anion mobility determines the acid base properties and the ion-exchange behaviour of the LDH (Yun and Pinnavaia, 1995).

The interlayer thickness is dependent on the number, size and strength of the bonds between the anions and hydroxyl groups (Yun and Pinnavaia, 1995; Cavani *et al.,* 1991). Dehydrated LDH can absorb water from the surroundings (Hou *et al.,* 2003). The amount of interlayer water is dependent on the size and nature of the anion, water vapour pressure and temperature. This results in the formation of mono-, di- or trilayers (Miyata, 1975; Khan and O'Hare, 2002; Miyata and Kumura,

1973). Yun and Pinnavaia (1995) identified two types of water molecule for all air-dried LDH-CO_3 samples. The water due to capillary condensation between LDH crystallites is called 'interparticle pore water'. The last layer of water, called 'adsorbed surface water', is bonded to the gallery and external surfaces. Kagunya and co-workers (1996 and 1997) identified two types of water molecule water in LDH. The first is the intrinsic water, which is the structural water intercalated in LDH as a monolayer, and the second is the extrinsic water, consisting of water molecules bound to the external surfaces.

Unlike brucite, LDH is characterised by its three-dimensional structure as a result of the electrostatic and hydrogen bonds between the layers and the interlayer region (Cavani *et al.,* 1991; Ogawa and Kaiho, 2002). The general formula is

$$[M(II)_{1-x}M(II)_x(OH)_2]^{x+} A^{n-}_{x/n} .mH_2O$$

where
M(II) represents a divalent cation Mg^{2+}, Fe^{2+}, Cd^{2+}, Co^{2+}, Zn^{2+} or Cu^{2+}
M(III) represents Al^{3+}, Cr^{3+}, Fe^{3+}, or Ga^{3+}
A^{n-} is an interlayer anion CO_3^{2-}, SO_4^{2-}, NO_3^- or Cl^-
x ranges from 0.2 to 0.33 (Costantino *et al.,* 1998).

The crystal layer structure is shown in Figure 1. The brucite-like sheets are stacked on top of each other (Cavani *et al.,* 1991). The surface area of LDH is usually lower than 100 m^2/g and the layer thickness is approximately 0.48 nm (Kanoh *et al.,* 1999; Chibwe and Jones, 1989; Choy *et al.,* 2007). The brucite-like sheet spacing varies from 0.78 nm to 0.76 nm, depending on the value of x (Chibwe and Jones, 1989; Carlino and Hudson, 1994).

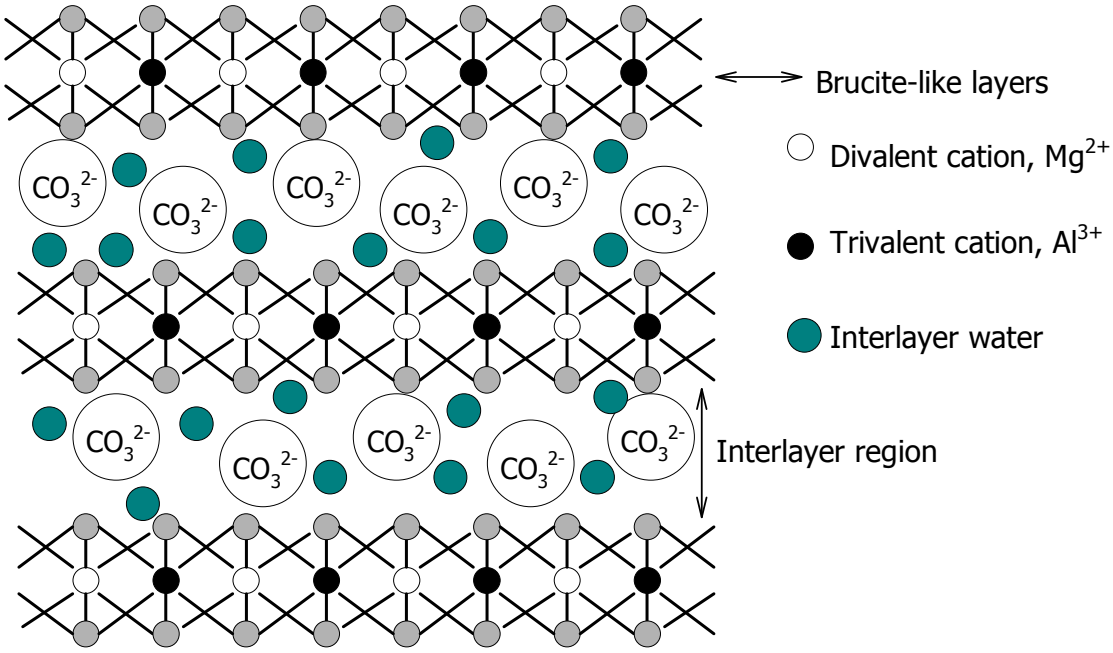

Figure 1: Structure of LDH (adapted from Carlino, 1997)

The di- and trivalent cations are metallic cations with oxidation states of +2 and +3 respectively. These cations can be exchanged with desired ones for specific purposes (Carrado and Kostapapas, 1988). The cations with atomic radii similar to that of Mg^{2+} and Al^{3+} can be accommodated in the octahedral sites of brucite-like layers (Cavani *et al.,* 1991). In the literature, wide varieties of cations in LDH have been reported (Auerbach *et al.*, 2004). Table 2 shows some of the reported di- and trivalent cations and their atomic radii. LDH containing the rare earth metals Ce^{3+}, Eu^{3+} has been reported (Chang *et al.,* 2006; Fernandez *et al.,* 1997).

Table 2: Atomic radii of some of the reported di- and trivalent metal cations in LDH brucite-like layers (adapted from Auerbach 2004 and Cavani *et al.,* 1991)

Divalent, M^{2+}	Radius, nm	Trivalent, M^{3+}	Radius, nm
Mg	0.072	Al	0.054
Ni	0.072	Co	0.063
Co	0.065	Ga	0.062
Zn	0.074	In	0.081
Fe	0.061	Y	0.090
Mn	0.083	V	0.074
Cu	0.073	La	0.103
Cd	0.097	Ti	0.076
Be	0.030	Cr	0.069

In the literature, LDH with tetravalent cations in place of trivalent cations has been reported. These include Zn-Si-LDH and Zn-Sn-LDH (Saber and Tagaya, 2003a, 2003b and 2007). The other reported tetravalent cations are V^{4+}, Ti^{4+}, Zr^{4+} (Intissar *et al.*, 2003). However, the replacement of trivalent cations by ones with radii that differ from that of Mg^{2+} and Al^{3+} may result in a different final product, i.e. not LDH. Das *et al.* (2004) tried to replace Al^{3+} with Zr^{4+} in Zn_3-Al, Zn_2-Al and Mg_3-Al-LDH. This resulted in the formation of Zn hydroxycarbonates and Zn-Al-Zr mixed oxides. The replacement of trivalent cations with tetravalent cations results in LDH with lower basal spacing and a decrease in the layer thickness compared with Mg-Al-LDH (Muramatsu *et al.,* 2007; Saber and Takagi, 2007). In some cases the trivalent cation has also been replaced by the hexavalent cation, Mo^{6+}, in Zn/Mo-LDH with Mo:Zn atomic ratios of 3:7, 2:8 and 1:9 (Muramatsu *et al.,* 2007).

LDH containing three different cations on the layers has been reported and this includes di-, tri- and tetravalent cations, i.e. Zn-Al-Sn-LDH, Cd-Al-Fe-LDH and Mg-Zn-Al, Cd-Al-Fe-LDH, Ni-Al-Cr and Ni-Al-Fe (Saber and Tagaya, 2003b; Perez-Ramirez *et al.,* 2007; Kooli *et al.,* 1995).

The charge density and stability of LDH layers is dependent on the M(II)/M(III) ratio (Boclair and Braterman, 1999a and 1999b). LDH with a variety of M(II)/M(III) ratios has been reported (Itoh *et al.,* 2003). The exchange capacity is controlled by controlling this ratio (Newman and Jones, 1998; Leroux *et al.,* 2003; Reichle, 1986b).

Although in nature hydrotalcite is found containing carbonates, in practice, a variety of charge-balancing anions may be incorporated in between the LDH layers. The anions may vary in geometry, size and charge, resulting in a large class of isostructural materials with different physicochemical properties (Evans and Duan, 2006). Some of the reported anions are listed below.

- **Organic anions:** Carboxylates, acetate, sebacate, carprate, laurate, palmitate, myristate, stearate and oleate oxalate, citrate, tartarate, succinate, adipate and malate, pamoate and aliphatic α, ω-dicarboxylic acids (Kandare and Hossenlopp, 2006; Prevot *et al.,* 1998; Kanoh *et al.,* 1999; Miyata and Kumura, 1973).
- **Inorganic anions:** Halides, (X^-), CO_3^{2-}, NO_3^-, OH^-, SO_4^{2-}, Cl^-, I^-, Br^-; MnO_4^-, CrO_4^{2-}, $Cr_2O_7^{2-}$, ClO_4^- (Bontchev *et al.,* 2003; Choudhary *et al.,* 2004; Malherbe and Besse, 2000).
- **Surfactants:** Sodium dodecylsulphate (SDS), sodium dodecylbenzenesulphate (SDBS), sodium octylsulphate (SOS), sodium octylbenzenesulphonate (SOBS), dodecyl glycol ether sulphate, sodium tetradecyl sulphate, octanesulphonic acid sodium salt, octylbenzene sulphonate acid sodium salt, octyldodecylsulphonic acid sodium salt and sodium dodecylbenzene sulphonic acid salt (Costa *et al.,* 2008; Meyn *et al.,* 1993; Trujillano, 2006).
- **Antibiotic and pharmaceutical drugs:** Gramidicin, amphoterin B, ampicillin, nalidixic (Trikeriotis and Chanotakis, 2007), phenylphosphonic acid (Carlino *et al.,* 1996), dichlorophenac (Dupin *et al.,* 2004) and *L*-ascorbic acid (Aisawa *et al.,* 2007).
- **Biochemical anions:** Various amino acids (Fudala *et al.,* 1999), DNA and ATP (Choy *et al.,* 1999).

- **Complex and polymeric anions:** $CoCl_4^{2-}$, $NiCl_4^{2-}$, $Fe(CN)_4^{2-}$, $Fe(CN)_6^{3-}$, $Ru(CN)_6^{-}$, $[P_2O_7]^{4-}$, $[V_2O_7]^{4-}$, (Malherbe and Besse, 2000), nitrilotriacetate (NTA) (Kaneyoshi and Jones, 1998) poly (ethylene) (Leroux and Besse, 2001) and inorganic-organic pigment – azo dye methyl orange (Costantino *et al.,* 1999).

The basal spacing is dependent on the size and nature of the interlayer anions (Bar-on and Nadiv, 1988). In carboxylate anions, the basal spacing is mostly dependent on the length of the chain (Carlino, 1997). The anion orientation is dependent on the anion concentration and the reaction temperature (Auerbach *et al.*, 2004, p 179). The ionic radii of the anions determine the thickness of the brucite-like layers (Miyata, 1980). The amount of the adsorbed anions is determined by the ratio of divalent to trivalent layer cations (Hansen and Taylor, 1991). Mg-Al-LDH is stable in the pH range of 3 to 10 and its capacity is about 220 meq/100 g (Miyata and Kumura, 1973). The order of LDH anion preference is known and is as follows (Miyata, 1983; Auerbach *et al.*, 2004):

$NO_3^{-}<Br^{-}<Cl^{-}<F^{-}<OH^{-}<MoO_4^{2-}<SO_4^{2-}<CrO_4^{2-}<HAsO_4^{2-}<HPO_4^{2-}<$naphthol yellow $<CO_3^{2-}$

Weak anions are preferred for exchange reactions because they can be easily replaced (Miyata, 1983). LDH has a strong electrostatic interaction with the divalent anions due to their high anion charge density (Leroux and Besse, 2001). However, Kooli *et al.* (1996) claim that anions with smaller radii are more strongly bonded than those with larger radii. The only limitation is that the desired anion must not form complexes with the layer cations.

The crystallinity and the textual and structural properties of LDH are highly dependent on the nature of the interlayer anions, on the preparation route and on the conditions (Bar-on and Nadiv, 1988; Costantino *et al.,* 1998). In ion-exchange reactions, replacement of anions with large inorganic or organic anions may lead to the formation of pillared materials (Dimotakis and Pinnavaia, 1990). The solubility is greatly affected by the nature of the exchangeable species, i.e. the

layer cations and anions. The smaller the crystal size, the higher the solubility of the resulting LDH material (Choy *et al.,* 2007; Costantino *et al.,* 1998).

2.2 Intercalation

The intercalation reaction can be defined as a reaction in which an ion or molecule is inserted in between the layers of the crystal lattice, leaving the basic structure unchanged (Williams and O'Hare, 2006). The insertion process is reversible (Khan and O'Hare, 2002; Chibwe and Jones, 1999). After intercalation, this clay can later be incorporated into polymers to improve the chemical and physical properties of the materials, i.e. tensile strength, thermal stability, and optical and magnetic properties, and also to change the surface properties of the host from hydrophobic to hydrophilic (Khan and O'Hare, 2002; Adachi-Pagano *et al*., 2000).

It is necessary for a host material to have a charged layered structure (Khan and O'Hare, 2002). The intercalation compounds are formed when the mobile guest species comes into contact with the host lattice (Evans and Duan, 2006; Morioka *et al.,* 1995). Layered hosts adapt to the geometry of the inserted guest species by adjusting the interlayer separation, resulting in increased basal spacing. The intercalation process may involve ion exchange. In LDH, if the anionic guest contains long aliphatic chains, the anions may self-assemble to form a mono- or bilayer structure due to hydrophobic interactions between the layers and the anions (Khan and O'Hare, 2002).

Intercalation reactions involve an electrostatic interaction between the guest anionic charge and the cationic sites in LDH layers (Morioka *et al.,* 1995). Only anion guest species can be intercalated between the brucite-like layers of LDH. The amount of anionic species and water molecules intercalated depends on the charge density of the LDH layers (Adachi-Pagano *et al.,* 2000). The higher the layer charge density, the higher the content of intercalated anions and water molecules. This results in a strong interaction between the layers, leading to a tight stacking of the sheet (Adachi-Pagano *et al.,* 2003). The high layer charge

density of LDH makes exfoliation difficult. However, exfoliation of LDH has been reported (Leroux and Besse, 2003; Evans and Duan, 2006).

2.3 Review of the Intercalation Methods

LDH is characterised by a smooth, flexible structure which exhibits excellent chemical and physical properties (Newman and Jones, 1998). The final properties of LDH are dependent on the method of preparation employed. Highly crystalline materials can be produced by optimising experimental parameters such as pH, time and reaction temperature (Reichle, 1986b). The particle size, surface area and morphology are highly affected by these parameters. Ageing plays a major role in determining the textural properties of the final material (Costantino *et al.,* 1999). Carlino (1997) and Newman and Jones (1998) reviewed the methods for preparing organic anion intercalated LDH. Carlino (1997) identified five methods that can be used to intercalate carboxylate anions in LDH. The methods are:

1. ion exchange
2. coprecipitation
3. rehydration
4. thermal melt
5. glycerol effect.

However, only coprecipitation and rehydration were found to be effective since they gave single-phase products on powder X-ray diffraction (PXRD).

The indirect method employs a suitable LDH precursor prepared by direct synthesis. Crepaldi *et al.* (1999) identified three indirect techniques for preparing intercalated LDH: 1) direct ion exchange; 2) LDH reconstruction from the layered double oxide (LDO) form obtained by calcinations of a suitable precursor; and 3) anion replacement by elimination of the precursor interlamellar species.

2.3.1 Direct ion exchange

In the direct ion-exchange method the guest anions are intercalated by dispersing the LDH in an aqueous solution containing an excess of the desired anion. The

pre-existing interlayer anion is partially replaced when the guest anion diffuses through the LDH matrix. The exchange reaction is carried out under an inert atmosphere to avoid the incorporation of carbonate from the atmosphere (Cavani *et al.,* 1991). The guest anion and LDH layers must be stable at the pH of exchange (Miyata and Kumura, 1973). A higher layer charge density increases the exchange capacity. Monovalent anions like Cl^- are usually preferred in exchange reactions because they can be easily exchanged. Carboxylic acid anions can be intercalated by shaking the LDH in a solution of the desired carboxylic acid or its salts (Carlino, 1997).

Borja and Dutta (1992) and Dutta and Robins (1994) successfully exchanged LDH-Cl^- with laurate, myristate and palmitate anions into Mg_3Al-LDH and Li_3Al-LDH. This was achieved by shaking the LDH-Cl in ethanolic solutions in the presence of the carboxylic acids, C12 to C16. However, the ethanol was incorporated along with the carboxylic acids. This was confirmed with thermogravimetry (TG) by 30% mass loss upon heating to 90 °C. Jackrupca and Dutta (1995) also confirmed it with myristate-exchanged LiAl-LDH. Apart from ethanol contamination, the LDH intercalates were also contaminated with the chloride anions from the precursor, confirmed by X-ray fluorescence spectroscopy (XRF).

Miyata and Kumura (1973) reported an exchange reaction of anions in Zn_3-Al-LDH with a series of α, ω dicarboxylic acids. Itoh *et al.* (2003) exchanged the Cl^- anions in LDH-Cl with sodium aliphatic carboxylate salts from C16 to C26 by treatment with an aqueous solution of carboxylates under a nitrogen atmosphere. A similar procedure was used by Kanoh *et al.* (1999) who exchanged the chloride anions with stearate anions from sodium stearate and also C8 to C10. The intercalation was unsuccessful for C8 to C10 and this was attributed to the hydrophobicity of these carboxylates at lower temperatures. Carboxylate anions were intercalated as bilayers. However, the LDH intercalates were contaminated with the chloride anion from the precursor.

The exchange of interlayer nitrate anions with sodium fatty acid salts in water was reported by Meyn et *al.* (1990). Tartarate and citrate anions were found not to react easily with the LDH. Anbarasan *et al.* (2008) described synthetic methods involving the dispersion of LDH-CO_3 in water in the presence of dodedecane-1-12-diol, dodecanedioic acid, stearic acid and heptadecanoic acid. The reaction was carried out at 70 °C with vigorous stirring under a nitrogen atmosphere for 48 hours. Intercalation was successful and the article claims that the surfactants interacted with the LDH through ionic bonding.

Saber and Tagaya (2003 a, 2003 b, 2007) exchanged the carbonate anion in Zn^{2+} and Si^{4+} in LDH with mono-(n-caprate, myristate and stearate), dicarboxylate (sebacate, suberate and dodecanoate) and aromatic 4-chlorophthalic acid. The carbonate Zn/Si-LDH and Zn/Sn-LDH samples were first prepared by coprecipitation, followed by exchange reactions in carboxylic acid sodium salts.

A stearate-intercalated LDH containing the di-, tri-, and tetravalent cations Zn-Al-Sn-LDH was also prepared (Saber and Tagaya, 2003a, 2003b). The reactions were carried out in an argon atmosphere. Although the intercalation reactions were successful, the materials were found to be contaminated with carbonate anions. A similar procedure was followed to prepare n-caprate and suberate-intercalated Zn^{2+} and Mo^{6+} containing LDH (Muramatsu *et al.,* 2007). The carbonate impurity was also retained in the final material. Broad diffraction peaks were obtained, indicating poor crystallinity.

Prevot *et al.* (1998) reported the exchange of Cl^- anions by dicarboxylates, tartarate and succinate. The LDH intercalates were contaminated with atmospheric carbonate anions, as evident from a low intense diffraction peak at 11.4° on XRD. In the exchange of NO_3^- anions in LDH-NO_3 with alkylsulphate derivatives, the samples retained the nitrate anions from the precursor (Meyn *et al.,* 1993). In the exchange of Cl^- anions with the anionic surfactants SDS, SDBS, SOS and SOBS, poorly crystalline materials were obtained (You *et al.,* 2002). The exchange of surfactants was also reported (Meyn *et al.,* 1993).

The exchange of nitrate and chloride anions by anionic nitrilotriacetate (NTA) complexes [M(NTA]$^-$ (where M is Cu^{2+}, Ni^{2+} for Zn/Cr LDH) has been reported (Gutmann *et al.,* 2000). The NO^{3-} and Cl^- anions were found to compete for the interlayer sites in LDH for the $[Ni^{2+}(NTA)]^-$ complex. The exchange of chloride anions for the platinum complexes MgAlPt, ZnAlPt and CuAlPt in LDH has also been reported (Beaudot *et al.,* 2001). In both cases the LDH intercalates were contaminated with anions from the precursor. The exchange of Cl^- with a series of complexes has been reported (Malherbe and Besse, 2000). Newman and Jones (1998) reported anion-exchange reactions of layered Zn, Cu, Ni, or La hydroxide nitrates with different aqueous media and the organic anions acetate, terephthalate and benzoate.

Anion exchange of NO_3^- in M-Al_4-NO_3-LDH (M = Zn, Cu, Ni, and Co) with a series of dicarboxylates, mono- and disulphonates was reported by Williams and O'Hare (2006). LDH was reacted with excess salt at 60 °C for 24 hours. The LDH intercalates were then dried for 3 hours under vacuum. The authors claim that with dicarboxylate the reactions were completed in less than 2 minutes. Bontchev *et al.* (2003) studied the monovalent anion-exchange preferences of LDH in comparison with the hydrothermal and rehydration methods. However, incomplete ion-exchange reactions were obtained. The pH of the synthesis solution for anion-exchange reactions was reported by Kukkadapu *et al.* (1997).

Prevot *et al.* (1999) described an exchange reaction method involving the extraction, dissolution and reconstruction. The Al^{3+} cations were first extracted by oxalate anions to produce aluminium oxalate complex. The Cl^- anions in ZnAl-LDH-Cl are exchanged with oxalate anions simultaneously when the LDH is being reconstructed at 250 °C. Crepaldi *et al.* (1999) described an exchange reaction method involving salt formation between anionic and cationic surfactants. This salt surfactant is later removed to an organic phase. Dimotakis and Pinnavaia (1990) described an exchange reaction using a swelling agent. The exchange of hydroxides is claimed to be easier with this method.

2.3.2 Rehydration

The rehydration method also referred to as 'reconstruction' is based on the so-called '*memory effect*'. Miyata (1975) and Leroux and Taviot-Guého (2005) define the *memory effect* as the ability of mixed oxides (LDO) obtained by thermal decomposition of LDH to reconstruct their original layered structure in aqueous media. The mixed oxides (LDO) formed feature interesting properties such as high surface area, small crystal sizes and stability to thermal treatments (Rocha *et al.,* 1999). High temperature causes solid state diffusion between the cations while the crystalline structure is destroyed. The hydroxyl groups and the interlayer carbonate anions are lost and the LDH lamellar structure collapses. During this process the divalent cations migrate to tetrahedral sites, resulting in the formation of the mixed oxides MgO and $MgAl_2O_4$ (Rocha *et al.,* 1999; Labajos *et al.,* 1992).

The method involves hydrothermal reconstruction of LDH from LDO in the presence of the desired anion (Kaneyoshi and Jones, 1998; Miyata and Okada, 1997; Crepaldi *et al.,* 2002; Chibwe and Jones, 1989). The reaction is carried out under an inert atmosphere to avoid carbonate contamination and calcination is performed in the temperature range 400–500 °C (Cavani *et al.,* 1991). The calcination process is reported to be reversible, provided the heating does not exceed 600 °C (Reichle, 1986a). However, when applied to organic anions it is difficult to avoid carbonate contamination and in some instances mixed phases may be produced (Dimotakis and Pinnavaia, 1990). During the LDH calcination process, water evaporates while interlayer carbonate anions are released as gas (Rocha *et al.,* 1999; Costantino *et al.,* 2007).

Dimotakis and Pinnavaia (1990) described the rehydration method in the presence of the swelling agent glycerol. The reconstruction was carried out in a water-glycerol solution, followed by reaction with the carboxylic acid. The absence of glycerol resulted in the mixed phases observed on XRD. Therefore, the swelling agent facilitated carboxylic acid intercalation. Greenwell *et al.* (2007) described the synthesis of dicarboxylate anion (adipate, succinate, malonate and glutarate)

intercalated LDH using the co-hydration route. The method consisted of stirring the MgO and Al_2O_3 in distilled water at 60 °C, followed by addition of excess dicarboxylic acid. Broad diffraction peaks and the carbonate impurity were observed on XRD and FT-IR.

Morioka *et al.* (1995) reconstructed LDH by treatment with water under a nitrogen atmosphere (see Figure 2). The LDH-CO_3 was calcined and reconstructed to LDH-OH by treatment with water. Water-treated samples were dried *in vacuo,* followed by the reaction with acid chlorides in acetonitrile. The authors claim that the LDH intercalates obtained were esterified. The reconstruction method was used to intercalate dicarboxylic acid, tartarate and succinate (Prevot *et al.,* 1998). No reconstruction was observed for tartarate anions. The LDH intercalates were also contaminated with carbonate, as evidenced by FT-IR.

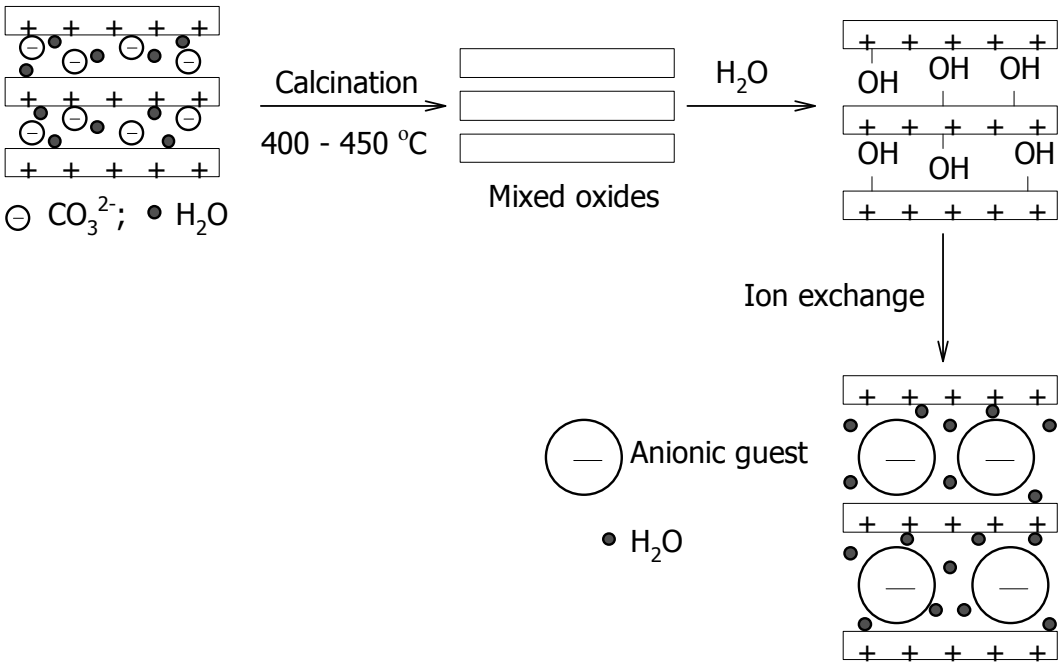

Figure 2: Schematic presentation of the reconstruction method followed to produce LDH intercalated material (adapted from Morioka *et al.,* 1995)

Chibwe and Jones (1989) used this method to prepare MgAl-LDH intercalated with sebacic acid, dodecyl sulphate and potassium salts. The LDH was calcined in air at 450 °C for 18 hours. Poorly crystalline LDH intercalates contaminated with carbonate were obtained. Sako and Okuwaki (1991) reported using the reconstruction method for the synthesis of benzene carboxylate intercalated LDH.

Stearate and oleate intercalated LDH were reported using reconstruction under hydrothermal conditions (Inomata and Ogawa, 2006). Incomplete intercalation of the oleate anions was observed at lower temperatures. Fogg *et al.* (1998) used the reconstruction method followed by anion exchange of Cl^- in Li-Al_2-LDH-Cl with a series of sodium dicarboxylate anions. LDH reconstruction in the presence of the anionic surfactants SDS and SDBS was reported by Costa *et al.* (2008). The atmospheric carbonate anion was incorporated along with the surfactants. This was indicated by FT-IR spectroscopy.

Del-Arco *et al.* (2003) attempted the reconstruction of Mg_2-Al-LDH in the presence of chromium oxalate complexes, but the method did not lead to the desired product. Aisawa *et al.* (2006) reported intercalation of L-ascorbic acid in Mg_3-Al, Mg_3-Fe and Zn_3-Al-LDHs. In comparison with coprecipitaion and ion exchange, intercalation barely occurred with coprecipitation and rehydration.

2.3.3 Direct synthesis by coprecipitation

Coprecipitation is one of the methods commonly used for the preparation of LDH intercalated materials. The metal (MII) and M(III) salts are mixed together and added to a solution of a base containing the desired anion (Carlino, 1997). Coprecipitation is achieved at either constant or increasing pH, depending on the conditions applied (Reichle, 1986b). The reaction is carried out under conditions of super-saturation.

It is necessary to precipitate at a pH higher than or equal to the one at which the LDH structure is more stable to avoid the formation of $M(OH)_2$ or $M(OH)_3$ impurities (Cavani *et al.,* 1991). The general coprecipitation reaction adapted from

Costantino *et al.* (2007) is shown in Scheme 1. The morphology and particle size depends on the conditions of super-saturation (Aramendia *et al.,* 2002). To prepare the intercalated LDH, the guest anion must have a high affinity for the brucite-like layers, otherwise the LDH intercalate may be contaminated with counter-anions from the metal salts. Hydrothermal treatment is usually performed to improve the crystallinity. The method is divided into two parts, i.e. coprecipitation at low and high super-saturations.

$$M^{II}(salt) + M^{III}(salt) + Guest\ (anion\ solution) \xrightarrow[pH = 10]{NaOH} M^{II}M^{III}\text{-(Guest)-LDH}$$

Scheme 1: Schematic presentation of the coprecipitaion method (from Costantino *et al.,* 2007)

Coprecipitation at low super-saturation

At low super-saturation the reaction is carried out by slow addition of M(II) and M(III) salts in an excess solution of the desired anion (Auerbach, 2004). The ratio of M(II) to M(III) must be known to prevent the formation of impurity phases. The pH is maintained between 7 and 10 by addition of basic solution, in the temperature range of 333 to 353 K, and low concentrations of the reagents. Washing is carried out with warm water at temperatures not exceeding 393 K (Cavani *et al.,* 1991). Aramendia *et al.* (1999) prepared LDH with the cation combinations Mg_3-Al and Mg_3-Ga using this method. The metal nitrate salts were employed as the starting materials, followed by anion exchange.

This method was employed for the intercalation of a series of dicarboxylic acids, succinic, adipic, subaric, sebacic and dodecanedionic acid, as well as Cl^-, CO_3^{2-}, NO_3 and SO_4^{2-} intercalated in MnAl, and ZnAL-LDH tartarate and succinate in Zn_3Al and Zn_2Cr-LDH from the carboxylate sodium salts (Prevot *et al.,* 1998). Poorly crystalline LDH intercalates contaminated with anions from the precursor were obtained. The researchers claim that the orientation change of dicarboxylic acid is

influenced by the length of the carboxylic acid chain. Acetate was also intercalated in Zn/Ni-LDH, and terephthalate and benzoate in Mg-Al-LDH (Kandare and Hossenlopp, 2006; Newman and Jones, 1998). Kooli *et al.* (1996) claimed that the terephthalate anion intercalation follows an indirect reaction.

Zhang *et al.* (2004) described a coprecipitation method for the preparation of citrate, oxalate, tartarate and malate pillared LDH intercalates. The method involved the dissolution of a suspension of LDH-CO_3 by addition of the desired amount of carboxylic acid. The acid-LDH mixture was re-precipitated by addition of an aqueous solution of NaOH. The method works well for the intercalation of dicarboxylate anions in LDH. Intercalation of acetate in Co-Al, Ni-Al and Mg-Al-LDH has been reported (Kelkar and Schutz, 1997). This method involved the peptisation of aluminium in the presence of acetic acid. Poorly crystalline materials were obtained.

Coprecipitation at high super-saturation

In this method mixed di- and trivalent salt solutions are added to a basic solution of the desired carboxylic acid (Reichle, 1986b). At high super-saturation, poorly crystalline materials are produced. The continuous change of pH causes the formation of the amorphous phases $M(OH)_2$ and $M(OH)_3$ (Adachi-Pagano *et al.*, 2003). The method is commonly used for the synthesis of pillared LDH intercalates, mostly for applications in catalysis (Reichle, 1986b; Costantino and Pinnavaia, 1995). Dredzon (1988) synthesised pillared terephthalate LDH for application in catalysis. Carlino and Hudson (1994) employed this method in the synthesis of caprate pillared LDH intercalates. Bilayer caprate intercalated LDH was obtained. Indole-2-carboxylate intercalated with Zn/Al-LDH has also been reported (Hussein and Long, 2004).

Costantino *et al.* (1998) described a method involving the addition of urea for the preparation of hydrotalcite. The method involves the decomposition of urea in a basic solution. Urea is added for better pH control and to allow homogenous precipitation as the pH increases. This leads to the formation of the fewer, well

crystallized particles. Rao and coworkers (2005) also used this method under hydrothermal conditions. No repetitive washings were required. Costa *et al.* (2008) produced highly crystalline Mg/Al-LDH with this method. The method is mostly used to prepare mono-dispersed LDH particles as a result of urea decomposition. It is good for the preparation of catalysts (Adachi-Pagano *et al.,* 2003).

Zhao *et al.* (2002) described a coprecipitation method involving separate nucleation and aging. The nucleation process is carried out by rapid mixing of the precursors in a colloid mill, followed by ageing. The crystallite is formed during nucleation and during ageing it undergoes growth, breakage, agglomeration and/or Ostwald ripening. Materials with higher crystallinity and high aspect ratios, and smaller crystallites with narrow size distribution are obtained (Zhao *et al.,* 2002). The method was recently employed for the preparation of LDH with different interlayer anions, divalent and trivalent cations (Feng *et al.,* 2006).

2.3.4 Thermal melt/reaction method

This method is used to prepare organo-intercalated LDH. The thermal reaction method, also referred to as the 'melt reaction' method, involves reacting molten acid with LDH. Carboxylic acid intercalation is achieved by heating the LDH-acid mixture slowly at a heating rate of less than 1 °C/min, followed by cooling at a rate of 10 °C/min. The method was first reported for the synthesis of sebacate intercalated LDH (Carlino and Hudson, 1994). Capric acid intercalated Mg_2-Al-LDH has also been reported (Carlino and Hudson, 1995). The LDH intercalate that was obtained contained an unreacted Mg-A-LDH-CO_3 phase, as evident from PXRD.

2.3.5 Sol-gel

A sol-gel can be defined as a process through which a product is formed by means of the gradual change of liquid involving the conversion of molecules in a sol (colloidal suspension of a solid in a liquid) to a gel. This method was used for the synthesis of LDH (Baron *et al.,* 2001). Two metal alkoxide solutions are mixed together to form a gel, followed by thermal treatment. The method involves hydrolysis of an organic precursor, achieved by addition of a strong acid such as

HCl. For example, if HCl is used for hydrolysis, acid addition results in LDH-Cl. Precipitation of the LDH phase occurs when working at a suitable pH. The method was used to study the thermal stability of LDH with a series of aluminium anions (Ramos *et al.,* 1997). The crystallinity depends on the nature of the precursors and the hydrolysis acid used (Prinetto *et al.,* 2000).

He *et al.* (2004) reported the synthesis of LDH-CO_3 using a water-in-oil emulsion solution. Octane, water and surfactant were mixed together at constant and variable pH. This method leads to a mesoporous LDH material.

2.4 Characterisation of LDHs

Various analytical techniques have been employed to characterise LDH intercalated materials. Some of the most commonly used analytical techniques are discussed in Sections 2.7.1 to 2.7.4 below. These include Fourier-transform infrared spectroscopy (FT-IR), powder X-ray diffraction (PXRD) and thermo-gravimetric techniques (TG/DTG).

2.4.1 FT-IR

FT-IR is one of the molecular vibrational spectroscopic techniques used for both quantitative and qualitative analysis (Pungor, 1995, p74). The infrared region is the region found in the wave number range 1.3 x 10^4 to 3.3 x 10^1 in the electromagnetic spectrum. This region is between the microwave and UV-visible light absorption spectra (Skoog *et al.,* 1996, p 502). FT-IR is used to investigate the structural bonding and chemical properties of compounds (Madejová, 2003). When a molecule absorbs radiation, the bonds stretch, vibrate or bend (Socrates, 1980, pp 1-3). Each molecule absorbs a specific IR radiation at a different frequencies – this is referred to as the 'molecular fingerprint'. Therefore each functional group has its own frequency and this is useful for revealing the presence or absence of these groups from the spectrum.

In this study samples are prepared using the KBr pellet-pressing method (Madejová, 2003). The pellet is prepared by crushing a small amount of sample

(2–5 mg) with 100 mg of dried KBr powder. The mixture is then pressed in a die under a specified pressure. KBr is used because it features a simple spectrum with no water or intense peaks (Sibilia, 1988, pp 13-19). The reference spectrum is then subtracted from the sample (Madejová, 2003).

In pure clays –OH absorptions can be detected (3 500-4 000 cm^{-1}) and the interlayer carbonate in the case of LDH-CO_3 (Labajos *et al.,* 1992; Williams and O'Hare, 2006). The inorganic lattice vibrations of the M-O and M-OH modes can be confirmed below 1000 cm^{-1} (Williams and O'Hare, 2006). In organo-LDHs the presence of the intercalated anionic species can be confirmed, e.g. in carboxylate intercalated LDH, the anion is identified by a strong asymmetric and symmetric stretching band in the region 1560 – 1400 cm^{-1} (Carlino, 1997). The undissociated form will be confirmed by the carbonyl stretch in the region 1725 – 1700 cm^{-1} (Borja and Dutta, 1992; Newman and Jones, 1998; Carlino and Hudson, 1994). The purity of the materials can also be confirmed. The carbonate impurity is observed by the band at 1360 cm^{-1} and other anions, such as nitrates, at 1360 cm^{-1} (Williams and O'Hare, 2006).

2.4.2 TG/DTG

TG is the analytical technique used to study the changes in thermal properties, i.e. the sample weight of the material as a function of temperature (Sibilia, 1988, p 205). The properties of the material are monitored under specified atmospheric conditions while the sample is subjected to a controlled temperature programme (Charles, 1988, p 1). Properties such as thermal stability, decomposition and the composition of the materials can be studied.

TG/DTG is mostly used to study the thermal decomposition and stability of the LDH intercalated materials (Williams and O'Hare, 2006). LDH contains different water molecules and an increase in temperature causes water to be released in the form of vapour. TG indicates the temperature at which this event takes place (Van de Pol *et al.*, 1994). Differential TG (DTG) enhances these events by showing the decomposition peaks in the range observed on TG (Sibilia, 1988, pp 206-207).

LDH intercalates decompose in three stages, namely loss of interlayer water (referred to as 'dehydroxylation') at 300 °C, dehydroxylation of brucite-like layers in the range 300-500 °C, and loss of interlayer anion (Reichle, 1986b; Williams and O'Hare, 2006). The temperature at which the interlayer anion is lost depends on the nature of the intercalated anion. The decomposition of LDH results in the formation of thermally stable mixed oxides that are mostly used in catalysis (Reichle, 1986b). The amount of intercalated anion can be estimated from the TG data.

2.4.3 PXRD

PXRD is one of the most powerful techniques for investigating the composition, purity and structural orientation of a material. The technique involves directing X-rays to the crystals. The radiation will be either reflected or diffracted at different angles. The interaction of X-rays with crystals results in the formation of secondary diffracted beams, as shown in Figure 3. The relationship between diffracted X-rays and the interplanar spacing is given by Bragg's law:

$$n\lambda = 2d_{hkl} \sin \theta \qquad (1)$$

where

n = diffraction order

λ = wavelength of the X-ray beam

d = interplanar spacing

θ = diffraction angle

hkl = diffraction or Miller indices of the plane where a, b and c are the axes.

XRD data are recorded as a plot of 2θ against the intensity (Sibilia, 1988, p 115; Pungor, 1995, p 151).

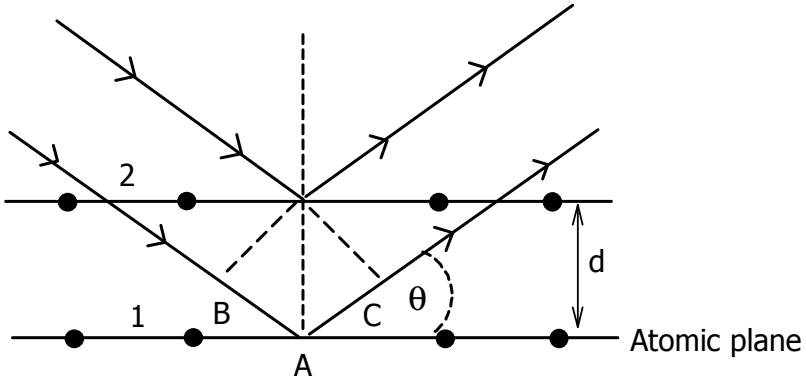

Figure 3: Diffraction of X-rays on crystal lattice according to Bragg

PXRD is used to study the purity of the LDH intercalated material. The phase purity of the material is determined by the sharpness and/or the broadness of the diffraction peaks. The broader reflections correspond to the amorphous phase, while the sharper reflections correspond to the crystalline phase. From the diffraction data the d-spacing of the intercalated LDH material can be determined. The reflection with the greatest d-spacing corresponds to the d-spacing of the intercalated LDH (Carlino, 1997).

In LDH the d-spacing depends on the size and orientation of the intercalated anion while n is the stacking sequence of the brucite-like layers (Williams and O'Hare, 2006). Carlino (1997) described three major reflections for carboxylate intercalated LDH, i.e. the greatest basal spacing, d_{003}, the half-height harmonic, d_{006}, which is equivalent to half d_{003}, and the d_{009} reflection, which is equivalent to one third of d_{003}. The rest are referred to as lesser reflections. The long-chain carboxylic acid guest can be intercalated to give mono- or bilayer structures. The d-spacing of a mono- and bilayer intercalated LDH structure can then be expressed by the following correction to the correlation equation presented by Carlino (1997) and Meyn *et al.* (1990):

$$\text{Monolayer: } d_L = d_0 + 1.27\ n \cos \alpha + d_1 \qquad (2)$$

$$\text{Bilayer: } \quad d_L = d_0 + 2.54\ n \cos \alpha + d_2 \qquad (3)$$

where

n = number of carbon atoms in the carboxylic acid

d_L = observed basal spacing from XRD data

d_0 = distance between the terminal ionised carboxyl group and the centre of the Mg-Al-$(OH)_x$ layer

d_1 = distance between the terminal methyl group and the centre of the Mg-Al-$(OH)_x$ layer

α = slant angle of the carboxylate chain from the normal to the LDH layer plane.

The interlayer height can be expressed by the following equation (Anbarasan *et al.,* 2005):

$$L = \text{d-spacing} - \text{layer thickness} \quad (4)$$

The bond lengths of metal-bonded oxygen can also be calculated from the PXRD data. Belloto *et al.* (1996) determined Al-O and Mg-O bond lengths in CO_3-LDH. The Mg-O bond length was found to be higher at 0.211 nm than the Al-O bond length at 0.190 nm.

2.4.4 Other characterisation techniques

Other techniques include scanning electron microscopy (SEM), differential scanning calorimetry (DSC) and X-ray fluorescence spectroscopy (XRF). SEM is used to study the surface topography of LDH intercalates – the particle morphology, porosity and phase composition within the material can be revealed. DSC, like TG, is also used to check the chemical and physical properties of a material corresponding to the temperature changes. It is used to detect the melting points (enthalpy of melting) and phase transitions of materials. This technique has not been explored very much in the study of LDH intercalates. XRF is employed for trace element analysis and is also used for the determination of the divalent to trivalent cation ratios.

2.5 Carboxylic/Fatty Acids

Carboxylic acids are characterised by the presence of the –COOH functional group. The suffix –oic is added to the end of the radical name (Gunstone, 1996). In linear fatty acids, the functional group is located at the end of the carbon chain. Carboxylic acids containing an even number of carbons from 16 to 36 are referred to as 'fatty acids' (MacMurry, 2000). The carboxylic acid anion is referred to as 'carboxylate' (Carlino, 1997). There are two types of fatty acid, namely saturated and unsaturated. The saturated fatty acids have long chains without double bonds or other functional groups along the chain. In unsaturated fatty acids, the chain consists of double or triple bonds and/or other functional groups along the chain (Markley, 1947).

Some fatty acids are found in ester and or sterol forms (Markely, 1947). In nature, these acids are found in plant or vegetable oils and animal fats. Typical examples are fish oil and cotton seed oil, which consist of 10-30% and 15-30% palmitic acid respectively, and fat from cow's milk, which contains 4% butyric acid (MacMurry, 2000; Gunstone, 1996; Markley, 1947). The short-chain fatty acids are retained in products containing milk fat (Gunstone, 1996). Fatty acids with carbon numbers greater than 18 are present in seed oils (Markley, 1947).

The fatty acids are extracted from natural resources by hydrolysis in aqueous NaOH, resulting in glycerol and fatty acid. (see Scheme 2 adapted from MacMurry (2000). Unsaturated fatty acids also exist in nature, e.g. 4-5 decanoic acid (Gunstone, 1996).

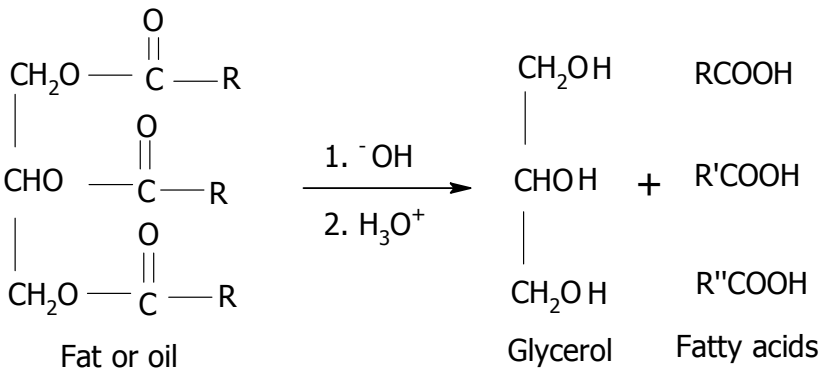

Scheme 2: Schematic presentation of the hydrolysis of fat or oil in aqueous NaOH, yielding glycerol and three fatty acids, where R, R', and R" = C11 – C19 (adapted from MacMurry, 2000)

Fatty acids exist in both the solid and liquid state. Short-chain carboxylic acids are usually liquids with low melting points and are isolated from plant or animal fat by carbonylation (Markley, 1947). The melting point and molecular mass of fatty acids increases with an increase in the chain length. Carboxylic acids have the ability to form hydrogen bonds with each other (MacMurry, 2000). The O-H bond is weak, which results in less stable molecules (Gunstone, 1996). Carboxylic/fatty acids are proton donors and dissociate into $RCOO^-$ and H^+ in aqueous solutions (MacMurry, 2000). Fatty acid salts are amphiphillic molecules produced by the reaction between carboxylic acid and a base. The functional group (carboxyl group) can be modified to produce surfactants (Lange, 1999).

With FT-IR, carboxylic acids are easily identifiable. They are characterised by strong absorption bands at 1710 and 1760 cm^{-1} due to the C=O (Carlino, 1997) functional group. The O-H bond of the carboxyl group results in a broad absorption band in the range 2500- 3300 cm^{-1} (Socrates, 1980). Free acids absorb at 1760 cm^{-1} while dimerics absorb at 1710 cm^{-1}.

2.6 Surfactants

Surfactants, also referred to as 'surface active agents', are amphiphilic molecules composed of parts of different polarity. These are usually dubbed the 'head' and

the 'tail' respectively. The head is hydrophilic (polar) and the tail hydrophobic (non-polar) (see Figure 4 (a)). The tail often consists of a long hydrocarbon chain (Moilliet *et al.,* 1961, p 6). Surfactants self-assemble to form micelles in solution (Lange, 1999, p 1). Khan and O'Hare (2002) define self-assembly as a process in which the small pre-existing subunits organise themselves into an ordered state or structural arrangement due to the electrostatic attraction, chemisorption, hydrophobicity and hydrophillicity of the materials.

Some surfactants occur naturally, while others are chemically modified lipids (Lange, 1999, p 3). Naturally occurring surfactants contain triglyceride ester from plant or animal oils (Lange, 1999). The separation is achieved by hydrolysis, resulting in glycerol and fatty or carboxylic acids with chain lengths from C8 to C22 (see Scheme 3). Synthetically, some surfactants are produced from plant and vegetable oils, followed by hydrolysis (Moilliet *et al.,* 1996, p 7). Surfactants are crystalline, amorphous solids and they can also be found in liquid form.

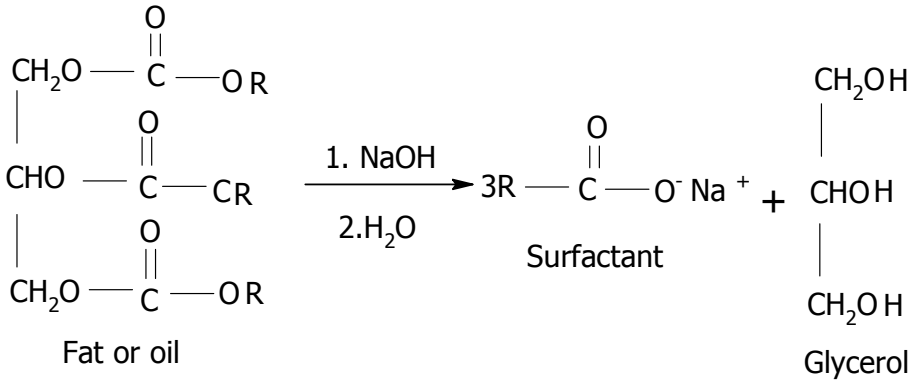

Scheme 3: Schematic representation of the hydrolysis process for the production of surfactant, where R = C11- C19 (adapted from MacMurry, 2000)

Surfactants orient themselves into extended structures at surfaces and also in water to form micelles (see Figure 4 (b)). Formation of a micelle allows the head to stay in the water phase while the tail is not (see Figure 4 (c)). In aqueous solution the surfactant molecules can form different microstructures, depending on factors such as temperature, composition and the surfactant's nature (Dong *et al.,*

2008). Disk-like and rod-like surfactant micelles are known (Hoffmann and Ebert, 1988). Surfactants have the ability to solubilise hydrocarbons. The solubility is mainly dependent on the critical micelle concentration, which is defined as the concentration at which micelles begin to form (Lange, 1999).

When dissolved in water/medium, the surfactant reduces the surface tension of the water/medium. The surfactant head can be positively (cationic) or negatively (anionic) charged or it can be non-ionic. It can also have both a positive and a negative charge (amphoteric or zwitternoic). Surfactants can be divided into four main groups, depending on the nature and the charge of the hydrophilic head. In a solution, charged surfactants can be adsorbed at the interfaces due to the electrostatic force (Lange, 1999, p 2).

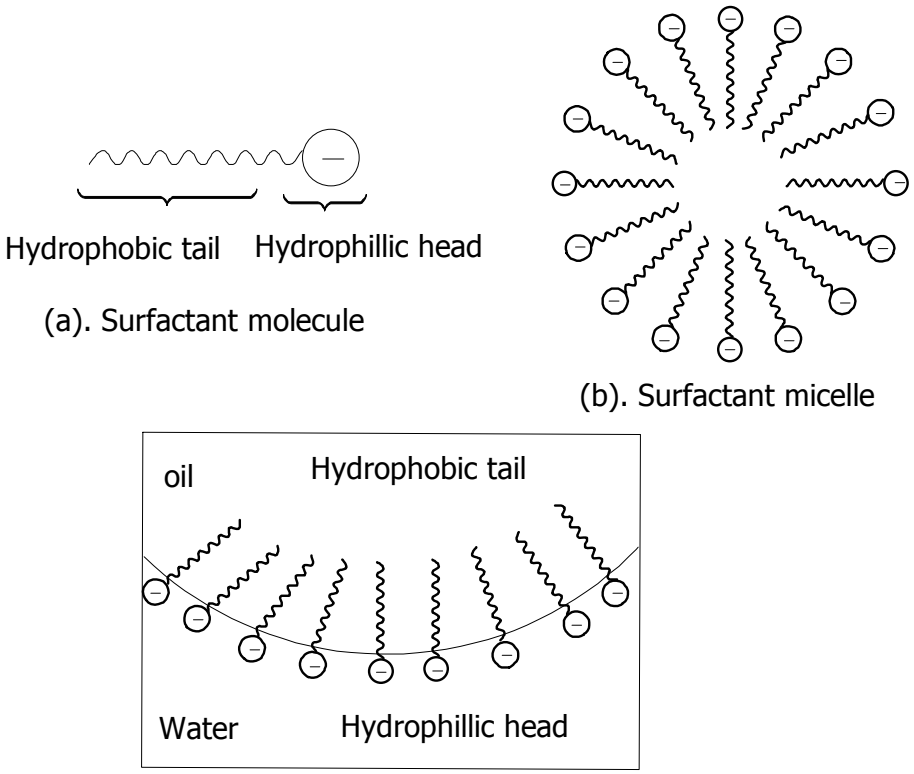

(a). Surfactant molecule

(b). Surfactant micelle

(c). Surfactant head in water and tail in oil

Figure 4: Representations of (a) a surfactant molecule; (b) a surfactant micelle; and (c) the surfactant head in water and tail in oil

Anionic surfactants consist of a negatively charged head. A typical example is sodium dodecylsulphate. This type of surfactant consists of a hydrocarbon tail of 12 carbons and a negatively charged sulphate head (see Figure 6). Anionic surfactants are characterised by their high surface activities. They adsorb easily on positively charged mineral surfaces. The adsorption process involves electrostatic and hydrophobic interactions with the mineral (Carrasco *et al.,* 2008; Reis *et al.,* 2004). It depends mainly on the nature of the structural groups on the surface, the molecular structure of the surfactant, the pH, the temperature and the concentration of the media (Reis *et al.,* 2004; Carrasco *et al.,* 2008). In the modification of minerals such as clay, the presence of surfactant changes the physico-chemical properties of the mineral surfaces via hydrophobic and electrostatic interactions (Fischer, 2003). Sodium alkyl sulphonate has attracted attention due to its high solubility in the presence of magnesium and calcium ions (Meyn *et al.,* 1990).

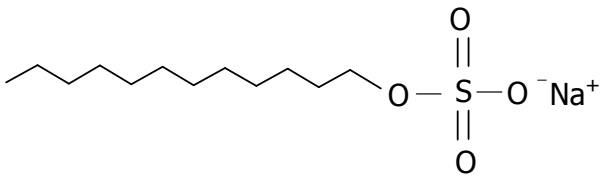

Figure 5: Chemical structure of sodium dodecylsulphate (SDS) – a typical example of an anionic surfactant

Cationic surfactants are usually composed of quaternary nitrogen. This type of surfactant interacts strongly with water molecules due to the presence of alkyl ammonium halides (Lange, 1999, p 3).

Zwitternoic surfactants are electro-neutral salts with a hydrophobic head that has both positive and negative charges. The negative charge arises from carboxylate or sulphate groups. These kinds of surfactant are characterised by their low toxicity, biodegradability and by not being irritant to skin (Wydro, 2007). They are amphoteric in nature and therefore their behaviour is similar to that of cationic and anionic surfactants (Lange, 1999, p. 4).

Non-ionic surfactants have an uncharged head. Unlike other surfactants, the interaction is governed by steric and osmotic forces (Lange, 1999, p 5). Their main application is in detergents, specifically fabric softeners. Their head groups consist of long ethoxylated chains. The availability of different kinds of surfactant allows tailoring for particular applications (Wydro, 2007).

Surfactants are mostly used in household products such as detergents, shampoos, cosmetics, stain removers, fabric softeners, etc. They can be used as suspension stabilisers and emulsifiers, for better solubility and dispersion (Wydro, 2007). In clay science, surfactants are used to modify the physical and chemical properties of clays, i.e. to improve the hydrophilicity in order to prepare polymer composites and/or nanocomposites (Fischer, 2003).

2.7 Potential Applications of LDH

Recently, much research has focused on potential applications of LDH intercalated materials. LDHs have found a wide variety of applications in the medical, pharmaceutical, catalysis and polymer industries. Some of these potential applications are discussed in the following sections.

2.7.1 Catalysis

LDH has attracted attention in the field of catalysis because of its small particle size, large specific surface area and the wide variety of chemical compositions attainable. In applications involving catalysis or ion exchange, it is desirable that the LDH be carbonate-free and have a high layer charge. LDH and LDO are very efficient catalysts for different chemical reactions (Cavani *et al.,* 1991). Some of the reported LDH and/or LDO base catalysed reactions are the Michael addition-type reaction, Aldol condensation of aldehydes and ketones, Claisen Schimide, Knoevenagel and Henry reactions (Prescott *et al.,* 2005; Evans and Duan, 2006).

LDO is characterised by high thermal stability, making it useful as a catalyst or catalyst support. LDO has been found to be catalytically active for the polymerisation of propiolactones and polypropylene oxide and for hydrogen-deuterium exchange of acetone and toluene (Carrado and Kostapapas, 1988).

In heterogeneous catalysis, LDH and LDO are useful precursors of multi-component oxide catalysts (Reichle, 1986b). LDH can also be used as a support for the metals used for the catalytic reduction of nitrates with hydrogen. LDO can be used for improving the catalytic reduction of nitrates in water (Palomares *et al.,* 2004).

Semi-conductor pillars incorporated in LDH material have been reported to provide excellent photocatalytic activity (Fujishiro *et al.,* 1999; Guo *et al.,* 2001). Catalysts prepared with LDH at low temperatures are characterised by higher activity, stability and lifetime, and there is no necessity for alkali metal additions; they therefore have good activity and thermal stability (Cavani *et al.,* 1991). Organo-modified Zn/Al-LDH has been reported for the polymerisation of ethylene as a catalyst support and reinforcement material (He and Zhang, 2007).

2.7.2 Pharmaceutical, medical and cosmetic applications

The most important properties that make LDH useful in these industries are their low toxicity, buffering effect and exchange capacity (Choy *et al.,* 2007). The problem facing modern pharmacology is to produce active medication that can be released at the required rate in the human body. LDH has proved to be useful as a matrix for most pharmaceutical and biologically active agents for this purpose (Choy *et al.,* 2007).

Solubility plays a major role in drug liberation, adsorption and bioavailability (Costantino *et al.,* 2007). Drugs must be highly soluble in biological fluid but some available drugs show poor solubility. Trikeriotis and Chanotakis (2007) reported the intercalation of the antibiotics gramidin, amphoterin B, ampicillin and nalidixic in LDH. Dupin *et al.* (2004) incorporated dichlorophenac, an anti-inflammatory

drug used mostly to treat fever, pain and inflammation in the body. This resulted in drugs being released at the required time and under appropriate conditions. The release of the drugs involves a long de-intercalation process, giving the medicine the required prolonged period of action (Choy *et al.,* 1999; 2007). DNA and nucleoside monophosphate intercalated LDH has also been reported (Choy *et al.,* 1999). These LDH nano-hybrids can be used for delivering the DNA into the cells.

LDH is an antacid, and can be used to neutralise the free HCl in the stomach gastric juices (Miyata and Okada, 1977; Choy *et al.,* 2007). Currently, LDHs are receiving considerable attention in the development of biosensors for enzymes, particularly for medical diagnosis. Urea biosensors based on LDH have been reported for the determination of urea in the human body in order to diagnose diabetes and dysfunction of the liver or kidneys. Carbonate-containing LDH can be used as agents for peptic ulcer treatment (Miyata and Okada, 1977; Miyata, 1980; 1983).

Solar radiation affects human skin badly, resulting in premature skin ageing, skin cancer and burning of the skin. Skin damage is caused mostly by sunscreens, moisturisers and skin lighteners which loose their specific functions when penetrating the skin (Anselim, 2001; Perioli et al., 2006). The skin lotions must remain on the skin for a required period of time (Anselim, 2001). LDH has shown the ability to solve some of these problems. It has proved to be a good matrix for intercalating sunscreens. This offers advantages such as photostability, easy formulation and no skin contact, and also removes shine and covers blemishes (Choy *et al.,* 2007). Perioli *et al.* (2006) intercalated 2-phenyl-1H-benzimidazole-5-sulfonic acid in LDH. This proved to be good for photoprotection and can also be used in underarm deodorants.

2.7.3 Polymers

LDH can be used in a polymer matrix to produce nanocomposite materials with reproducible chemical and physical properties (Adachi-Pagano, 2003; Fischer,

2003) Anion-exchange capacity (AEC) plays a major role in the preparation of nanocomposites. The smaller the AEC, the easier the formation of a nanocomposite (Leroux and Besse, 2001). Employing LDH in the preparation of nanocomposites results in materials with increased tensile and thermal properties, reduced permeability and solvent uptake, and lower flammability (Zammarano *et al.,* 2006; Frost *et al.,* 2003a). LDH nanocomposites can be used in many applications, including batteries (Leroux *et al.,* 2003).

PVC is one of the thermoplastic resins that are thermally unstable. Most thermal stabilisers in use contain toxic substances like lead, metal soaps and tin compounds that are environmental pollutants. Nanocomposites based on PVC and modified LDH have been investigated to improve the thermal stability of PVC (Lin *et al.,* 2006). LDHs are used as halogen scavengers in polyolefin production, for the production of ceramic aluminium nitride from LDH poly (acrylonitrile) complexes (Meyn *et al.,* 1990).

2.7.4 Other applications

LDH has been reported for applications in cleaning and water treatment. The process involves the removal of organic contaminants. The development of stabilisers and sorbents for hydrophobic organic compounds is a major challenge. LDHs have attracted attention due to their use as adsorbents and ion exchangers. LDH formation offers a mechanism for the disposal of radioactive wastes and also for removing heavy metals from water contaminated by heavy metals (Lin *et al.,* 2006). Dodecylsulphate intercalated LDHs have been used for trapping chlorinated pollutants in water (Allada *et al.,* 2002). Li/Al-LDH is reported to be an effective adsorbent for Cr (VI), while in de-intercalated form it can be used to recover the contaminants from the adsorbents used (Lin *et al.,* 2006). Mg-Al oxides can be used for the treatment of waste acids as both a neutraliser and an adhesive of anions (Kameda *et al.,* 2002).

LDHs can be used in separation processes for the removal of environmentally hazardous acid mine drainage or as scavenger (Frost *et al.,* 2003a). LDH

incorporated into polyelectrolytes can be employed to modify the proton conductivity and diffusion coefficient of the membrane in direct methanol fuel cell applications (Lee *et al.,* 2005).

3 EXPERIMENTAL

3.1 Reagents and Suppliers

All the reagents were used without further purification, unless otherwise stated. The hydrotalcite, also referred to as LDH-CO_3, contained silica and magnesium carbonate as minor impurities. In all the experiments distilled water was used. Table 3 gives all the reagents used, their chemical grades and the suppliers.

Table 3: Reagents used and suppliers

Reagent	Supplier
Hydrotalcite (HT-325 grade)	Charmotte Holdings
Sodium dodecylsulphate (SDS) 98%	Fluka
Behenic (docosanoic) acid (80% technical grade)	Fluka
Tween 60 (polyoxyethylene-20-sorbatin monostearate)	Sigma
Stearic acid (65-90 °C)	Biozone Chemicals
Caprylic (octanoic) acid	Croda Chemicals
Acetic acid (98%)	Saarchem
Acetone (99%) C.P.	Radchem Laboratory Suppliers
Hexanoic acid 98%	Croda Chemicals
Butyric acid	Fluka
Ammonia solution	Promark Chemicals
Ethanol 96% rectified	Dana Chemicals
Ethanol A.R. 99.9% absolute	Radchem Laboratory Suppliers
Lauric (dodecanoic) acid	Croda Chemicals

3.2 Experimental Set-up

A schematic presentation of the experimental set-up is shown in Figure 6. All the LDH intercalated samples were prepared using this set-up. All the reactions were carried out in a glass beaker. The hot plate was used to heat the reactants to the

required temperature by setting it on the temperature controller. A mechanical stirrer was used to stir the reactants in order to avoid agglomeration. Constant low-speed stirring was employed throughout the experiments. A pH meter was used to determine the reaction pH for all the experiments.

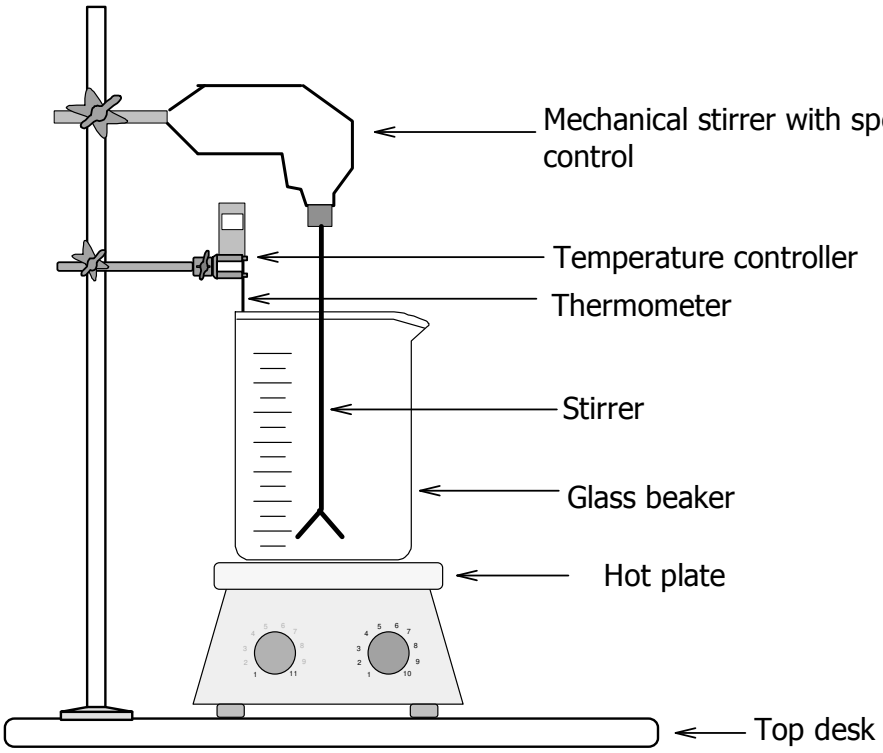

Figure 6: Schematic diagram of the experimental set-up

3.3 Standard Intercalation Method

Typical intercalation experiments were conducted according to the following procedure:

1. The molecular mass of LDH-CO_3 used was estimated at ca. 234.66 g/mol. 20 g of LDH-CO_3 ($[Mg_{0.689}Al_{0.311}(OH)_2](CO_3)_{0.156}.1.5H_2O$]) was used which amounted to 0.0852 mol. Thus 1 AEC was equivalent to 0.085 mol monocarboxylic acid. Therefore 4.12 and 4.5 AEC amounted to 0.351 mol and 0.384 mol monocarboxylic acid respectively.

2. 20 g of LDH-CO_3; 0.351 mol or 0.384 mol monocarboxylic acid; and 40 g (0.139 mol unless otherwise stated) of surfactant, SDS or Tween 60, were suspended in 1 500 ml of distilled water. The mixture was heated to and maintained at the required reaction temperature, e.g. at 80 °C for 9 hours, and cooled down overnight at room temperature. The cycle was repeated four times. Carboxylic acid was added partially in three cycles, i.e. until the overall total amount had been added. During the last cycle the mixture was simply allowed to stir without acid addition. The pH of the mixture was controlled by drop-wise addition of NH_4OH solution. The mixture was allowed to cool down slowly at room temperature. The solids were separated from the mother liquor by centrifugation, washed once with distilled water, four times with ethanol and once with acetone. After each washing the solids were separated from the liquid by centrifugation. The product (LDH-carboxylate) was allowed to dry at room temperature. In some instances the solids were further purified by Soxhlet extraction with absolute ethanol to remove the excess acid.

The above procedure was followed to prepare ethanoic (acetic), butanoic (butyric), hexanoic (caproic), octanoic (caprylic), decanoic (capric), dodecanoic (lauric), tetradecanoic (myristic), octadecanoic (stearic) and docosanoic (behenic) acid intercalated LDH. See Figure 7 for the melting points of these acids. All the experimental parameters, temperatures, pHs and product yields obtained for all the samples are shown in Appendix A.

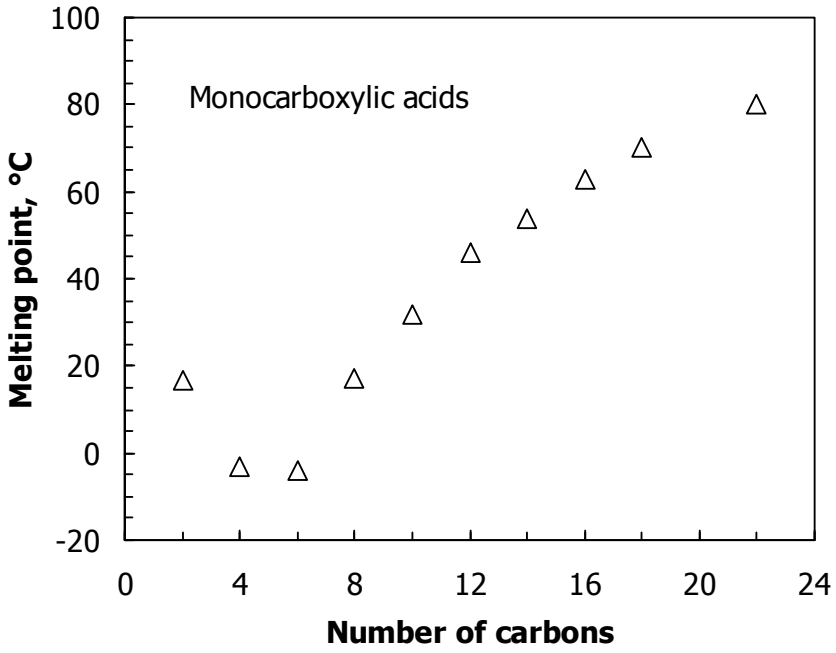

Figure 7: Carbon numbers and the melting points (∆) of the monocarboxylic acids

3.4 Effect of Surfactant on Intercalation

The effect of surfactant on intercalation was checked using the same standard procedure as in Section 3.3. Two samples were prepared using the surfactants SDS and Tween 60. In each case 40 g of the surfactant was added to 1 500 ml of distilled water at 80 °C, followed by addition of 20 g LDH-CO_3. The mixture was allowed to stir in four cycles as above, but without acid addition.

In some instances the samples were prepared using a smaller amount of surfactant. 2 g of SDS or Tween 60 was added to 1 500 ml of distilled water at 80 °C, followed by the addition of an excess amount of stearic acid (0.384 mol) and LDH-CO_3. The acid was added partially in three cycles, as stated in Section 3.3.

3.5 Leaching out the Excess Monocarboxylic Acid on LDH Intercalates

The main focus was on intercalating stearate anions. The excess stearic acid was leached out using a Soxhlet extractor. 3.9 g of stearate-intercalated LDH was

suspended in 100 ml of 99.9% absolute ethanol. The suspension was heated to 80 °C in a water bath under reflux for an hour. The mixture was cooled down slowly at room temperature. The product was recovered by centrifugation and allowed to dry at room temperature. The experimental set-up is shown in Figure 8.

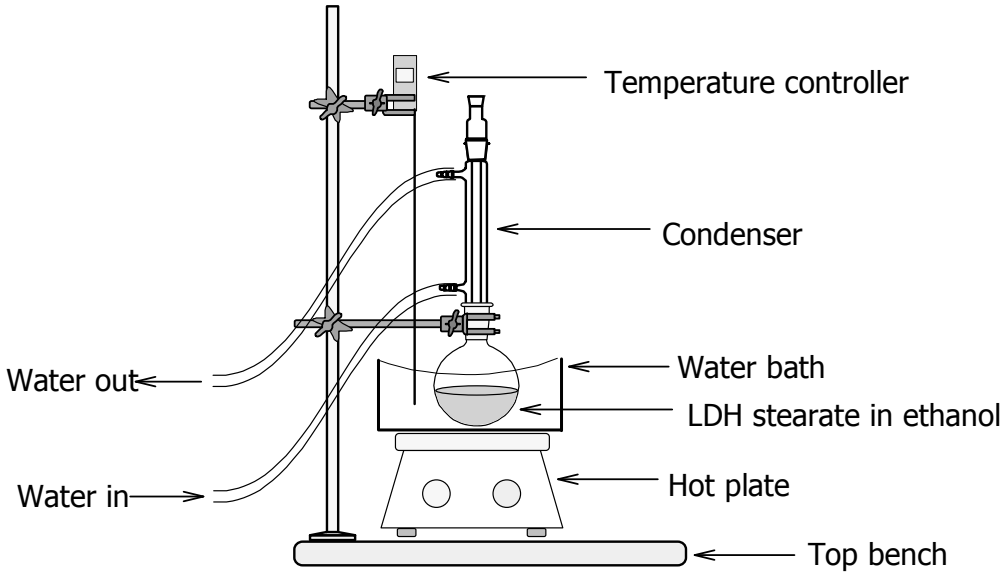

Figure 8: Schematic presentation of the experimental extraction set-up

3.6 Preparation of Mixture of Magnesium Stearate and LDH Stearate

To make sure that the LDH stearate obtained is an intercalate rather than simply magnesium stearate, a mixture of magnesium stearate and LDH stearate was prepared. The procedure described in Section 3.3 was employed. 40 g of the surfactant SDS, 20 g of LDH-CO_3, 2.25AEC (54.401 g) of stearic acid and 2.25 AEC (113.07 g) of magnesium stearate were dissolved in 1 500 ml of distilled water at 80 °C. The mixture was heated in four cycles as described in Section 3.3, but in this case the magnesium stearate was added partially in three cycles. The product was recovered and dried at room temperature.

3.7 Material Analysis

3.7.1 Instrumentation

Elemental analysis was performed by means of XRF. The carboxylate intercalated LDH sample was first ashed in a furnace at 700 °C for four hours to produce LDO. The elemental analysis was performed on the LDO sample. The samples were ground to <75 μm in a tungsten carbide milling vessel, then roasted at 1 000 °C for determination of the loss on ignition. The loss on ignition value was determined after addition of 1 g of sample to 9 g of $Li_2B_4O_7$ fused into a glass bead. Major element analysis was executed on the fused bead using an ARL9400XP+ spectrometer. Another aliquot of the sample was pressed into a powder briquette for trace element analysis.

Thermal degradation of the samples was checked on a simultaneous TGA/SDTA Mettler Toledo 851e instrument. 15 mg of the sample was placed in an open 70 μl aluminium pan. The sample was heated from 25 to 700 °C at a heating rate of 10 °C/min in air.

Identification of organic interlayer anions was performed on a Bruker FT-IR machine operating with Opus software, Version 2.1. The standard KBr pellet-pressing method was used. The pellets were prepared by crushing approximately 2 mg of sample together with 100 mg of KBr powder. The mixture was pressed in a die under vacuum for 5 minutes. The FT-IR absorption spectra were recorded by allowing the infrared radiation to pass through the pellet in the frequency range of 400 to 4 000 cm^{-1}. The data were collected from 32 scans at a resolution of 2 cm^{-1}. The data obtained were averaged and background-corrected using a pure KBr pellet.

DSC data were collected on a DSC Q100 TA instrument. 5–10 mg samples were placed in an open aluminium pan and heated from –20 °C to 150 °C and back to -20 °C at a rate of 10 °C/min and a flow rate of 50 ml/min using nitrogen.

Phase identification was carried out by XRD analysis on a PANalytical X-pert Pro diffractometer with variable divergence and receiving slits and an X'celerator detector using Fe-filter Co K-alpha radiation (0,17901 nm) operating with X'Pert High Score Plus software. The temperature-scanned XRD data were obtained using an Anton Paar HTK 16 heating chamber with Pt heating strip. Scans were measured between 2θ = 1 and 40 °C in a temperature range of 25–150 °C at intervals of 25 °C with a waiting time of 1 min and a measurement time of 6 min per scan. 99% pure Si (Aldrich) was added to the samples so that the data could be corrected for sample displacement using the X'Pert High Score Plus software. The results are presented as variable slit data as that allows for better data visualisation.

Sample morphology was checked on a JEOL 840 SEM (scanning electron microscope). A small fraction of sample was placed on carbon tape on a metal sample holder. The excess powder was removed by air blasting. SEM uses electrons to produce images and the sample must be electrically conductive. To make the samples conductive, SEM auto-coating unit, E2500 Polaron equipment LTD sputter coater, was used. The samples were placed in a chamber at vacuum and argon gas was introduced. They were coated five times with gold. The gold-coated samples were viewed at low magnifications.

4 RESULTS AND DISCUSSION

4.1 Elemental Analysis

Table 4 reports the XRF results for the chemical analysis of the LDH-CO_3 grade HT 325 that was used as raw material and the chemical composition of the ashed LDH stearate synthesised using the surfactants SDS and Tween 60. The reported composition of the LDH-CO_3 is consistent with the Mg:Al ratio of 2.21:1 (mol basis). The theoretical anionic exchange capacity (AEC) of this LDH-CO_3 is 402 meq/100 g. The ashed LDH-stearate (SDS) sample suggests instead a Mg:Al ratio of 1.93:1 (mol basis) and indicates the presence of 0.45 mol of sodium atoms for every mol of aluminium atoms for the LDH stearate sample synthesised using SDS. These results indicate that some sodium stearate was co-intercalated. The LDH stearate synthesised using Tween 60 suggests a Mg:Al ratio of 2.20:1.00 (mol basis). There is no change in the mol ratio obtained compared with LDH-CO_3. In this case only stearate anion was intercalated. The results show that non-ionic surfactants can be used to prevent co-intercalation of sodium. This is evident from the absence of sodium in the LDH stearate sample prepared using Tween 60.

Table 4: XRF composition analysis (mass %) of LDH-CO_3 and LDH-stearate synthesised with SDS and Tween 60 ashed at 700 °C

Sample	MgO	Al_2O_3	SiO_2	CaO	Fe_2O_3	Na_2O	NiO	LOI%
LDH-CO_3	35.05	20.09	1.05	0.26	0.10	0.00	0.08	43.31
Ash (SDS)	49.43	32.38	1.55	0.27	0.27	8.85	0.05	7.23
Ash (Tween 60)	55.23	31.76	1.24	0.36	0.15	0.01	0.04	12.00

4.2 Thermal Decomposition

Figure 9 shows the thermogravimetric mass loss and the mass loss derivative curves obtained for pure LDH-CO_3 heated from 25 to 700 ºC in air. The mass loss of LDH-CO_3 starts at room temperature and is complete by 700 ºC. Three major mass loss steps are observed on TG enhanced by three peaks on DTG. The first

sharp peak at 236 ºC observed in the range 25-250 ºC with a 86.3% mass loss is due to the loss of interlayer water (Rey *et al.,* 1992; Rocha *et al.,* 1999). The second peak centred at 325 ºC in the range 250–370 ºC is due to the loss of hydroxyl groups from the brucite-like layers (Rey *et al.,* 1992). The third peak at 428 ºC in the temperature range 370–700 ºC is reported as being due to a combination of dehydroxylation and loss of interlayer anion or decarbonation (Reichle, 1985; Miyata and Okada, 1995). The Mg-Al-LDH structure starts to decompose at temperatures higher than 400 ºC and the MgO phase starts to form (Kanezaki, 1998).

Despite the claim by Kanezaki (1998) that decarbonation occurs at temperatures above 400 and 500 ºC, Hibino *et al.* (1995) found that in this temperature range the process is not complete for Al-rich compounds. Rey *et al.* (1992) claim that the decarbonation process starts from 227 ºC and overlaps with the dehydration, and that the Al content has no influence on the thermal behaviour of hydrotalcites. All the thermal processes were found to be to be reversible at room temperature in contact with the atmosphere (Rey *et al.,* 1992). Kloprogge and Frost (1999) claim that decarbonation occurs in the region 80 to 230 ºC.

The present results show 58.3% total residue at 700 ºC on TG. The expected TGA residues for $[Mg_2Al(OH)_6](CO_3)_{1/2}.1.5H_2O$ after the first and final steps are 88.45 and 56.08% respectively. The full calculation of the expected % mass loss after the first and last thermal events is shown in Appendix B. The experimentally observed values for the LDH-CO_3 are 86.33 (at T = 250 °C) and 58.3% (at T = 700 °C) respectively.

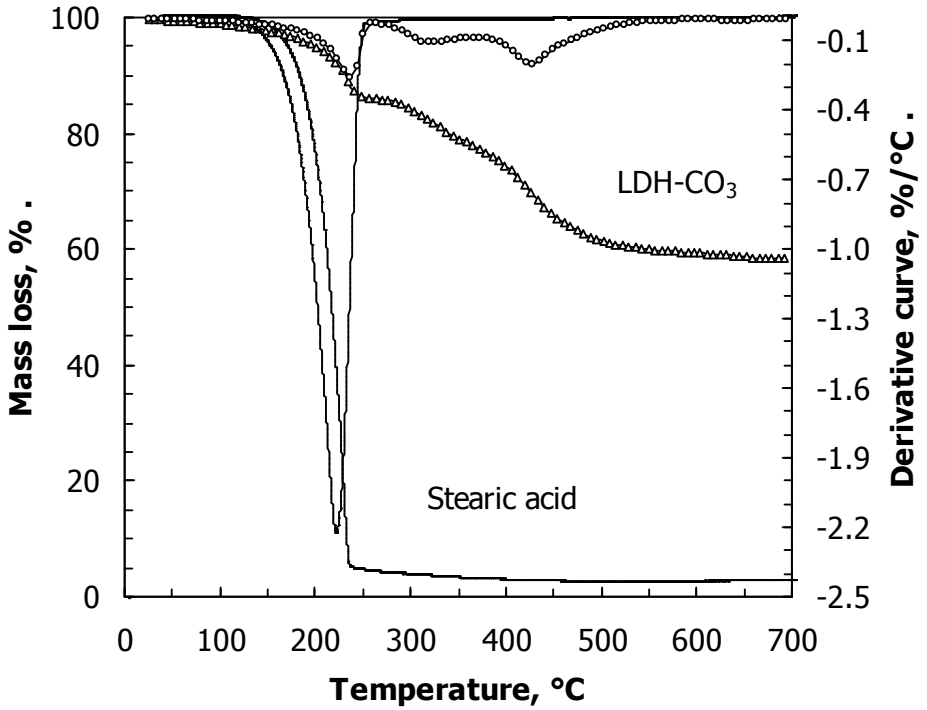

Figure 9: TG and DTG curves of LDH-CO_3 and stearic acid in air

The thermal decomposition product of the $[Mg_2Al(OH)_6](CO_3)_{1/2}.nH_2O$ can be represented as follows:

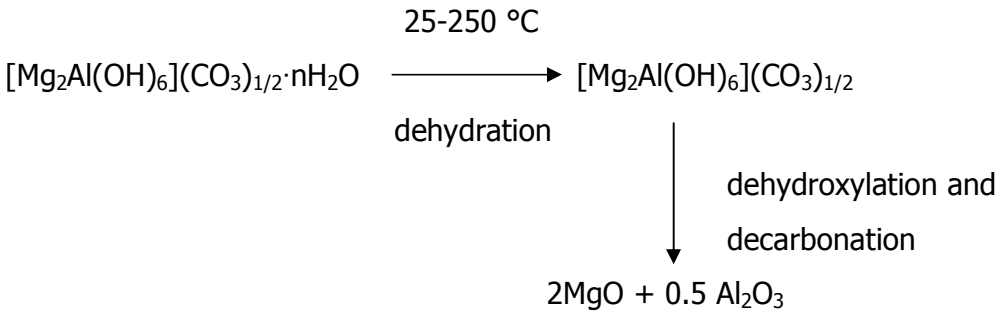

Scheme 4: Schematic presentation of the LDH decomposition process

Kanezaki claims that water molecules thermally oxidise the interlayer carbonate and carbon dioxide, and that hydroxyl anions are released by the reaction (Kanezaki, 1998)

$$[CO_3^{2-} + H_2O]_{interlayer} \longrightarrow CO_{2(g)} + 2OH^-_{(g)}$$

Stearic acid shows only one mass loss step. The peak observed is centred at 225 °C on DTG. This peak is attributed to the vaporisation of carboxylic acid and its degradation products. This mass loss is also complete at 700 °C.

Figures 10 and 11 show the TG and DTG curves for fatty acid intercalated LDH from 25–700 °C in air. The individual curves are shown in Appendix B. Three thermal events similar to those observed in LDH-CO_3 are observed. These are loss of interlayer water, dehydroxylation and a combination of dehydroxylation and the loss of interlayer anion.

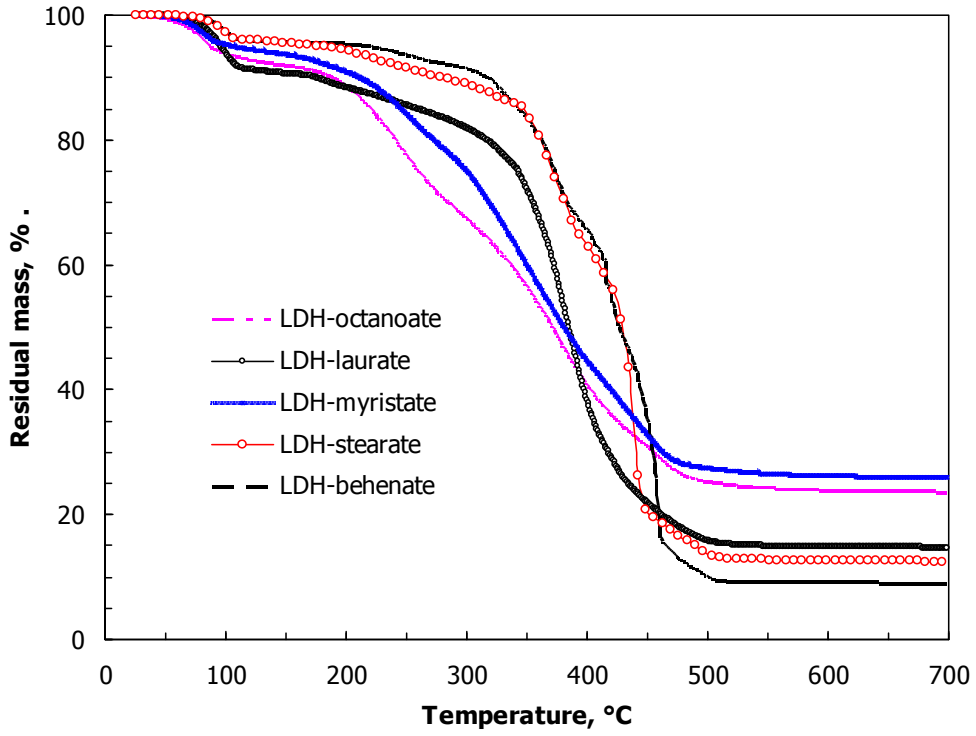

Figure 10: TG curves of LDH-octanoate, laurate, myristate, stearate and behenate prepared at 80 °C (octanoate and stearate), 70 °C (laurate), 60 °C (myristate) and 90 °C (behenate)

The sharp DTG peaks centred at 82, 90, 85, 97 and 100 °C corresponding to ca. 4% mass loss are attributed to the loss of interlayer water for the LDH-octanoate, laurate, myristate, stearate and behenate samples respectively. The peak at

225 °C observed in LDH-CO_3 in Figure 9 is suppressed and new peaks are observed at 250, 237, 260, 380 and 425 °C for the LDH-octanoate, laurate, myristate, stearate, and behenate samples respectively. An attempt was made to intercalate acetic, butyric, hexanoic and decanoic acid anions in LDH. However, the intercalation failed. The TG/DTG results are shown in Appendix B.

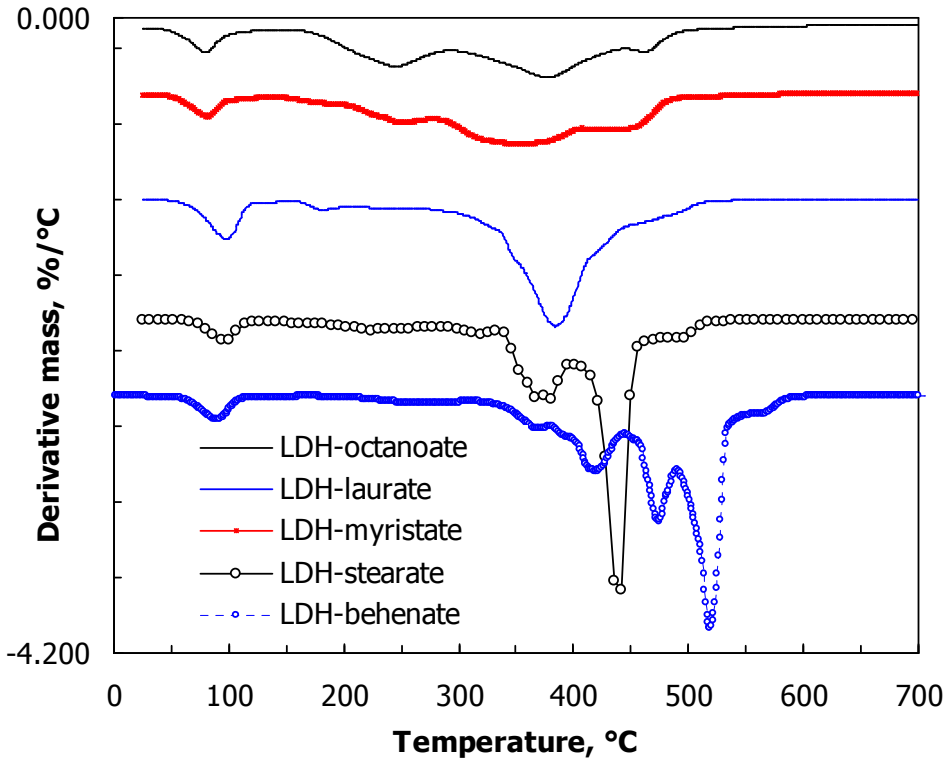

Figure 11: DTG curve of LDH-octanoate, laurate, myristate, stearate and behenate prepared at 80 °C (octanoate and stearate), 70 °C (laurate), 60 °C (myristate) and 90 °C (behenate**)**

The amount of intercalated carboxylate in the interlayer was estimated from TG data as follows:

The interlayer water content was estimated from the mass loss recorded at 148 °C. This is based on the fact that at this temperature the physically adsorbed and interlayer water has been lost. The effective clay content was calculated from the residue at a high temperature of 700 °C. The carboxylic acid content was

calculated from the difference (see Table 5). This was based on the fact that the residue contains MgO, Na_2O and Al_2O_3 as is evident from the presence of sodium in the samples prepared using SDS. A high carboxylate content was observed for LDH-laurate, stearate and behenate. This high organic content is attributed to the presence of sodium in the interlayer region.

Table 5: TG data for LDH-CO_3, octanoate (80 °C), laurate (70 °C), myristate (60 °C), stearate (80 °C) and behenate (90 °C) intercalated LDH prepared using SDS

Sample	Residual mass at 148 °C	Residual mass at 700 °C	% Effective clay content	% Carboxylate
LDH-CO_3	97.78	58.33	100	
LDH-octanoate	91.98	23.63	43.06	56.94
LDH-laurate	90.70	14.71	27.17	72.82
LDH-myristate	93.77	25.94	46.36	53.64
LDH-stearate	95.63	12.48	21.87	71.28
LDH-behenate	95.73	9.00	15.75	84.24

Figure 12 illustrates the effect of reagent stoichiometry on stearate intercalation obtained at 80 °C in comparison with the data obtained by Itoh *et al.* (2003). The degree of stearate intercalation in the present data lies slightly above the theoretical limit for the product obtained at a feed composition of stearate/LDH = 4.12, purified by Soxhlet extraction with absolute ethanol. In contrast, Itoh *et al.* (2003) obtained values that are slightly below the theoretical limit at a feed composition of 5 mm of the sodium stearate, with appropriate amounts of LDH, at 60 °C.

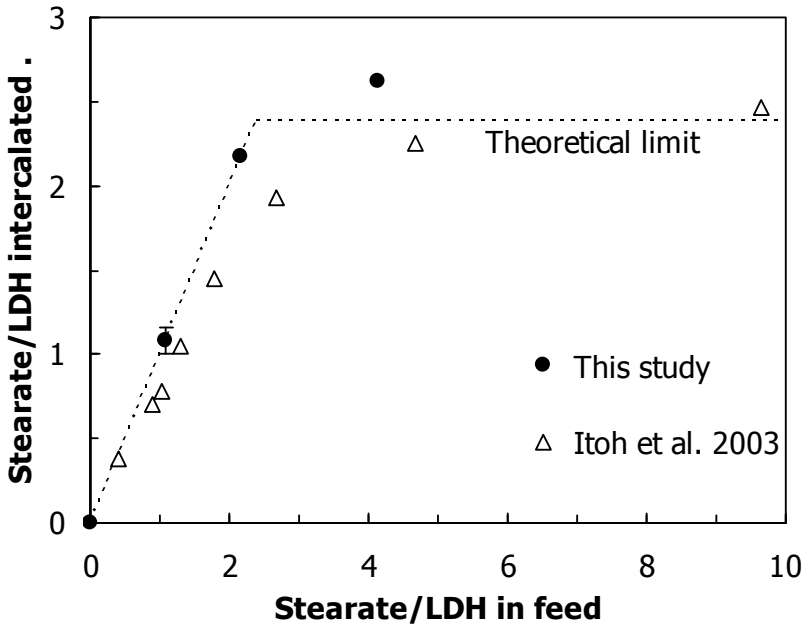

Figure 12: Effect of reagent stoichiometry on the degree of stearic acid intercalation at 80 °C, where (•) represents the present data and (Δ) represents the values obtained by Itoh *et al.* (2003) for sodium stearate

4.3 FT-IR

Figure 13 shows the FT-IR results of the precursors (LDH-CO_3, stearic acid and the surfactant SDS) used in the intercalation reactions. LDH-CO_3 shows a broad band at 3455 cm^{-1} due to the (-OH) hydroxyl stretching vibration of free hydrogen and hydrogen bonded to the octahedral layer and water molecules (Labajos *et al.,* 1992). The shoulder at 3063 cm^{-1} is due to the hydrogen bonding of H_2O to CO_3^{2-} ions in the interlayer space (Perez-Ramirez, 2001). The carbonate peak is observed at 1360 cm^{-1}. The shoulder at 917 cm^{-1} is due to the M-OH deformation mode. The bands at 763, 672 and 549 cm^{-1} are due to the Mg-OH translation mode, the v_4 (in-plane bending) vibrations of CO_3^{2-} and the Al-OH translation mode respectively (Kloprogge and Frost., 1999).

Stearic acid shows a broad O-H stretching mode in the range 3300-2500 cm^{-1}. The C-H symmetric and asymmetric stretching vibrations are observed at 2954, 2914 and 2870 cm^{-1}. Carboxylic acid salts are characterised by a strong absorption at

1700 cm^{-1} as is evident from C=O in dimeric carboxylic acids. The C-H bending and scissoring modes are observed at 1472 and 1464 cm^{-1}. The C-O-H bending mode is observed at 1410 cm^{-1} and the C-O stretching modes at 1313 and 1297 cm^{-1}. The CH_2 wagging modes are observed in the range 1300-1250 cm^{-1}. The number of these peaks is dependent on the length of the carboxylic acid chain, i.e. for even-number carbons the number of peaks will be equal to half carbon numbers, while for odd-number carbons they will be half plus one (Socrates, 1980). The O-H out-of-plane bending mode is observed at 936 cm^{-1}.

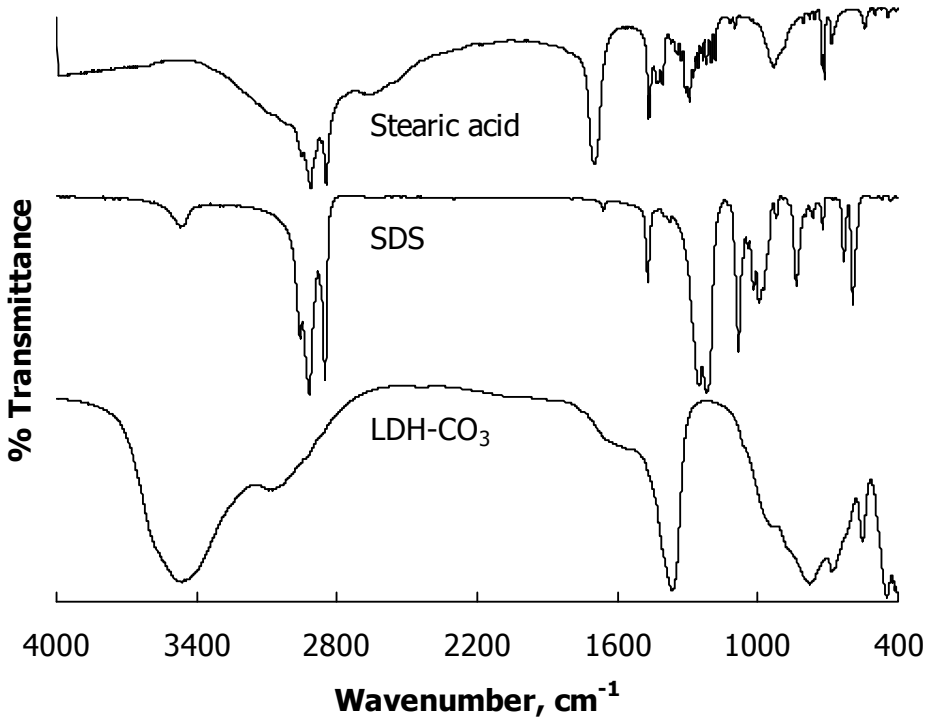

Figure 13: FT-IR spectra of the precursor LDH-CO_3, stearic acid and the surfactant SDS used in the intercalation reactions

The O-H stretching mode of the surfactant, SDS, is observed at 3447 cm^{-1}. The strong absorptions at 2915 and 2848 cm^{-1} are due to the -CH symmetric and asymmetric stretching of the alkyl chain. A strong and sharp absorption due the bending and scissoring mode of the $–CH_2-$ surfactant tail is observed at 1467 cm^{-1} (Crepaldi *et al.,* 2002). The band at 1382 cm^{-1} is attributed to the CH_3 deformation

mode. SDS is mainly characterised by the presence of $–SO_4$. The bands due to the asymmetric and symmetric stretching mode of $-SO_4$ are observed at 1206 and 1062 cm^{-1}. These bands are sometimes observed at 1214 and 1132 cm^{-1} or 1229 and 1065 cm^{-1} (Crepaldi *et al.,* 2002; Costa *et al.,* 2008). The shift to lower frequencies is attributed to the disturbance due to $–SO_3$ (Crepaldi *et al.,* 2002). Irrespective of C-H absorptions, carboxylic acids and SDS are easily distinguished by the presence of the carbonyl region for carboxylic acids and sulphate in the surfactant SDS.

Figure 14 compares the FT-IR spectra of fatty acid (octanoic, lauric, myristic, stearic and behenic) intercalated LDH. The separate spectra are shown in Appendix C. A broad band due to the -O-H vibration mode bonded to metal in the brucite-like layered sheet is observed in the range 3448–3387 cm^{-1} for all the samples (Frost *et al.,* 2002). The shoulder at 3247–3225 cm^{-1} is attributed to the water molecules that are hydrogen bonded to the interlayer anion (Perez-Ramirez *et al,* 2001). The strong and sharp-intensity peaks at 2915 and 2848 cm^{-1} are attributed to the asymmetric and symmetric stretching modes of the $–CH_2-$ group of the alkyl chain respectively (Labajos *et al.,* 1992).

LDH-octanoate, laurate and myristate show a very weak-intensity peak at 2936 cm^{-1} due to the $–CH_2$ vibration mode. However, these peaks are absent in the stearate and LDH-behenate samples. Several absorption bands are observed in the carboxyl region of 1750–600 cm^{-1} and this is discussed separately. The M-OH deformation and translation modes are observed at 983, 769 and 775 cm^{-1} (Perez-Ramirez *et al.,* 2001; Labajos *et al.,* 1992). The O-M-O and M-O bending and stretching modes are observed at 723 and 667 cm^{-1} and the $–CH_2-$ rocking mode at 716 cm^{-1} (Perez-Ramirez *et al.,* 2001).

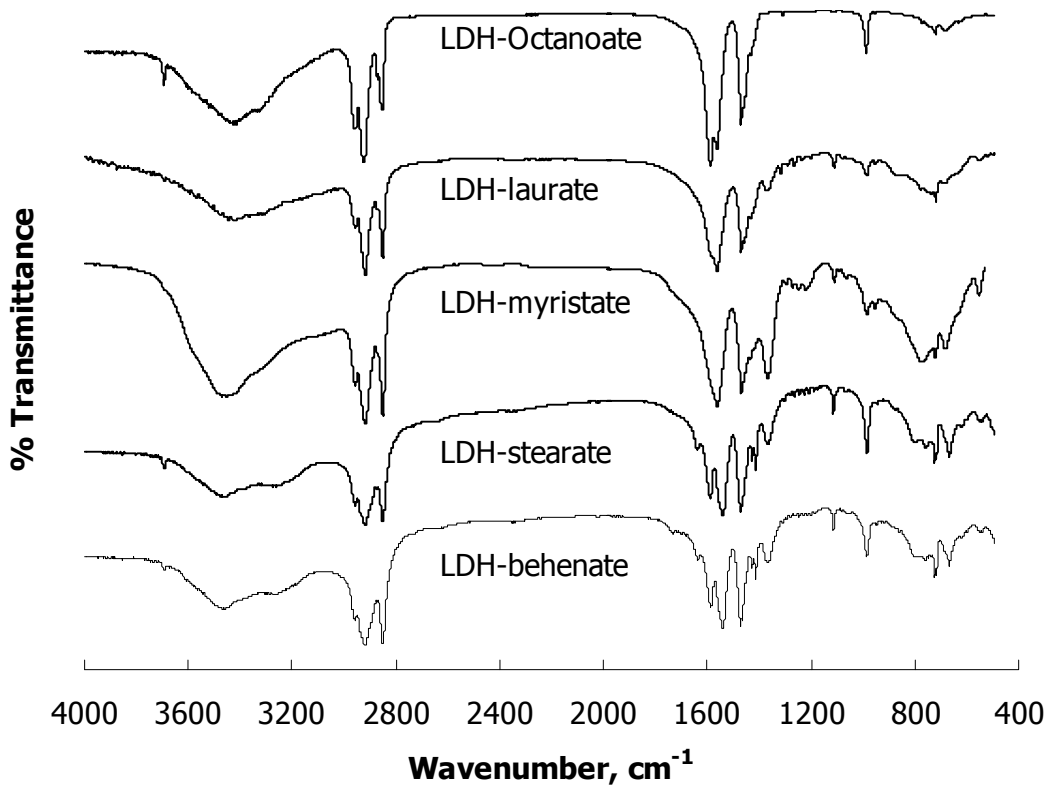

Figure 14: Comparison of FT-IR spectra of LDH-octanoate, laurate, myristate, stearate and behenate prepared at 80, 70, 60, 80 and 90 °C respectively

4.4 State of Intercalated Carboxylic Acid

Figure 15 shows the FT-IR spectra of the carboxyl group in the vibration region 1750-600 cm-1 of octanoate, laurate, myristate, stearate and behenate intercalated LDH obtained at 80, 70, 60, 80 and 90 °C respectively. The absence of a peak due to undissociated carboxylic acid at 1720 cm^{-1} and at 1210 cm^{-1} for sulphate indicates the purity of the intercalates obtained. LDH-Stearate and behenate show absorption bands similar to those obtained by Borja and Dutta (1992). A weak absorption band is observed at 1634 cm^{-1} in the LDH-stearate and behenate samples. This peak is attributed to the –OH stretching mode of the interlayer water (Labajos *et al.,* 1992). However, Borja and Dutta (1992) obtained the bands at 1637 cm^{-1} and 1588 cm^{-1}, and these bands were attributed to carboxylic acid being intercalated in the form –RCOOH, where H^+ is ionised in the interlayer as $C(O)O^{-\delta}H^{+\delta}$. The band at 1588 cm^{-1} is present in all the samples. The

LDH-octanoate shows a weak band at 1559 cm^{-1} due to the symmetric stretching mode of the ionised –C-O group in the interlayer (Carlino and Hudson, 1994). This band is observed at 1558, 1555, 1538 and 1536 cm^{-1} for the LDH-laurate, myristate, stearate and behenate samples respectively. The asymmetric mode is observed at 1425, 1426, 1413 and 1412 cm^{-1} in the LDH-laurate, myristate, stearate and behenate samples respectively (Perez-Ramirez *et al.,* 2001). However, these bands are absent in the LDH-octanoate sample. The medium-intensity bands at 1467, 1468, 1466, 1472 and 1470 cm^{-1} for the LDH-octanoate, laurate, myristate, stearate and behenate samples respectively are attributed to the $–CH_2$ bending mode of the carboxylic acid chain (Borja and Dutta, 1992).

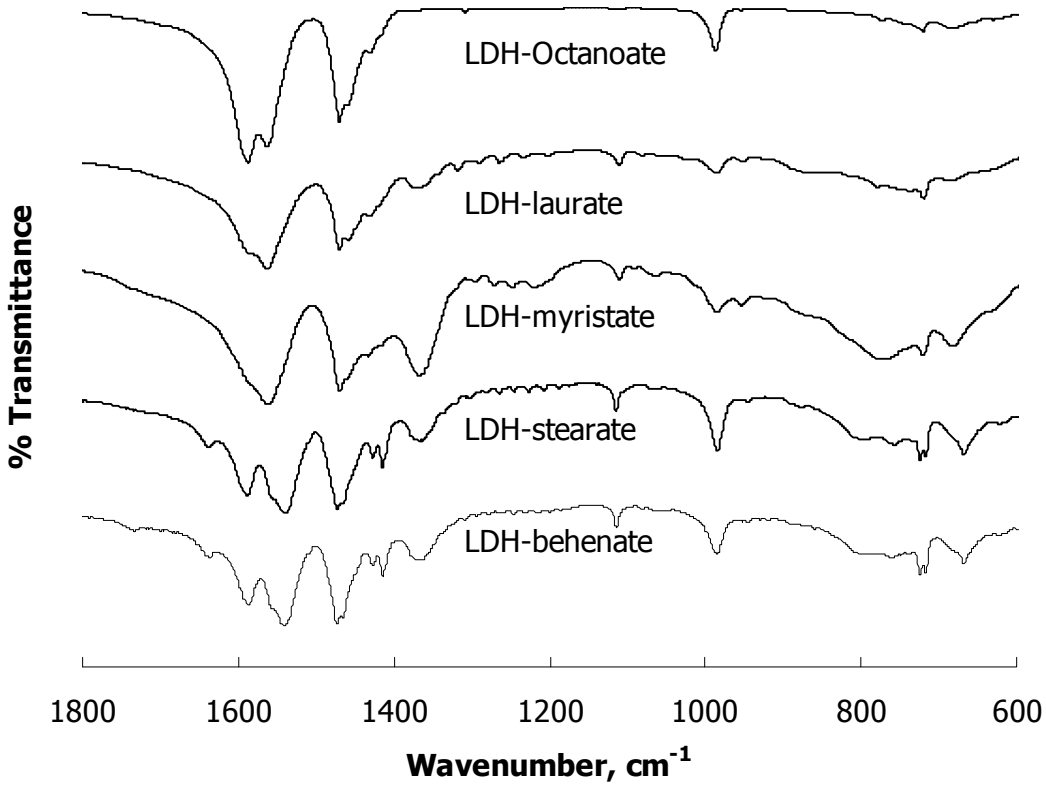

Figure 15: FT-IR spectra of fatty acid (octanoic, lauric, myristic, stearate and behenic) intercalated LDH showing only the carboxyl region

The high affinity of LDH for carbonate anion is confirmed by the presence of the band at 1360 cm^{-1} due to carbonate impurity from the LDH-CO_3 precursor. These bands are observed for the LDH-laurate, myristate, stearate and behenate

samples and are absent in LDH-octanoate. These results indicate that the carboxylic acid was intercalated in different forms, i.e. ionised and non-ionised, in between the LDH layers. Intercalation of short-chain fatty acids (acetic, butyric, hexanoic and decanoic) failed completely, as already mentioned. However, the FT-IR spectra are also shown in Appendix C. Kanoh *et al.* (1999) tried to intercalate short-chain fatty acids, but failed. This was attributed to the hydrophilicity of the acids at lower temperatures.

4.5 X-ray Diffraction

The PXRD pattern (obtained using cobalt Kα) of fatty acids, octanoate, laurate, myristate, stearate and behenate intercalated LDH prepared at 80 °C (octanoate and stearate), 70 °C (laurate), 60 °C (myristate) and behenate (90 °C) in comparison with LDH-CO_3 is shown in Figure 16. The individual XRD patterns are shown in Appendix D.

Two diffraction peaks are observed at 0.76 nm (2θ = 13.49°) and 0.38 nm (2θ = 27.21°). The first and greatest reflection d_{003} corresponds to the d-spacing of LDH. In this case a d-spacing of 0.76 nm is observed.

Several reflections are observed and the main reflections d_{003}; d_{006} and d_{009} are shown in Table 6. LDH intercalates show unreacted LDH-CO_3. This is evident from the reflections at 2θ = 13.49° and 27.21°. These are observed for the samples LDH-laurate, myristate, stearate and behenate and are absent in LDH-octanoate. This is in agreement with the FT-IR results obtained for all the samples. The sharp reflection peaks observed are an indication that the LDH intercalates obtained are highly crystalline. However, Carlino and Hudson (1995) reported the intercalation of octanoate in LDH using coprecipitation and the thermal reaction method, and obtained a polyphasic XRD pattern.

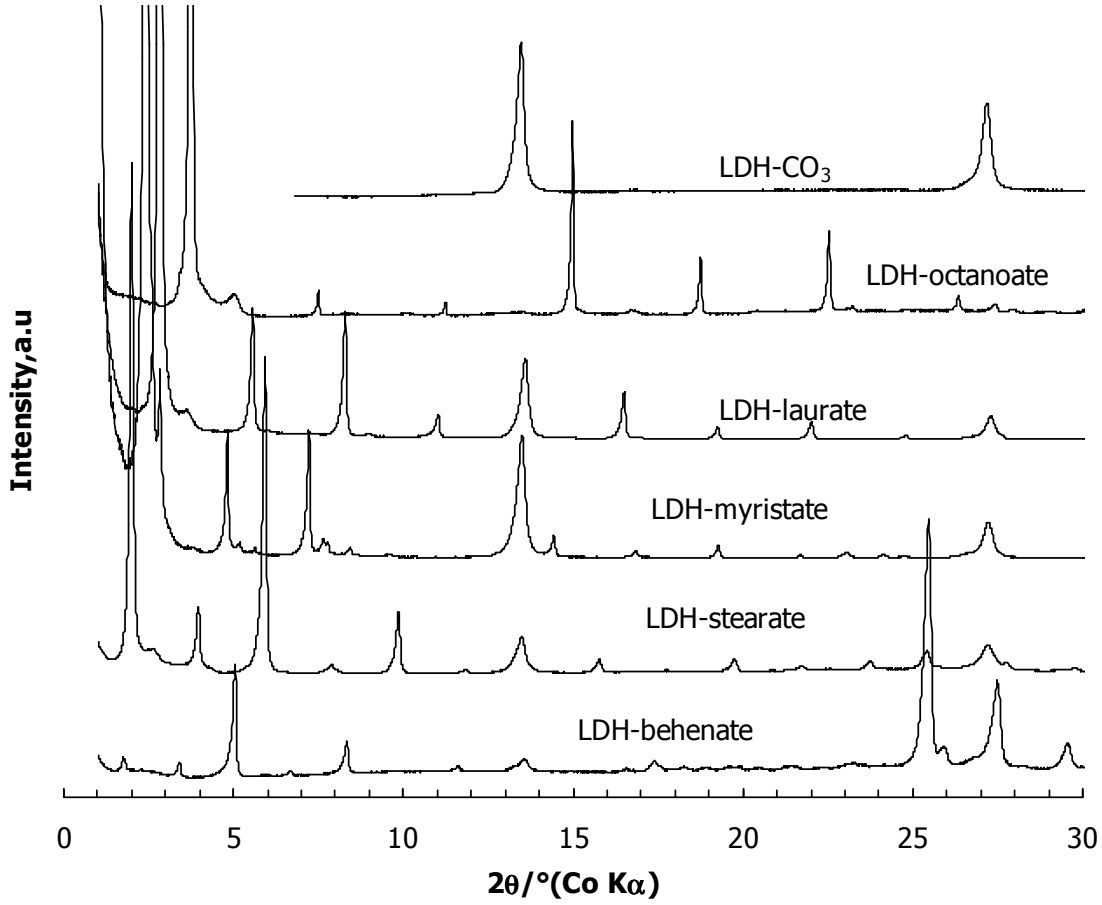

Figure 16: XRD pattern of fatty acid (octanoic, lauric, myristic, stearic and behenic) intercalated LDH samples prepared at 80 °C (LDH-octanoate, laurate and stearate), 60 °C (LDH-myristate) and 90 °C (LDH-behenate) respectively

An increase in the basal spacing from 0.76 nm is observed for all the samples. This is evident from the XRD data obtained. The basal spacings increased to 2.72, 3.66, 4.22, 5.04 and 5.81 nm for the LDH-octanoate, laurate, myristate, stearate and behenate samples respectively. These basal spacings suggest a bilayer intercalated LDH structure (Carlino, 1997; Meyn *et al.,* 1993). The bilayer structure is illustrated in Figure 17.

Borja and Dutta (1992) reported a monolayer structure in intercalated laurate, myristate and palmitate with $LiAl_2$-LDH. However, with Mg_3Al-LDH a bilayer structure was obtained. These structures were achieved using an ion-exchange method.

In the present study the observed basal spacings result in interlayer gallery heights of 2.24, 3.18, 3.74, 4.56 and 5.33 nm for the LDH-octanoate, laurate, myristate, stearate and behenate samples respectively. These interlayer gallery heights were calculated from the difference of 0.84 nm between the basal spacing and the thickness of the brucite-like LDH layers (Chibwe and Jones, 1989; Kanoh *et al.,* 1999).

Table 6: Observed XRD data of LDH intercalated samples

Sample	**Observed reflections**		
	d_{003}	**d_{006}**	**d_{009}**
LDH-octanoate: 2θ/°	3.77	5.02	7.50
d/nm	2.72	2.04	1.37
LDH-laurate: 2θ /°	2.80	5.56	8.29
d/nm	3.66	1.85	1.24
LDH-myristate: 2θ/°	2.43	4.83	7.22
d/nm	4.22	2.13	1.42
LDH-stearate: 2θ/°	2.04	4.01	5.97
d/nm	5.04	2.56	1.72
LDH-behenate: 2θ/°	1.76	2.61	3.39
d/nm	5.81	3.93	3.03

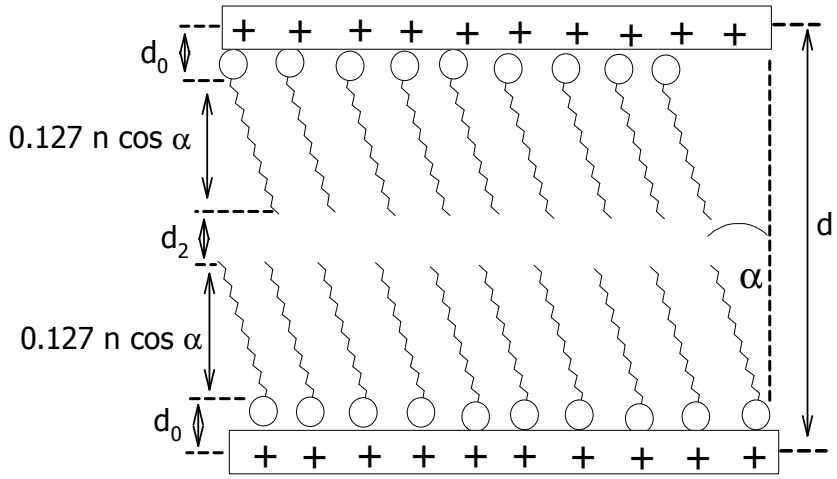

Figure 17: Schematic representation of the bilayer structure of fatty acid intercalated LDH with corrected slant angle (adapted from Carlino, 1997)

The effect of the chain length of carboxylic acid on the d-spacing was studied by plotting the observed d-spacing against the number of carbon atoms in carboxylic acid (see Figure 18). The data suggest that the d-spacing of the LDH intercalates increases linearly with an increase in the length of the carboxylic acid chain. Figure 18 also plots the d-spacing reported by Borja and Dutta (1992) and the values reported by Itoh *et al.* (2003). The literature values are slightly higher than the ones obtained in this study. The difference might be due to the presence of impurities that were incorporated into the clay galleries, i.e. ethanol in the case of the results obtained by Borja and Dutta (1992), and sodium ions in the case of the results obtained by Itoh *et al.* (2003). Miyata and Kumura (1973) and Meyn *et al.* (1993) also reported a linear increase in d-spacing with an increase in chain length for dicarboxylate and surfactant intercalated LDH.

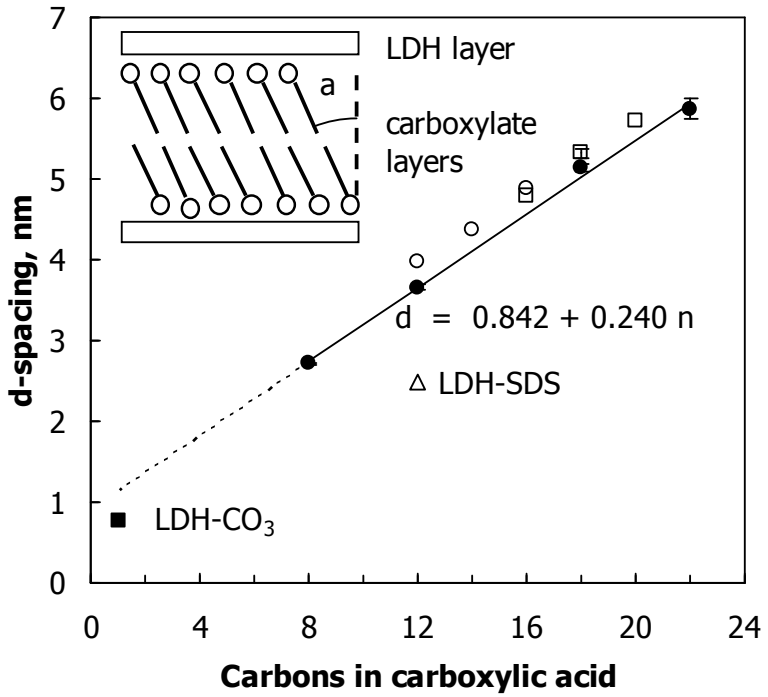

Figure 18: Effect of carboxylic acid chain length on the d-spacing of the LDH intercalates prepared by the SDS-mediated intercalation method, represented by (●). The d-spacing values for LDH-CO_3 (■) and LDH-SDS (△) (i.e. the sample in which an attempt was made to intercalate acetate) are shown, as well as the d-spacing values reported by Borja and Dutta (1992) (○) and Itoh *et al.* 2003 (□).

It is assumed that the slant angle of the alkyl chain length is dependent on the length and that the methylene bond lengths are equal to 0.127 nm (Carlino, 1997). The d-spacing of the bilayer intercalated LDH-carboxylate is calculated using equation 3. The present results, suggesting a slope of slope of 0.24 nm per unit charge, are similar to those reported by Kanoh *et al.* (1999) and Itoh *et al.* (2003) (see equation 5).

$$d = 0.842 + 0.240\,n \qquad (5)$$

The slope of 0.24 nm per $-CH_2-$ unit is similar to previously reported values of 0.235 and 0.2454 nm (Itoh *et al.,* 2003; Kanoh *et al.,* 1999). This slope corresponds to the slant angles of 19.3°, 22.3 and 15° using equation 3. These

values are slightly higher than the theoretical values reported in the literature. This is because of the presence of the sodium ion and ethanol impurities observed (Itoh *et al.,* 2003; Kanoh *et al.,* 1999). The aluminium atoms are probably randomly distributed within the Mg-Al-$(OH)_x$ sheets. However, an idealised regular arrangement is shown in Figure 19. This figure supports the estimation of the projected surface area per formula weight of the LDH. This was based on the predicted brucite-like Mg-Al-$(OH)_x$ sheet area per LDH formula weight ($[Mg_{2+x}Al_{1-x}(OH)_6]$ $(CO_3)_{(1-x)/2}.nH_2O$), which is given by equation6 below.

$$A(LDH) = \frac{3\sqrt{3}}{2}a^2 \qquad (6)$$

The lattice parameter a = 0.305 nm for the present LDH-CO_3 (Belloto *et al.,* 1996). This results in the projected LDH area A_{LDH} = 0.2404 nm^2. Based on the assumption that the sample has a hexagonal close-packing structure, the cross-sectional area per stearic acid chain is given by equation 7.

$$A(chain) = \frac{2}{\sqrt{3}}t^2 \qquad (7)$$

The reflection 2θ = 25.422° for CoKα results in a layer spacing of 0.407 nm and an area per stearic acid chain of 0.191 nm^2. Therefore, for bilayer intercalated LDH, incorporating a correction for the slant angle leads to the following maximum intercalation level (equation 8):

$$\left(\frac{Carboxylate}{LDH}\right)_{max} = 2\frac{A_{LDH}}{A_{chain}}\cos\alpha = \frac{9}{2}\left(\frac{a}{t}\right)^2\cos\alpha \qquad (8)$$

In the present case the slant angle is estimated at α = 19.1°. This yields a limit of 2.39 mol carboxylate/LDH for close-packed carboxylate chains.

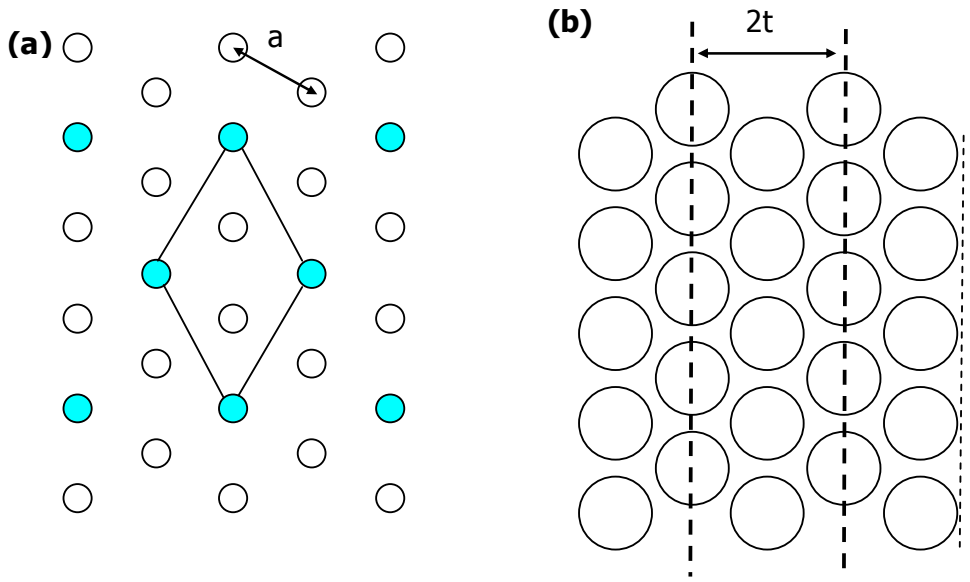

Figure 19: (a) Idealised regular arrangement of aluminium (○) and magnesium atoms (○) in the brucite-like metal hydroxide sheet of $[Mg_{2+x}Al_{1-x}(OH)_6]$ $(CO_3)_{(1-x)/2}.nH_2O$) with $\alpha \cong 0$, the lattice parameter a = 0.305 (Belloto *et al.,* 1996); and (b) the hexagonal close packing structure of the stearate chains

4.6 Effect of Surfactant on Intercalation

Figure 20 shows the FT-IR spectra obtained by dispersing the LDH-CO_3 in distilled water at 80 °C in the presence of the surfactants SDS and Tween 60 in comparison with LDH-CO_3. The absorption bands obtained fit perfectly with all the bands obtained in LDH-CO_3. This result indicates that the surfactants did not intercalate on their own.

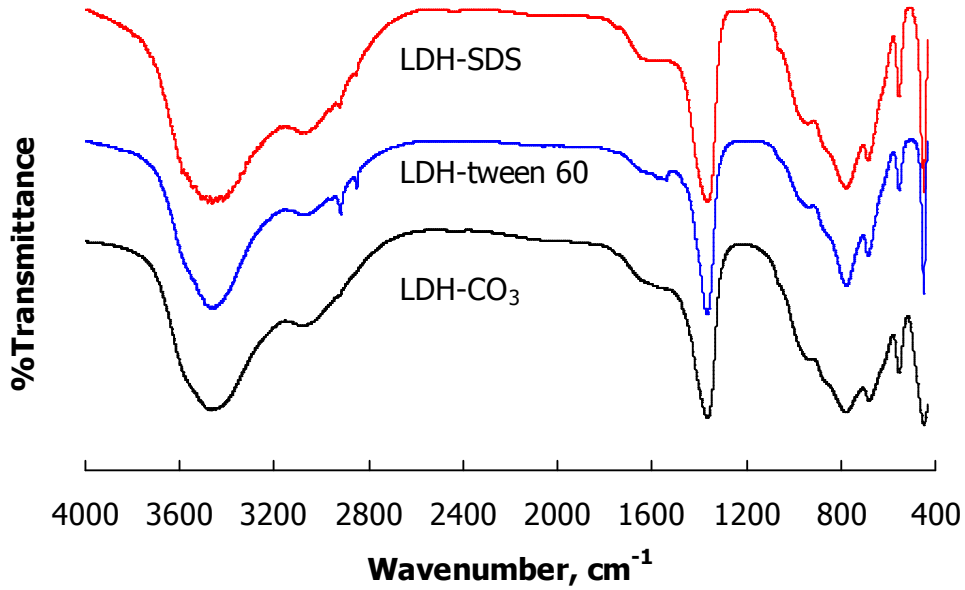

In this case a large amount of surfactant is required for better dispersion and purity of the LDH intercalates.

Figure 20: FT-IR spectra of LDH-SDS and LDH-Tween 60 in comparison with LDH-CO_3

The results in Figure 20 are in agreement with the XRD pattern in Figure 21. The observed XRD pattern is similar to the LDH-CO_3 pattern – in fact, no difference can be observed. Only two diffraction peaks due to LDH-CO_3 are observed.

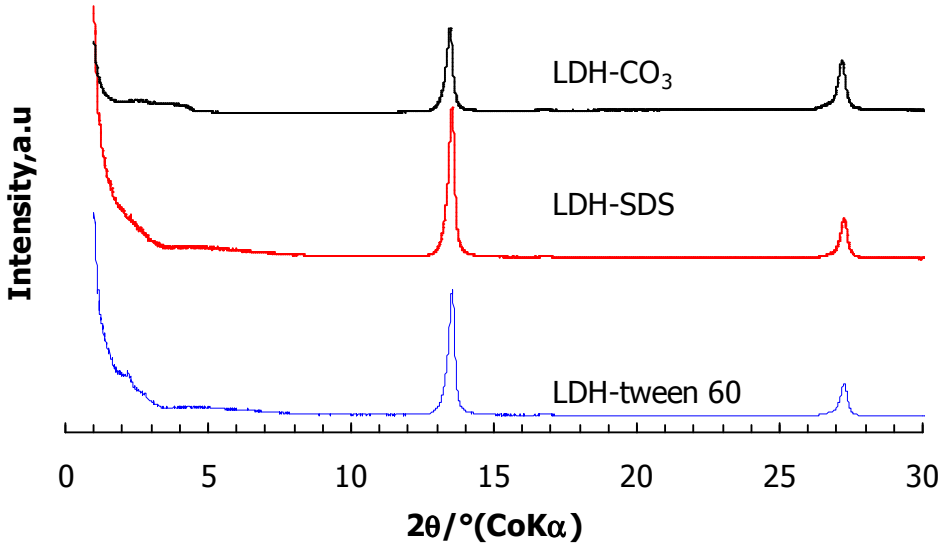

Figure 21: XRD pattern of LDH-SDS and LDH-Tween 60 synthesised at 80°C in comparison with LDH-CO_3

Figure 22 shows the TG/DTG curves for the LDH-SDS and LDH-Tween 60 samples prepared at 80 °C. Three thermal events similar to those of LDH-CO_3 are observed. The observed residual masses at 700 °C are 58.33, 58.68 and 58.43% for the LDH-CO_3, LDH-SDS and LDH-Tween 60 samples respectively. These results show that the surfactants SDS or Tween 60 did intercalate on their own. This is in agreement with the FT-IR and XRD results obtained, shown in Figures 20 and 21 respectively.

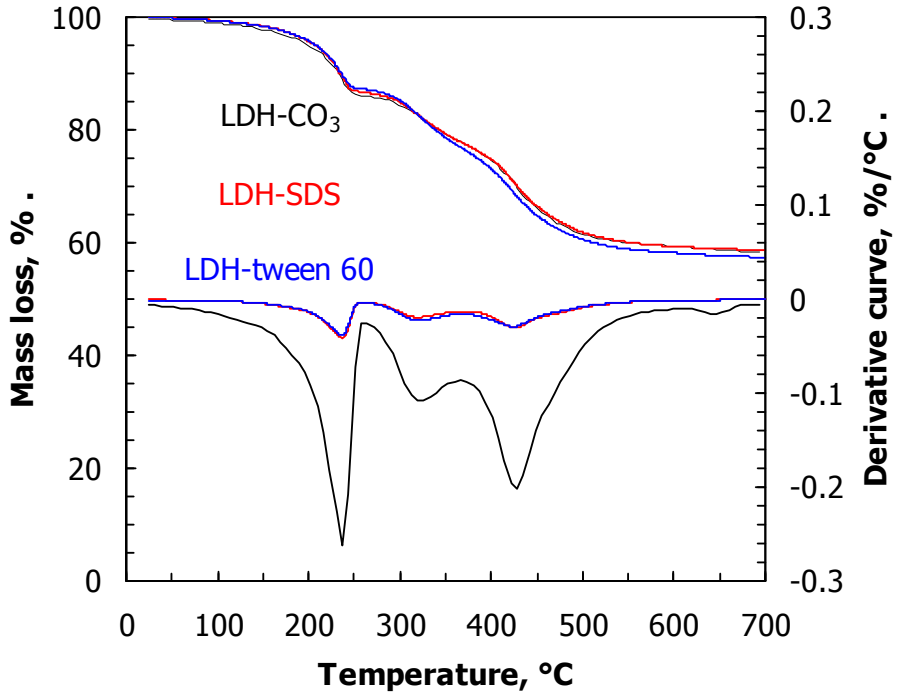

Figure 22: TG/DTG curves of the product obtained by dispersing the LDH in water in the presence of the surfactants SDS (LDH-SDS) and Tween 60 (LDH-Tween 60), in comparison with LDH-CO_3 heated from 25–700 °C in air

In contrast, when acetic acid is used the sulphate vibration modes are observed (see Figure 23). All the SDS bands discussed in Section 4.4 are observed. These indicate that the surfactant anions were intercalated in the LDH, instead of the desired acetic acid anions. The results obtained in this case show that in the presence of short-chain fatty acids such as acetic acid, which is also a weak acid, the LDH prefers SDS anions and not acetate. Miyata and Kumura (1973) reported that acetate intercalated in LDH. In the study, the acetate anions were successfully intercalated.

The present method works well with long chain carboxylic acids. However, high anionic or non-ionic surfactant concentration is required. When less surfactant is used in carboxylic acid intercalation, incomplete reactions are observed indicating that prolonged periods of heating is required and the materials also retains large

amounts of impuruties. Carboxylate intercalation is successful at the melting point or at temperatures higher than the melting point of the carboxylic acid.

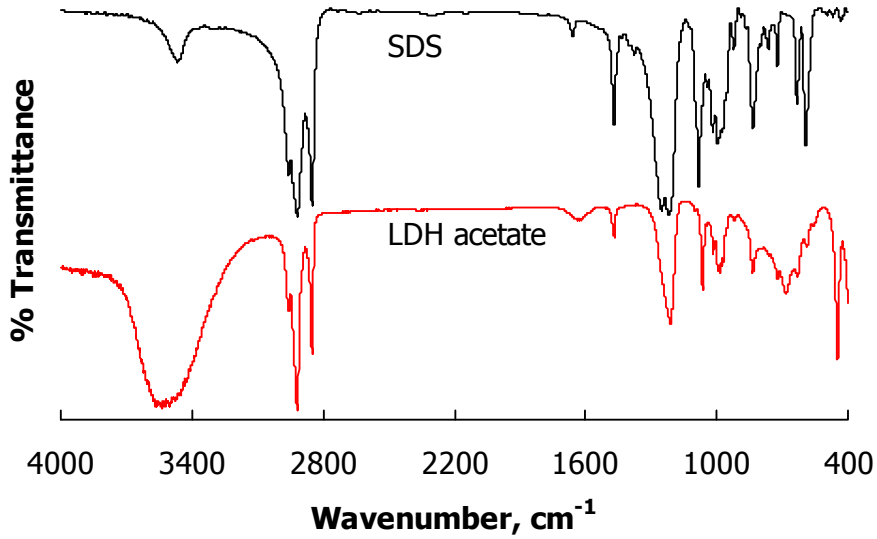

Figure 23: FT-IR spectra of LDH-acetate obtained at room temperature in comparison with the surfactant SDS

4.7 Effect of Reaction Temperature on Carboxylate Anion Intercalation

The effect of reaction temperature on the degree of intercalation for lauric and stearic acid is shown in Figure 24. The current method results in an incomplete reaction at temperatures below the melting point of the carboxylic acid, i.e. below 60 and 53 °C for stearic and lauric acid respectively. However, Itoh *et al.* (2003) and Kanoh *et al.* (1999) reported the intercalation of water-soluble sodium stearate at temperatures as low as 5 °C. The apparent degrees of intercalation exceeded the theoretical limit for intercalation at temperatures above 60 °C. This is attributed to the presence of sodium in the interlayers of LDH.

The results obtained by Kanoh *et al.* (1999) indicate that the structure of stearate intercalated LDH changes reversibly to form a monolayer or bilayer intercalated LDH structure, depending on the intercalation temperature. This was supported by the monolayer LDH-stearate structure obtained at lower temperatures for 1 AEC, and by the bilayer structures obtained at higher temperatures, above 70 °C. However, bilayer intercalated LDH was also formed at lower temperatures when excess sodium salts, 3 AEC, were used (Kanoh *et al.,* 1999). The calculated size of the stearate anion is 2.25 nm (Kanoh *et al.*, 1999). Anbarasan *et al.* (2008) reported monolayer intercalated LDH-stearate at 70 °C with a d-spacing of 2.67 nm. This result was obtained by dispersing LDH in water in the presence of stearic acid.

Bilayer and monolayer intercalated stearate anions in Zn-Si-LDH with interlayer spacings of 3.72 and 3.12 nm, and 3.71 and 2.89 nm for Zn-Sn-LDH, were reported for samples prepared by stirring at room temperature for 72 hours (Saber and Tagaya, 2003 a, 2003 b and 2007). Similar results were also obtained for myristate intercalated Zn/Si-LDH and Zn/Sn-LDH (Saber and Tagaya, 2007). Carlino and Hudson (1995) reported mono- and bilayer caprate and sebaccate intercalated LDH obtained using coprecipitation and the thermal reaction method at 150 °C.

The present results suggest only a bilayer intercalated carboxylic acid LDH structure. Inomata and Ogawa (2006) obtained bilayer stearate and oleate intercalated LDH at room temperature and at 60 °C using the rehydration method under hydrothermal conditions. However, the results showed incomplete reaction, indicating that a prolonged period of heating was required at room temperature and at 60 °C. Temperature proves to be the most important parameter to control in order to obtain highly crystalline LDH intercalates. It therefore appears that the packing of the chains in the interlayers of LDH depends on the route taken to prepare the LDH intercalates. This observation is based on the different results obtained by different authors at different temperatures.

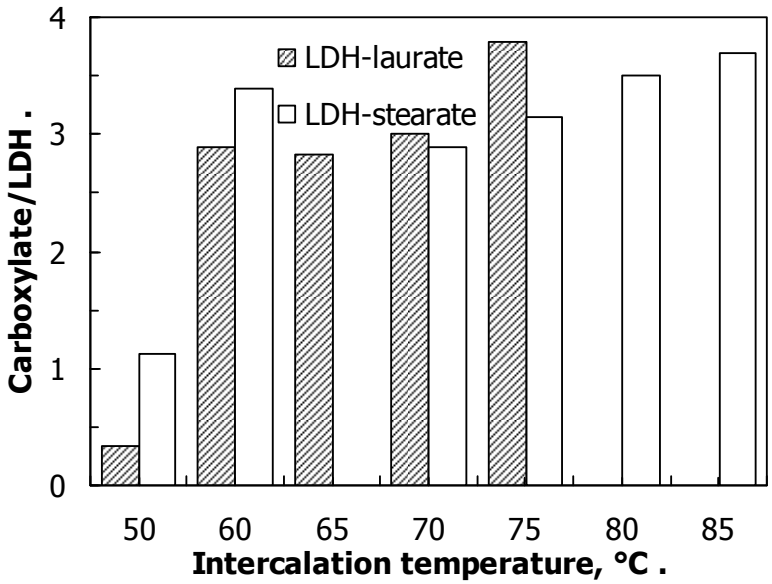

Figure 24: Effect of reaction temperature on the degree of lauric and stearic acid intercalation

4.8 Differential Scanning Calorimetry (DSC)

Figure 25 shows the DSC melting endotherms for pure and technical-grade stearic acid, magnesium stearate and LDH stearate synthesised using SDS. The technical-grade stearic acid shows a low melting enthalpy compared with the 99% grade because it contains significant amounts of palmitic acid, as shown in Table 7. The technical-grade stearic acid was used in the preparation of LDH-stearate. This compound shows two endotherms: the one centred at ca. 107 °C corresponds to the dominant endothermic event. The main endotherm is positioned at about 50 °C higher than the parent stearic acid. These reflect the effect of the two-dimensional constraints imposed by the rigid inorganic sheet on the stearate bilayers. The magnesium stearate shows the highest melting range. Its melting enthalpy is higher than that observed for the stearic acids, but lower than that observed for LDH-stearate. In this compound all the stearic acid radicals are fully ionised and directly co-ordinated to the magnesium atoms in an octahedral site (Vold and Hattiangdi, 1949; Bracconi *et al.,* 2003). In contrast, in LDH stearate only a portion of the stearic acid molecules in the LDH galleries are expected to be ionised.

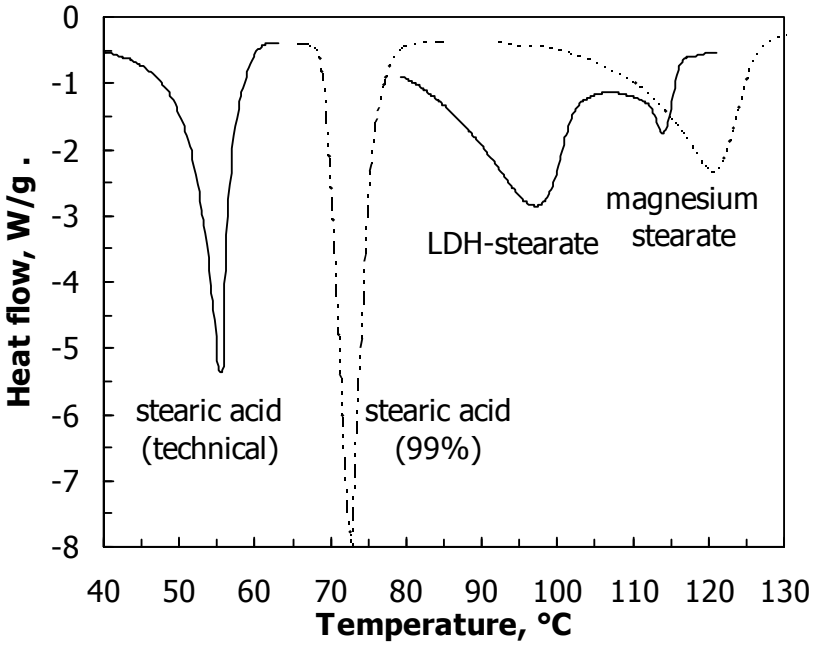

Figure 25: DSC melting endotherms for technical-grade stearic acid, pure stearic acid (99%), LDH-stearate prepared at 80 °C using SDS and magnesium stearate. The measured enthalpies were -185, -221, -241 and -173 kJ/kg respectively

Table 7: Differential scanning calorimetry (DSC) results for selected compounds

Compound	**Stearic acid (technical grade)**	**Stearic acid (99% pure)**	**LDH-stearate (SDS)**	**Magnesium stearate**
Endotherm peak, °C	55.6	72.8	107.2 & 117.8	121.0
Enthalpy, J/g	-158	-173	-241	-221

Figure 26 shows a hot-stage microscopic image at different temperatures and a DSC heating scan of the LDH-stearate prepared using Tween 60. The two melting endotherms are also observed, as in the sample prepared using SDS. However, in this case the second endotherm is more pronounced than that of LDH-stearate as shown in Figure 27. The crystals appear superficially intact at temperatures

exceeding the second endothermic peak. At 140 °C both the LDH-stearate samples are fully molten.

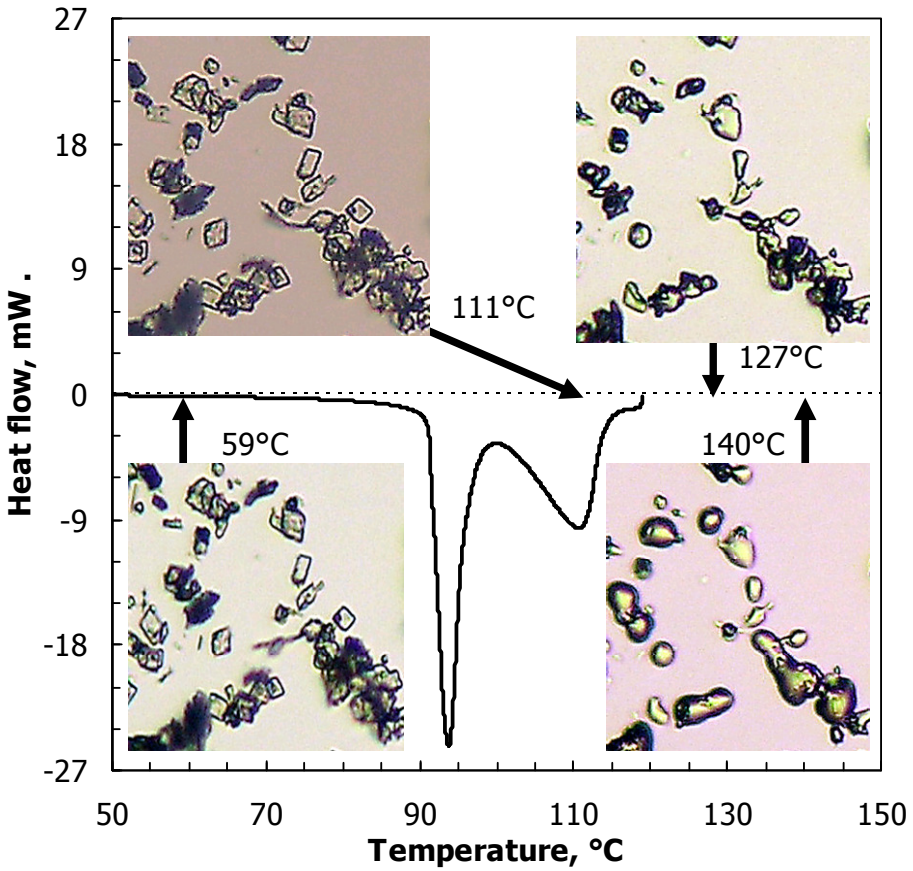

Figure 26: DSC melting endotherm and hot-stage microscopic image of LDH-stearate prepared at 80 °C using Tween 60

The same behaviour is observed with LDH-stearate (SDS). Figure 27 shows a microscopic image of LDH-stearate (SDS) at 100 to 170 °C. The sample starts to melt at 136 °C and at 170 °C it is fully molten. Inomata and Ogawa (2006) obtained an endotherm and a shoulder at 78 and 87 °C respectively for LDH-stearate. This behaviour was reversible since on cooling these peaks were observed at lower temperatures, namely 66 and 74 °C. In contrast, in the present data no recrystallisation was observed when cooling to lower temperatures. The observed thermal behaviour is non-reversible. In this case the presence of the interlayer recrystallisation water may be required for recrystallisation.

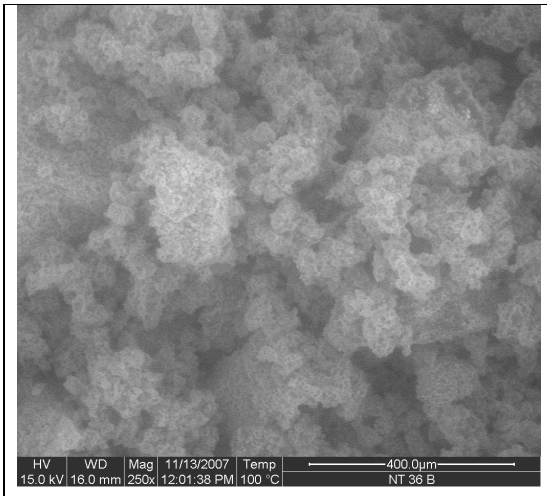

LDH-stearate (SDS) 100 °C

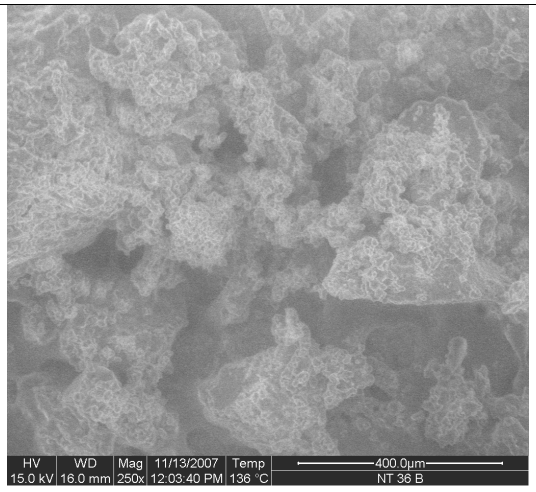

LDH-stearate (SDS) 136 °C

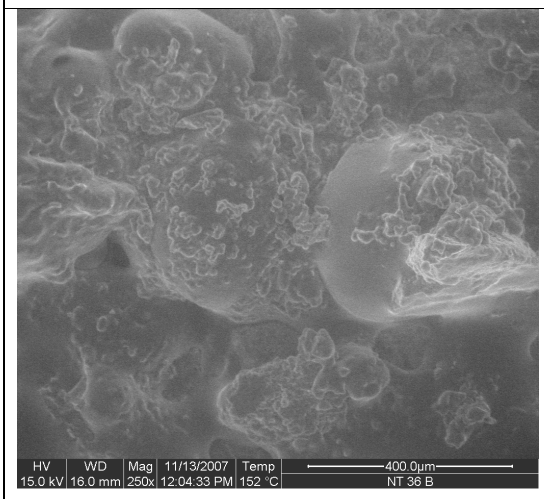

LDH-stearate (SDS) 152 °C

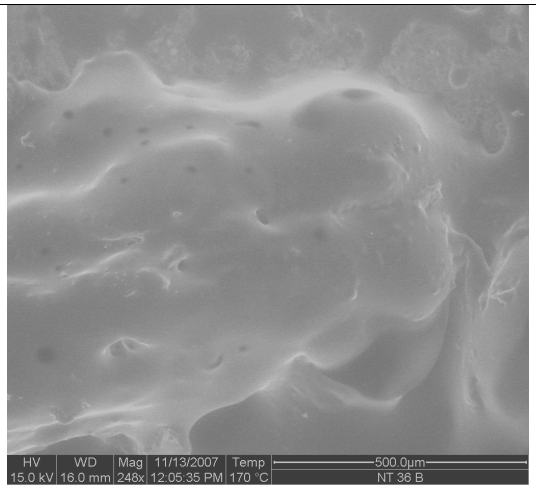

LDH-stearate (SDS) 170 °C

Figure 27: Microscopic images o f LDH-stearate (SDS) taken at 100, 136, 152 and 170 °C

Magnesium stearate shows an endothermic peak at 121 °C and LDH-stearate at 117.8 °C, as seen in Figures 25 and 26. Due to the close similarities between these two samples, it could be suggested that the LDH stearate contains magnesium stearate.

In order to check whether or not the LDH-stearate sample contains magnesium stearate, a mixture of the two was prepared at 80 °C. Figure 28 compares the

XRD patterns obtained for LDH-stearate, the mixture of LDH-stearate and magnesium stearate, and magnesium stearate recrystallised in Tween 60.

Similar reflections are observed in the LDH-stearate and recrystallised magnesium stearate samples. However, the mixture of magnesium stearate and LDH-stearate shows completely different reflections. Two twin reflection peaks are observed, indicating the presence of two different phases. These double diffraction peaks are observed at 2θ = 4.39, 4.37° and 6.54, 6.22° respectively. However, none of these peaks is observed in the LDH-stearate sample and the recrystallised magnesium stearate sample. This polyphasic XRD pattern proves that LDH-stearate is not a mixture with magnesium stearate. Thus, it is a stearate intercalated LDH.

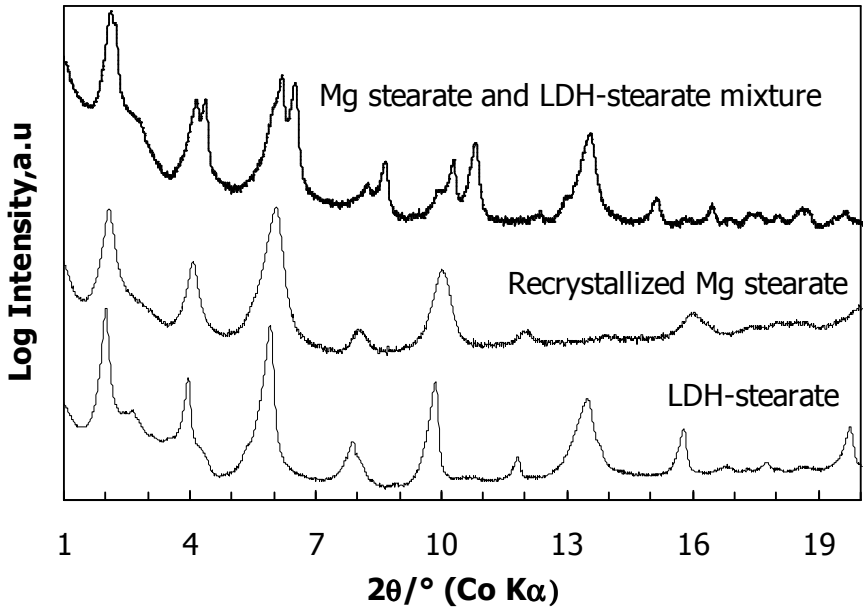

Figure 28: XRD pattern of LDH-stearate in comparison with the mixture of stearate-LDH and magnesium stearate

Figure 29 shows the DSC curve for LDH-stearate prepared at 80 °C using SDS. Only one endothermic peak and a shoulder are observed. The main endotherm is centred at 91 °C and there is a shoulder at 102 °C. Similarly to LDH-stearate, non-reversible thermal behaviour is also observed in this case. No recrystallisation

is observed on cooling. The theoretical melting point of lauric acid is 53 °C, which is lower than that observed for LDH-laurate.

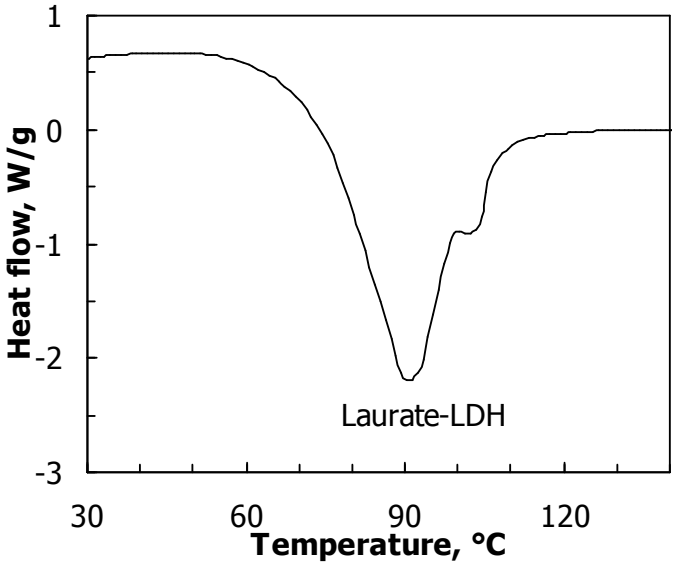

Figure 29: DSC curve for LDH-laurate prepared at 80°C using SDS

4.9 Temperature-scanned XRD

Figures 30 to 32 show the XRD spectra of stearate-LDH (Tween 60) and stearate-LDH (SDS) as a function of temperature. There is a notable shift in the diffraction peak positions at temperatures above ca. 85 °C. This is an indication of a phase change. The first observed shift coincides with the onset of the first melting endotherm observed in the DSC scans in Figures 30 and 31. The observed phase change is associated with a decrease in the LDH d-spacing from ca. 5.1 nm to about 4.7 nm and at the same time there is an increase in the separation between the alkyl chains from 0.406 nm (2θ = 25.42°) to about 0.425 nm (2θ = 24.6°). This change in peak positions results in a peak broadening, which suggests a transition towards disorder. This is due to the loss of water and melting of the intercalated chains. This behaviour is non-reversible and coincides with the results obtained on DSC.

Figure 32 indicates that the layer starts to contract above 85 °C. Above 135 °C the material becomes amorphous, possibly due to reaction between the free carboxylates and the magnesium and aluminium hydroxide groups. Borja and Dutta (1992) attributed this disordering behaviour of the bimolecular film to the formation of kinks and gauge blocks in the alkyl chains. However, the LDH-CO_3 impurity peak remains visible and only disappears slowly at higher temperatures.

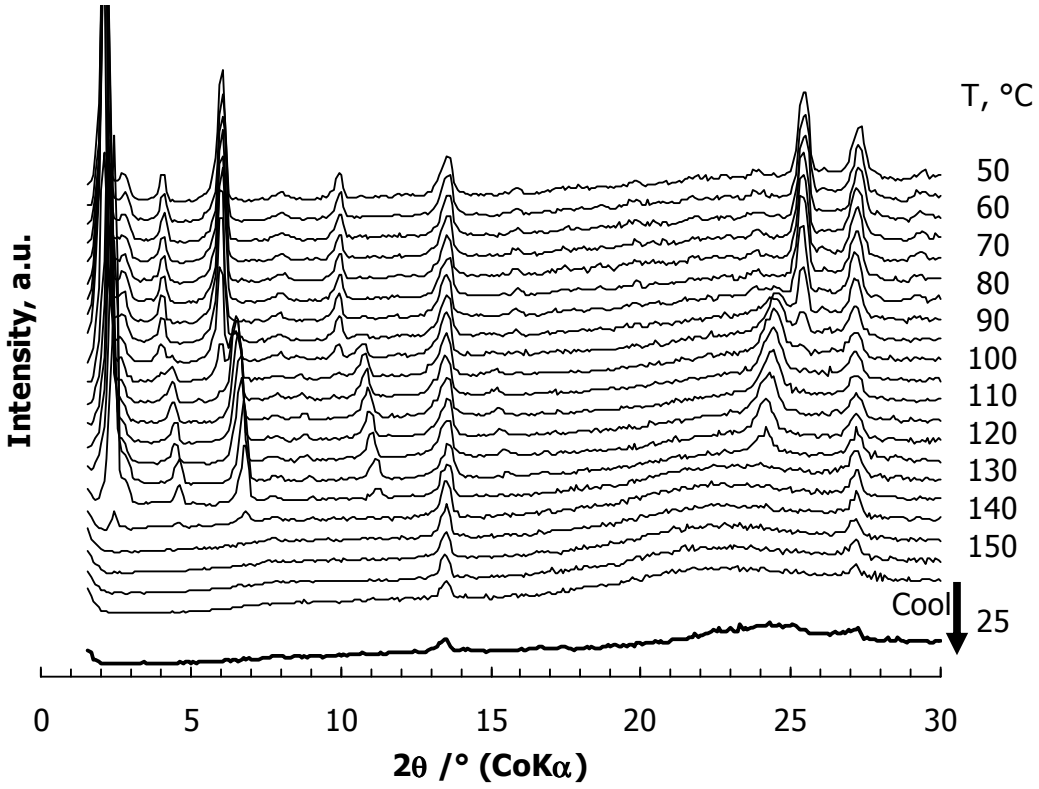

Figure 30: Effect of temperature on the X-ray diffraction spectra of LDH-stearate synthesised at 80 °C using Tween 60 (scans taken at 5 °C/min intervals**)**

The effect of temperature on the corresponding peak intensities for stearate-LDH (SDS) is shown in Figure 31. This confirms that the onset temperature for the transition is at ca. 85 °C and disappears at ca. 125 °C.

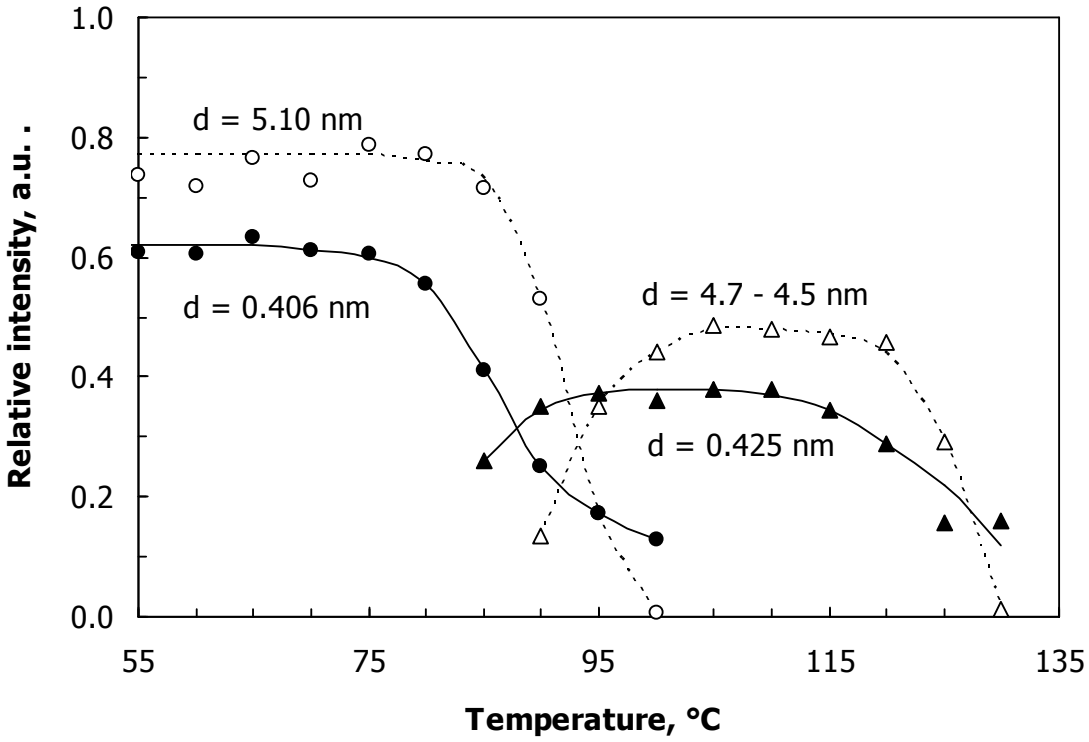

Figure 31: Effect of temperature on the intensity of the selected X-ray diffraction peaks of LDH-stearate (SDS) (scans taken at 5 °C/min intervals)

Recovery of this material is possible when the upper temperature to which the sample is heated is limited to 100 °C and it is subsequently cooled down to 30 °C, as shown in Figure 32. In contrast, Inomata and Ogawa (2006) reported a reversible behaviour of the stearate-LDH by *in situ* XRD in the temperature range 16 to 140 °C. The original d-spacings were also recovered on cooling.

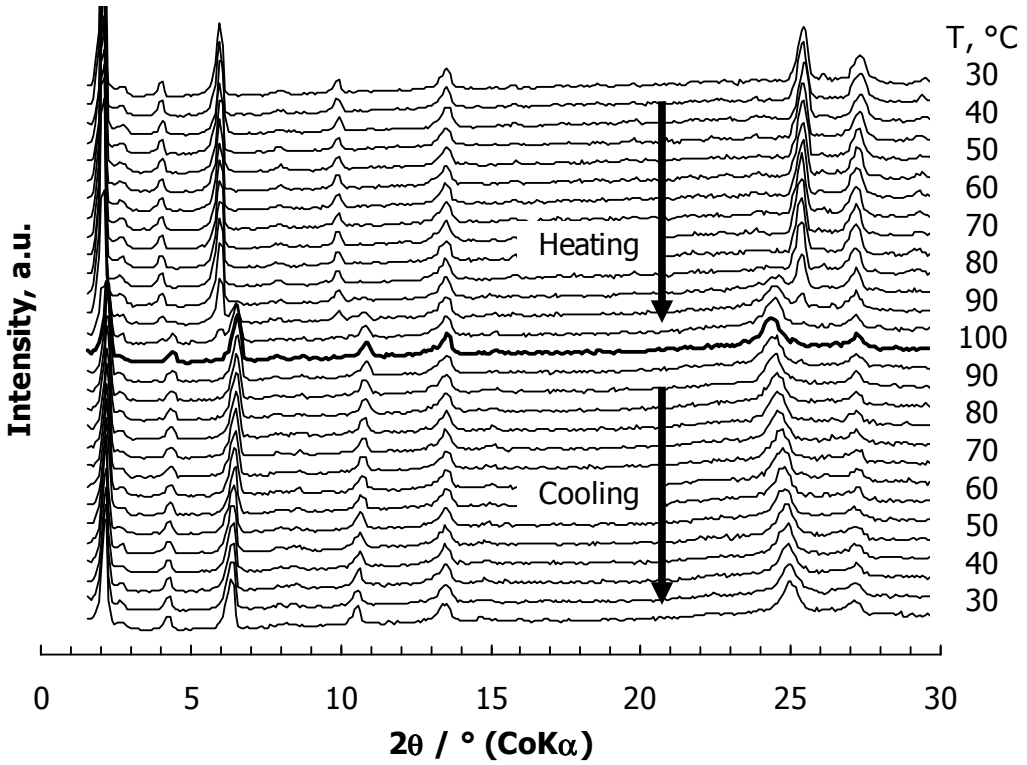

Figure 32: Changes in the X-ray diffraction spectra on heating LDH-stearate (SDS) to 100 °C and cooling it to 30 °C (scans taken at 5 °C/min intervals)

Similar behaviour is observed in the LDH-laurate sample shown in Figure 33. In this case the phase transition starts at ca. 65 to 95 °C. This result coincides with the DSC results given in Figure 29, which show the melt endotherm at ca. 97 °C. In this case the LDH layers start to contract in this range. At temperatures above 95 °C, the amorphous phase starts to form. The diffraction peak in plane d_{003} broadens at 115 °C, indicating the phase change to amorphous. However, the LDH impurity peaks remain unchanged.

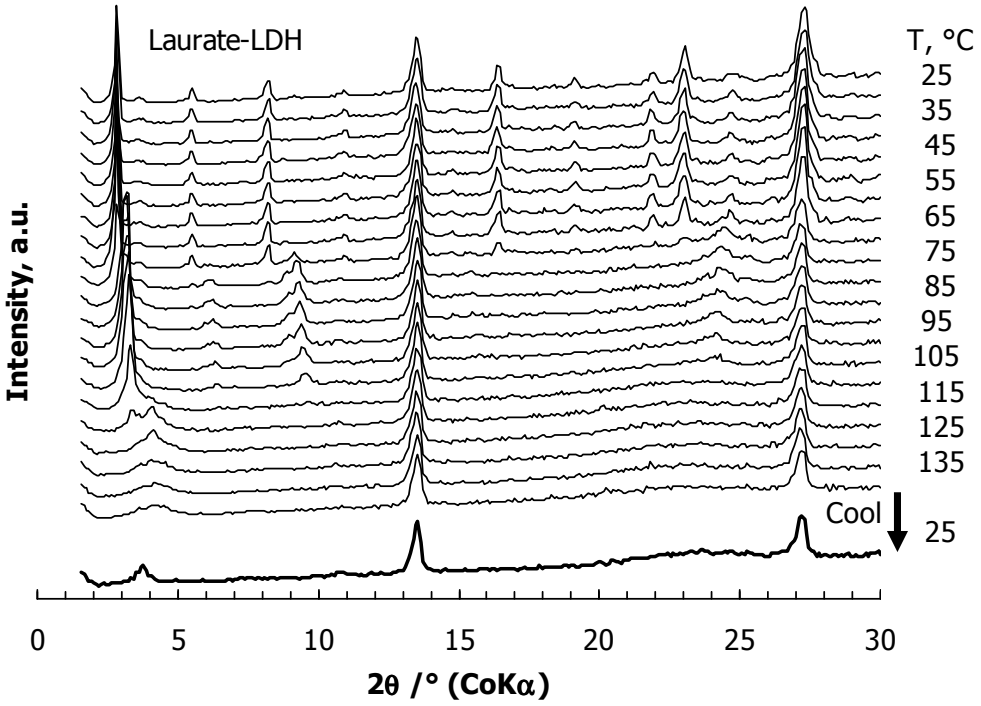

Figure 33: Changes in X-ray diffraction spectra of LDH-laurate on heating to 135 °C and cooling to ambient (scans taken at 5 °C/min intervals)

4.10 Particle Morphology

Figure 34 shows SEM images of pure fatty acid intercalated LDH in comparison with LDH-CO_3. The LDH-CO_3 consisted of numerous smaller crystals inter-grown in a 'sandrose' arrangement, as shown in Figure 34(a) (Adachi-Pagano *et al.,* 2000). After the reaction with stearic acid (as shown in Figure 28 b), this structure was replaced by the low-aspect-ratio flakes which were significantly larger – as much as 20 µm across. The change in crystal size morphology indicates that the intercalation was accompanied by a recrystallisation process. The stearate-LDH crystals are larger than those of the precursor before (Figure 34 b) and after (Figure 36 c) extraction with ethanol.

Dimotakis and Pinnavaia (1990) reported that intercalation occurs in a topotactic manner. In contrast, the present reactions did not proceed in a topotactic manner. This is an expected behaviour considering that the stearate monolayers provide a template for Mg-Al-LDH growth (He *et al.,* 2004). Well-defined crystal morphology

is obtained in stearate-LDH (Tween 60). However, flaky rod-like crystal morphology is obtained for LDH-laurate. The reason for this is not well understood. The other fatty acid intercalated-LDH SEM images are shown in Appendix E.

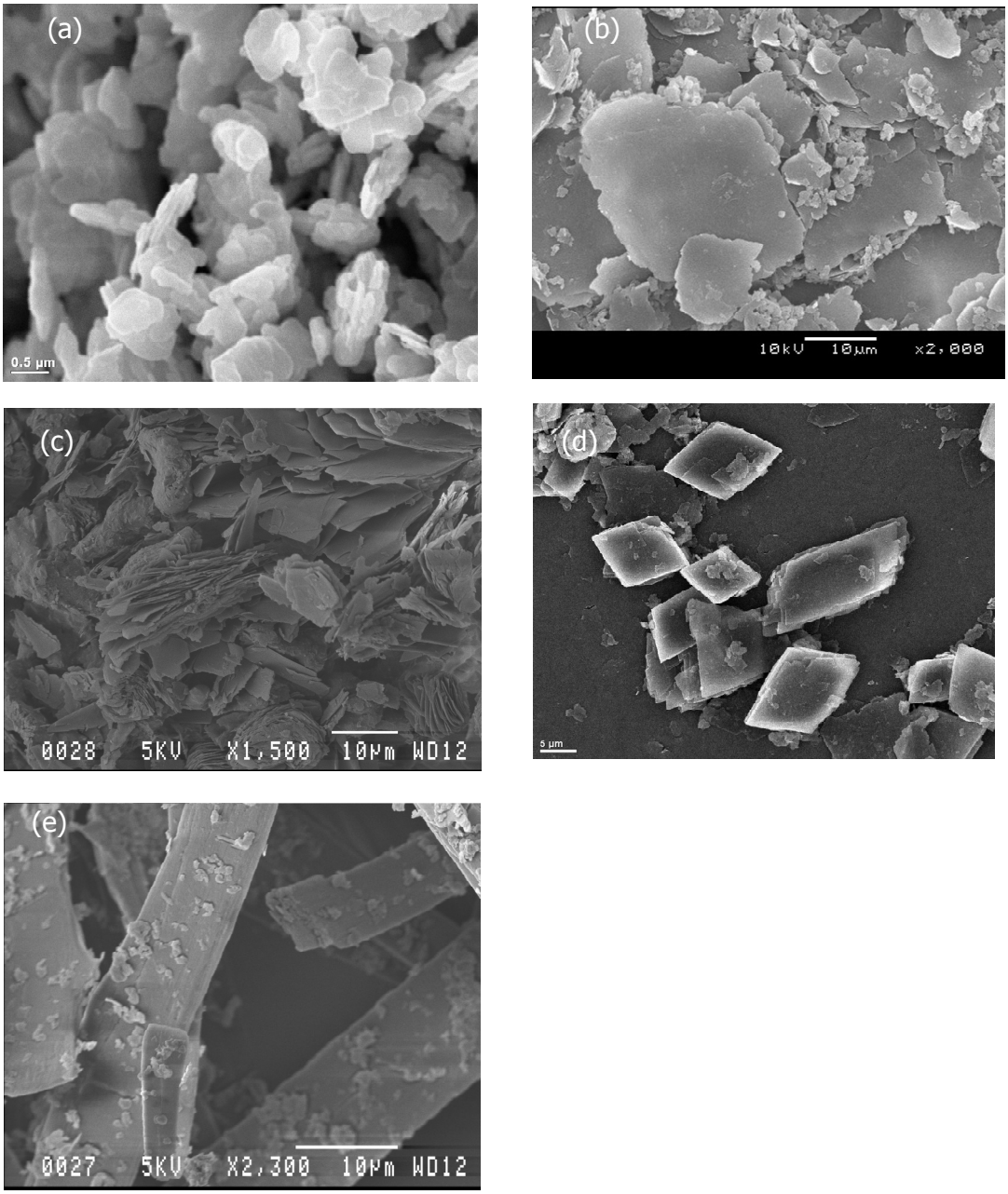

Figure 34: SEM images showing: (a) the 'sandrose' morphology of LDH-CO_3 crystals; (b) the flake-like habit of LDH-stearate (SDS); (c) the delamination of the LDH-stearate crystals after extraction with ethanol; (d) the LDH-stearate crystals obtained with Tween 60; and (e) the LDH-laurate crystals

5 CONCLUSION

Molten carboxylic acid reacts with LDH-CO_3 when dispersed in an aqueous medium under atmospheric conditions to form a bilayer intercalated LDH. The interlayer carbonate anions can be easily replaced by the carboxylate anions in the LDH galleries. The greater stability of the bilayer intercalated LDH-stearate compared with LDH-CO_3 arises from the stabilising effect of the hydrophobic interactions between the chains (Choy *et al.,* 1999; Takagi *et al.,* 1993).

The carboxylate anions are intercalated in different forms, as evident from FT-IR. The stearate and behenate anions exist in the forms –RCOOH and –$RCOO^-$ in between the brucite-like LDH sheets. This is evident from the absorption peaks at 1558, 1536 and 1538 cm^{-1} for both samples (Borja and Dutta, 1992). However, in the LDH-octanoate, laurate and myristate samples only the ionised carboxylate form is present, as evident by the FT-IR absorption bands at 1559, 1558, and 1555 cm^{-1} respectively. The close agreement between the XRD and FT-IR analyses of the present results and those previously obtained (Borja and Dutta, 1992; Kanoh *et al.,* 1999) suggests successful carboxylate intercalation.

The addition of an anionic surfactant (SDS) positively influenced the intercalation process. It acts as a dispersant for the LDH-CO_3 particles and keeps the unreacted stearic acid in emulsion, thereby facilitating its removal from the final product. The purer carboxylate intercalated LDH is obtained with less mixing and purification effort, as is evident from the sharp diffraction peaks obtained in the XRD results.

The method works well with long-chain carboxylic acids, i.e. C12 to C22. However, at low reaction temperatures with short-chain carboxylic acids – C2, C4, C6 and C10 – the LDH layers preferred to intercalate the anionic surfactant instead of the desired carboxylate anion. Kanoh *et al.* (1999) attributed this to the hydrophobicity of the sodium salts used in the attempt to intercalate these anions at low temperatures. In contrast, the present method employs neat acids and even octanoic acid was intercalated as a bilayer with ease. Temperature is

therefore the most important parameter to control during the intercalation process. In the present method the intercalation was successful at temperatures higher than the melting point of the carboxylic acids. Bilayer intercalated LDH products were previously obtained by exchanging the Cl^- in LDH-Cl with fatty acids in ethanol and with sodium carboxylates in aqueous media (Borja and Dutta 1992; Kanoh *et al.,* 1999). Inomata and Ogawa (2006) also obtained bilayer intercalated LDH-stearate using the reconstruction method. In the present method all the carboxylate anions (laurate, myristate, stearate and LDH-behenate) were intercalated as bilayers.

The surfactant-mediated intercalation method is an environmentally friendly option compared with the methods reported in the literature. The anionic surfactant (SDS) solution should be recyclable and no volatile or flammable organic solvents are necessary to free the product from the excess stearic acid. However, XRF analysis reveals that the use of SDS also leads to sodium carboxylate in addition to the carboxylic acid forms. This problem can be avoided by replacing SDS with a non-ionic surfactant, such as Tween 60.

The LDH carboxylate intercalates obtained with either surfactant showed similar thermal behaviours. Specifically, two phase transitions are observed at elevated temperatures. At temperatures that are higher than the melting point of the corresponding free acids, the alkyl chains assume a disordered liquid-like state within the clay galleries. In addition, an increase in temperature results in a decrease in the interlayer spacing. This state is reversible to some extent. However, at even higher temperatures, the material becomes completely amorphous and behaves like a true melt. Cooling does not lead to the recovery of the well-ordered crystalline state. Inomata and Ogawa (2006) reported a reversible thermal behaviour of LDH-stearate.

The effects of temperature on the material properties of intercalated LDH are very important when the materials are to be used in polymeric materials. This is because the degree of dispersion is very important and depends on the

intermolecular interaction between the polymer and the modified clay surface. This has an influence on the performance of the final material (Inomata and Ogawa, 2006). The temperature effects on the properties of LDH-carboxylate obtained in the present method have two important implications. First, it appears that, once the LDH-carboxylate is fully molten, the presence of interlayer water may be required for recrystallisation. Secondly, exfoliation is the main requirement for conventional polymer melt-blending. However, exfoliation of stearate intercalated LDH is unlikely to proceed when conventional melt-blending techniques are used because this sample melts below typical polymer processing temperatures. Furthermore, crystals are only stable if they form a stacking structure of at least 20 sheets (He *et al.,* 2002).

6 REFERENCES

Adachi-Pagano, M., Forano, C. and Besse, J.-P. (2000). Delamination of layered double hydroxides by use of surfactants. *Chem. Commun*. 91-92.

Adachi-Pagano, M., Forano, C. and Besse, J-P. (2003). Synthesis of Al-rich hydrotalcite-like compounds by using the urea hydrolysis reaction-control of size and morphology. *J. Mater. Chem.* 13: 1988–1993.

Aisawa, S., Higashiyama, N., Takahashi, S., Hirahara, H., Ikematsu, D., Kondo, H., Nakayama, H. and Narita, E. (2007). Intercalation behaviour of L-ascorbic acid into layered double hydroxides, *Appl. Clay Sci.* 35: 146–154.

Aisawa, S., Sasaki, S., Takahashi, S., Hirahara, H., Nakayama, H. and Narita, E. (2006). Intercalation of amino acids and oligopeptides into Zn–Al layered double hydroxide by coprecipitation reaction. *J. Phys. Chem. Solids* 67: 920–925.

Allada, R.K., Navrotski, A., Berbeco, H.T. and Casey, W.H. (2002). Thermochemistry and aqueous solubilities of hydrotalcite-like solids. *Science* 296: 721-726.

Allmann, R. (1968). The crystal structure of pyroaurite. *Acta Cryst*. 24: 972-977.

Allmann, R. (1970). Lattice parameter of the hexagonal subcell that contains two OH groups. *Chimia* 24: 99-108.

Ambrogi, V., Fardella, G., Grandolini, G., Perioli, L. and Tiralti, M.C. (2002). Intercalation compounds of hydrotalcite-like anion clays with anti-inflammatory agents II: Uptake of dichlofenac for a controlled release formulation. *AAPS Pharm. Sci. Tech.* 3: Article 26. (http://www.aapspharmsci.org).

Anbarasan, R., Lee, W. and Im, S.S. (2008). Modification of nano-sized layered double hydroxides by long-chain organic aliphatic surfactants. *J. Serb. Chem. Soc.* 73: 321-331.

Anbarasan, R., Lee, W. D. and Im, S. S. (2005). Adsorption and intercalation of anionic surfactants onto layered double hydroxides-XRD study. *Bull. Mater. Sci.* 28: 145–149.

Anselim, C., Centini, M., Rossi, C., Ricci, M., Rastrelli, A., Andreassi, M., Buonocore, A. and La Rosa, C. (2002). New microencapsulated sunscreens: technology and comparative evaluation. *Int. J. Pharm.* 242: 207-211.

Aramendia, M.A., Avilés, Y., Borau, V., Luque, J.M., Marinas, J.M., Ruiz, J.R. and Urbano, F.J. (1999). Thermal decomposition of Mg/Al and Mg/Ga layered-double hydroxides: A spectroscopic study. *J. Mater. Chem.* 9: 1603-1607.

Aramendía, M.A., Borau, V., Jiménez, C., Marinas, J.M., Ruiz, J.R. and Urbano, F.J. (2002). Comparative study of Mg/M(III) (M=Al, Ga, In) layered double hydroxides obtained by coprecipitation and the sol-gel method. *J. Solid State Chem*. 168: 156-161.

Auerbach, S.M., Carrado, A.C. and Dutta, P.K. (2004). *Handbook of Layered Materials*. New York: Taylor and Francis Group.

Baron, M., Fox, R.B., He, J., Hess, M., Horie, K., Kahovec, J., Kitayama, J., Kubisa, P., Maréchal, E., Mormann, W., Swift, G., Vohlídal, J. and Work, W.J. (2001). Definition of Terms Relating to Reactions and to Fundamental Polymeric Materials. *IUPAC Working Group IV-1, Macromolecular Nomenclature Commission,* Project 34/99, Draft 9.

Bar-on, P. and Nadiv, S. (1988). The effect of raw material type on the characteristics of Mg-Al double hydroxides synthesised by hydrothermal method. *Thermochim. Acta* 133: 119-124.

Beaudot, P., De Roy, M.E. and Besse, J.P. (2001). Intercalation of platinum complex in LDH compounds. *J Solid State Chem*. 161: 332-340

Bellotto, M., Rebours, B., Clause, O. and Lynch, J. (1996). A reexamination of hydrotalcite crystal chemistry. *J. Phys. Chem.* 100: 8527-8524.

Bergaya, F.A. (2008). Layered clay minerals. Basic research and innovative composite applications. *Microporous and Mesoporous Materials* 107: 141–148.

Boclair, J.W. and Braterman, P.S. (1999a) Layered double hydroxide stability. 1. Relative stabilities of layered double hydroxides and their simple counterparts. *Chem. Mater.* 11: 298-302.

Boclair, J.W., Braterman, P.S., Jiang, J., Lou, S. and Yarberry, F. (1999b). Layered double hydroxide stability. 2. Formation of Cr(III)-containing layered double hydroxides directly from solution. *Chem. Mater.* 11:303-307.

Bontchev, R.P., Liu, S., Krumhansl, J.L., Voigt, J. and Nenoff, T.M. (2003). Synthesis, characterization, and ion exchange properties of hydrotalcite $Mg_6Al_2(OH)_{16}(A)_x(A')_{2-x}$ $4H_2O$ (A, A') Cl^-, Br^-, I^-, and NO_3^-, $2 \geq x \geq 0$) derivatives. *Chem. Mater*. 15: 3669-3675.

Borja, M. and Dutta, K. (1992). Fatty acids in layered metal hydroxides: Membrane-like structure and dynamics. *J. Phys. Chem*. 96: 5434-5444.

Bracconi P., Andres, C. and Ndiaye, A. (2003). Structural properties of magnesium stearate pseudopolymorphs: Effect of temperature. *Int. J. Pharm.* 262: 109-124.

Brindley, G.W. and Kikkawa S. (1979). A crystal-chemical study of Mg, Al and Ni, Al hydroxyl-perchlorates and hydroxyl-carbonates. *Am. Mineral*. 64: 836-843.

Bujdák, J. (2006). Effect of the layer charge of clay minerals on optical properties of organic dyes. A review. *Appl. Clay Sci.* 34: 58–73.

Carlino S. and Hudson, M.J. (1995). Thermal intercalation of layered double hydroxides: Capric acid into an Mg-Al LDH. *J. Mater. Chem*. 5: 1433-1442.

Carlino, S. (1997). The intercalation of carboxylic acids into layered double hydroxides: A critical evaluation and review of different methods. *Solid State Ionics* 98: 73-84.

Carlino, S. and Hudson, M.J. (1994). Reaction of molten sebacic acid with a layered (Mg/Al) double hydroxide. *J. Mater. Chem*. 4: 99-104.

Carlino, S., Hudson, M.J., Husain, S.W. and Knowles, J.A. (1996).The reaction of molten phenylphosphonic acid with a layered double hydroxide and its calcined oxide. *Solid State Ionics* 84: 117-129.

Carrado, K.A. and Kostapapas, A. (1988). Layered double hydroxides (LDHs). *Solid State Ionics* 26: 77-86.

Carrasco, N., Kretzschmar, R., Pesch, M.-L. and Kraemer, S. M. (2008). Effects of anionic surfactants on ligand-promoted dissolution of iron and aluminum hydroxides. *J. Colloid Interface Sci.* 321: 279-287.

Cavani, F., Trifirò, F. and Vaccari, A. (1991). Hydrotalcite-type anionic clays: Preparation, properties and applications. *Catal. Today.* 11: 173-301.

Chang, Z., Evans, D., Duan, X., Boutinaud, P., De Roy, M. and Forano, C. (2006). Preparation and characterization of rare earth-containing layered double hydroxides. *J. Phys. Chem. Solids* 67: 1054–1057.

Charles, M.E. (1988). *Compositional Analysis by Thermogravimetry.* American Society for Testing and Materials, Baltimore, p 291.

Chibwe, K. and Jones, W. (1989). Intercalation of organic and inorganic anions into layered double hydroxide *J. Chem. Soc. Chem. Commun.* : 926-927.

Choudhary, V.R., Indurkar, J.R., Narkhede, V.S. and. Jha, R. (2004). MnO_4^{-1} exchanged Mg-Al hydrotalcite: A stable and reusable/environmentally-friendly catalyst for selective oxidation by oxygen of ethylbenzene to acetophenone and diphenylmethane to benzophenone. *J. Catal.* 227: 257-261.

Choy, J.-H. (2004). Intercalative route to heterostructured nanohybrid. *J. Phys. Chem. Solids* 65: 373–383.

Choy J.-H., Choi, S.-J. Oh, J.-M. and Park, T. (2007). Clay minerals and layered double hydroxides for novel biological applications. *Appl. Clay. Sci.* 36: 122-132.

Choy, J.-H., Kwak, S.-Y., Park, J.-S., Jeong, Y.-J. and Portier, J. (1999). Intercalative nanohybrids of nucleoside monophosphates and DNA in layered metal hydroxide. *J. Am. Chem. Soc.* 121: 1399-1400.

Costa, F.R., Leuteritz, A., Wagenknecht, U., Jehnichen, D., Häußler, L. and Heinrich, G. (2008). Intercalation of Mg–Al layered double hydroxide by anionic surfactants: Preparation and characterization. *Appl. Clay Sci.* 38: 153-164.

Costantino, U., Coletti, N. and Nocchetti, M. (1999). Anion exchange of methyl orange into Zn-Al synthetic hydrotalcite and photophysical characterization of the intercalates obtained. *Langmuir* 15: 4454-4460.

Costantino, U., Ambrogi, V., Nocchetti, M. and Perioli, L. (2007). Hydrotalcite-like compounds: Versatile layered hosts of molecular anions with biological activity. *Microporous and Mesoporous Materials* (Article in press).

Costantino, U., Marmottini, F., Nocchetti, M. and Vivani, R. (1998). New synthetic routes to hydrotalcite-like compounds: Characterisation and properties of the obtained materials. *Eur. J. Inorg. Chem.* 10: 1439-1446.

Costantino, V.R.L. and Pinnavaia, T.J. (1995). Basic properties of $Mg^{2+}_{1-x}Al^{3+}_{x}$ layered double hydroxides intercalated by carbonate, hydroxide, chloride and sulfate anions. *Inorg. Chem.* 34: 883-892.

Crepaldi, E.L., Pavan, P.C. and Valim, J.B. (1999). A new method of intercalation by anion exchange in layered double hydroxides. *Chem. Commun.* 155-156.

Crepaldi, E.L., Tronto, J., Cardoso, L.P. and Valim, J.B. (2002). Sorption of terephalate anions by calcined and uncalcined hydrotalcite-like compounds. *Colloids Surf. A* 211:103-114.

Das, N.N., Konar, J., Mohanta, M.K. and Srivastava, S.C. (2004). Adsorption of Cr(VI) and Se(IV) from their aqueous solutions onto Zr^{4+} substituted ZnAl/MgAl-layered double hydroxides: Effect of Zr^{4+} substitution in the layer. *J. Coll. Int. Sci.* 270: 1–8.

Del Arco, M., Gutiérrez, S., Martín, C. and Rives, V. (2003). Intercalation of $[Cr(C_2O_4)_3]^{3-}$ complex in Mg,Al layered double hydroxides. *Inorg. Chem*. 42: 4232-4240.

Dimotakis, E.D. and Pinnavaia, T.J. (1990). New route to layered double hydroxides intercalated by organic anions: Precursors to polyoxometalate-pillared derivatives. *Inorg. Chem.* 29: 2393-2394.

Dong, B., Zhang, J., Zheng, L., Wang, S., Li, X. and Inoue, T. (2008). Salt-induced viscoelastic worm-like micelles formed in surface active ionic liquid aqueous solution. *J Colloid Interface Sci.* 319, 338–343.

Drezdzon, M.A. (1988). Synthesis of isopolymetalate-pillared hydrotalcite via organic-anion-pillared precursors. *Inorg. Chem*. 27: 4628-4632.

Dupin, J.-C., Martinez, H., Guimon, C., Dumitrio, E. and Fechete, I. (2004). Intercalation compounds of Mg-Al layered double hydroxides with dichlophenac: Different methods of preparation and physico-chemical characterization. *Appl. Clay Sci.* 27: 95-106.

Dutta, P.K and Robins, D.S. (1994). Interlayer dynamics of a fatty acid exchanged lithium aluminium layered double hydroxide monitored by IR spectroscopy and pyrene fluorescence. *Langmuir* 10: 4681-4687.

Evans, D.G. and Duan, X. (2006). Preparation of layered double hydroxides and their applications as additives in polymers, as precursors to magnetic materials and in biology and medicine. *Chem. Commun* : 485–496.

Feitknecht, W. (1942). Über die Bildung von Doppelhydroxyden zwischen zwei und dreiwertigen Metallen. *Helv. Chim. Acta* 25: 555-569.

Feitknecht, W. and Gerber, M. (1942). Zur Kenntnis der Doppelhydroxide und der basichen Doppelsalze. III. *Helv. Chim. Acta* 25: 131-137.

Feng, Y., Li, D. Wang, Y., Evans, D.G. and Duan, X. (2006). Synthesis and characterization of a UV absorbent-intercalated Zn-Al layered double hydroxide. *Polymer Degradation and Stability* 91: 789-794.

Fernández, J.M., Barriga, C., Ulibarri, M.A., Labajos, F.M. and Rives, V. (1997). New hydrotalcite-like compounds containing yttrium. *Chem. Mater.* 9: 312-318.

Fischer, H. (2003). Polymer nanocomposites: From fundamental research to specific applications. *Mater. Sci. Eng. C*. 23: 763-772.

Fogg, A.M., Dunn, J.S. and O'Hare, D. (1998). Formation of second-stage intermediates in anion-exchange intercalation reactions of the layered double hydroxide $[LiAl_2(OH)_6]Cl^{-}H_2O$ as observed by time-resolved, in situ X-ray diffraction. *Chem. Mater.* 10: 356-360.

Frost, R.L., Martens, W., Duong, L. and Kloprogge, J.T. (2002). Evidence for molecular assembly in hydrotalcites. *J. Mater. Sci. Lett.* 21: 1237-1239.

Frost, R.L., Martens, W., Duong, L. and Kloprogge, J.T. (2003a). Raman spectroscopy of some natural hydrotalcite with sulphate and carbonate in the interlayer. *J. Raman Spectroscop.* 34: 760-768.

Frost, R.L., Weier, M.L., Clissold, M.E. and Williams, P.A. (2003b). Infrared spectroscopic study of natural hydrotalcites carrboydite and hydrohonessite. *Spectrochimica Acta Part A* 59: 3313-3319.

Fudala, Á., Pálinkó, I. and Kiricsi, I. (1999). Preparation and characterization of hybrid organic-inorganic composite materials using the amphoteric property of amino acids: Amino acid intercalate layered double hydroxide and montmorillonite. *Inorg. Chem*. 38: 4653-4658.

Fujishiro, Y., Uchida, S. and Sato, T. (1999). Synthesis and photochemical properties of semiconductor pillared layered compounds. *Int. J. Inorg. Mater*. 1: 67-72.

Greenwell, H.C., Marsden, C.C. and Jones, W. (2007). Synthesis of organo-layered double hydroxides by an environmentally friendly co-hydration route. *Green Chem.* 9: 1299–1307.

Gunstone, F. (1996). *Fatty Acids and Lipid Chemistry*. First edition, London: Chapman and Hall, p 252.

Guo, Y., Li, D., Hu, C., Wang, Y. and Wang, E. (2001). Layered double hydroxides pillared by tungsten polyoxometalates: Synthesis and photocatalytic activity. *Int. J. Inorg. Mater.* 3: 347–355.

Gutmann, N.H.,. Spiccia, L. and Turney, T.W. (2000). Complexation of Cu(II) and Ni(II) by nitrilotriacetate intercalated in Zn-Cr layered double hydroxides. *J. Mater. Chem.* 10: 1219-1224.

Hansen, H.C.B. and Taylor, R.M. (1991). The use of glycerol intercalates in the exchange of carbonate with sulphate, nitrate or chloride in pyroaurite-type compounds. *Clay Miner.* 26: 311-327.

He, F.-A. and Zhang, L.-M. (2007). Organo-modified ZnAl layered double hydroxide as new catalyst support for the ethylene polymerization. *J. Colloid Interface Sci.* 315: 439–444.

He, J., Li, B., Evans, D.G. and Duan, X. (2004) Synthesis of layered double hydroxides in an emulsion solution. *Colloids and Surfaces A: Physicochem. Eng. Aspects* 251: 191–196.

Hibino, T., Yamashita, Y., Kosuge, K. and Tsunashima, A. (1995). Decarbonation behavior of Mg-Al-CO_3 hydrotalcite-like compounds during heat treatment. *Clays Clay Miner.* 43: 427-432.

Hibino, T. and Jones, W. (2001). New approach to the delamination of layered double hydroxides. *J. Mater. Chem.* 11: 1321-1323.

Hickey, L., Kloprogge, J.T. and Frost, R.L. (2000). The effects of various hydrothermal treatments on magnesium-aluminium hydrotalcites, *J. Mater. Chem*. 35: 4347-4355.

Hoffmann, H. and Ebert, G. (1988). Surfactants, micelles and pascinating phenomena. *Angew. Chem. Int. Ed. Engl.* 27: 902-912.

Hou, X., Bish, D.L., Wang S.-L., Johnston, C.T. and Kirkpatrick, R.J. (2003). Hydration, expansion, structure, and dynamics of layered double hydroxides. *Am. Mineral.* 88: 167-179.

Hussein, M.Z.B. and Long, C.W. (2004). Synthesis of organo-mineral nanohybrid material: Indole-2-carboxylate in the lamella of Zn–Al-layered double hydroxide. *Mater. Chem. Phys.* 85: 427–431.

Inomata, K. and Ogawa, M. (2006). Preparation and properties of Mg/Al layered double hydroxide-oleate and –stearate intercalation compounds. *Bull. Chem. Soc. Jpn.* 79: 336-342.

Intissar, M., Jumas, J.-C., Besse, J.-P. and Leroux, F. (2003). Reinvestigation of the layered double hydroxide containing tetravalent cations: Unambiguous response provided by XAS and Mössbauer spectroscopies. *Chem. Mater.* 15: 4625-4632.

Itoh, T., Ohta, N., Shichi, T., Yui, T. and Takagi, K. (2003). The self-assembling properties of stearate ions in hydrotalcite clay composites. *Langmuir.* 19: 9120-9126.

Iyi, N., Matsumoto, T., Kaneko, Y. and Kitamura, K. (2004). Deintercalation of carbonate ions from a hydrotalcite-like compound: Enhanced decarbonation using acid-salt mixed solution. *Chem. Mater.* 16: 2926-2932.

Jackrupca, M. and Dutta, P.K. (1995). Thermal and spectroscopic analysis of fatty acid layered double hydroxides and its application as a chromatographic stationery phase. *Chem. Mater.* 7: 989-994.

Kagunya, W.W., Dutta, P. K. and Lei, Z. (1997). Dynamics of water in hydrotalcite. *Physica B* 234-236: 910-913.

Kagunya, W.W. (1996). Properties of water adsorbed in anionic clays: A neutron scattering study. *J. Phys. Chem*. 100: 327-330.

Kameda, T., Yoshioka, T., Uchida, M., Miyano, T. and Okuwaki, A. (2002). New treatment method for dilute hydrochloric acid using magnesium-aluminium oxide. *Bull. Chem. Soc. Jpn.* 75: 595-599.

Kandare, E. and Hossenlopp, J.M. (2006). Thermal degradation of acetate-intercalated hydroxyl double and layered hydroxyl salts. *Inorg. Chem.* 45: 3766-3773.

Kaneyoshi, M. and Jones, W. (1998). Formation of Mg-Al layered double hydroxides intercalated with nitrilotriacetate anions. *J. Mater. Sci.* 9: 805-811.

Kanezaki, E. (1998). Thermal behavior of the hydrotalcite-like layered structure of Mg and Al-layered double hydroxides with interlayer carbonate by means of in situ powder HTXRD and DTA/TG. *Solid State Ionics* 106:279–284.

Kanoh, T., Shichi, T. and Takagi, K. (1999). Mono- and bilayer equilibria of stearate self-assembly formed in hydrotalcite interlayers by changing the intercalation temperature. *Chem. Lett*. 117-118.

Kelkar, C.P. and Schutz, A.A. (1997). Ni-, Mg- and Co-containing hydrotalcite-like materials with a sheet-like morphology: Synthesis and characterization. *Microporous Mater.* 10: 163-172.

Khan, A.I. and O'Hare, D. (2002). Intercalation chemistry of layered double hydroxides: Recent developments and applications. *J. Mater. Chem*. 12: 3191-3198.

Kloprogge, J.T. and Frost, R.L. (1999). Infrared emission spectroscopy study of the thermal transformation of Mg, Ni and Co hydrotalcite catalysts. *Appl. Catal. A.* 1814: 61-74.

Kooli F., Chisem, I.C., Vucelic, M. and Jones, W. (1996). Synthesis and properties of terephthalate and benzoate intercalates of Mg-Al layered double hydroxides possessing varying layer charges. *Chem. Mater*. 8: 1969-1977.

Kooli, F., Kosuge, K. and Tsunashima, A. (1995). Mg-Zn-Al-CO_3 and Zn-Cu-Al-CO_3 hydrotalcite-like compounds: Preparation and characterization. *J. Mater. Sci*. 30: 4591-4597.

Kukkadapu, R.K., Witkowski, M.S. and Amonette, J.E. (1997). Synthesis of a low-carbonate high-charge hydrotalcite-like compound at ambient pressure and atmosphere. *Chem. Mater.* 9: 417-419.

Labajos F.M., Rives, V. and Ulibarri, M.A. (1992). Effect of hydrothermal and thermal treatments on the physicochemical properties of Mg-Al hydrotalcite materials. *J. Mat Sci*. 27: 1546-1552.

Lange, K.R. (1999). *Surfactants: A Practical Handbook*. Munich: Hanser Publishers, p 237.

Lee, K., Nam, J.-H., Lee, J.H., Lee, Y., Cho, S.M., Jung, C.H., Choi, H.G., Chang, Y.-Y., Kwon, Y.-U. and Nam, J.-D. (2005). Methanol and proton transport control by using layered double hydroxide nanoplatelets for direct methanol fuel cell. *Electrochemistry Communications* 7: 113–118.

Leroux, F. and Besse, J.-P. (2001). Polymer interleaved layered double hydroxide: A new emerging class of nanocomposites. *Chem*. *Mater.* 13: 3507-3515.

Leroux, F. and Taviot-Guého, C. (2005). Fine tuning between organic and inorganic host structure: New trends in layered double hydroxide hybrid assemblies. *J. Mater. Sci.* 15: 3628-3642.

Leroux, F., Aranda, P., Besse, J.-P. and Ruiz-Hitzky, E. (2003). Intercalation of poly(ethylene oxide) derivatives into layered double hydroxides. *Eur. J. Inorg. Chem*. 1242-1251.

Lin, Y., Wang, J., Evans, D.G. and Li, D. (2006). Layered and intercalated hydrotalcite-like materials as thermal stabilizers in PVC resin. *J. Phys. Chem. Solids* 67: 998–1001.

Lopez, T. Ramos, E., Bosch, P., Asomoza, M. and Gomez, R. (1997). DTA and TGA characterization of sol-gel hydrotalcites. *Mater. Lett*. 30: 279-282.

Madejová, J. (2003). *Vibrational Spectroscopy* 31: *Review: FTIR Techniques in Clay Mineral Studies*. pp 1–10.

Malherbe, F. and Besse, J.-P. (2000). Investigating the effects of guest-host interactions on the properties of anion-exchanged Mg-Al hydrotalcites. *J. Solid State Chem.* 155: 332-341.

Markley, K.S. (1947). *Fatty acids: Their Chemistry and Physical Properties.* London: Interscience Publishers, p 668.

MacMurry, J. (2000). *Organic Chemistry*. Fifth edition, USA: Brooks/Cole, p 1284.

Meyn, M., Beneke, K. and Lagaly, G. (1990). Anion-exchange reactions of layered double hydroxides. *Inorg. Chem*. 29: 5201-5207.

Meyn, M., Beneke, K. and Lagaly, G. (1993). Anion-exchange reactions of hydroxy double salts. *Inorg. Chem.* 32: 1209-1215.

Miyata, S. (1975). The synthesis of hydrotalcite-like compounds and their structures and physico-chemical properties: The systems Mg^{2+}-Al^{3+}- SO_4^{2-} and Mg^{2+}-Al^{3+}- CrO_4^{2-}. *Clays Clay Miner*. 23: 369-375.

Miyata, S. and Kumura, T. (1973). Synthesis of new hydrotalcite-like compounds and their physico-chemical properties. *Chem. Lett.*: 843-848.

Miyata, S. and Okada, A. (1977). The synthesis of hydrotalcite-like compounds and their structures and physico-chemical properties: I. The systems Mg^{2+}-Al^{3+}- NO_3^-, Mg^{2+}-Al^{3+}- Cl^-, Mg^{2+}-Al^{3+}- ClO_4^-, Ni^{2+}-Al^{3+}- Cl^- and Zn^{2+}-Al^{3+}- Cl^-. *Clays Clay Miner*. 25: 14-18.

Miyata, S. (1970). Process for the preparation of hydrotalcite. *U.S. Patent* 3: 539-306.

Miyata, S. (1980). Physico-chemical properties of synthetic hydrotalcites in relation to composition. *Clay Min.* 28: 50-56.

Miyata, S. (1983). Anion exchange properties of hydrotalcite-like compounds. *Clays Clay Miner.* 31: 305-311.

Moilliet, J.L., Collie, B. and Black. W. (1961). *Surface Activity: The Physical Chemistry, Technical Applications and Chemical Constitution of Synthetic Surface Active Agents*. Second edition, London: E & F.N. Spon, p 518.

Morioka, H., Tagaya, H., Karasu, M., Kadokawa, J. and Chiba, K. (1995). Preparation of new useful materials by surface modification of inorganic layered compounds. *J. Solid State Chem*. 117: 337-342.

Muramatsu, K., Saber, O. and Tagaya, H. (2007). Preparation of new layered double hydroxide, Zn-Mo LDH. *J. Porous Mater*. 14: 481–484.

Newman, S.P. and Jones, W. (1998). Synthesis, characterization and layered double hydroxides containing organic guests. *New J. Chem*. 105-115.

Ogawa, M. and Kaiho, H. (2002). Homogeneous precipitation of uniform hydrotalcite particles. *Langmuir* 18: 4240-4242.

Palomares, A.E., Prato, J.G., Rey, F. and Corma, A. (2004). Using the "memory effect" of hydrotalcites for improving the catalytic reduction of nitrates in water. *J. Catal.* 221: 62–66.

Perez-Ramirez, J., Abello, S. and Van der Pers, N.M. (2007). Influence of the divalent cation on the thermal activation and reconstruction of hydrotalcite-like compounds. *J. Phys. Chem. C.* 111: 3642-3650.

Perez-Ramirez, J., Mul, G., Kapteijn, F. and Moulijn, J.A. (2001). A spectroscopic study of the effect of the trivalent cation on the thermal decomposition behaviour of Co-based hydrotalcites. *J. Mater. Sci.* 11: 2529-2536.

Perioli, L., Ambrogi, V., Rossi, C., Latterini, L., Nocchetti, M. and Costantino, U. (2006). Use of anionic clays for photoprotection and sunscreen photostability:

Hydrotalcites and phenylbenzimidazole sulfonic acid. *J. Phys. Chem. Solids* 67: 1079–1083.

Prescott, H.A., Li, Z.-J., Kemnitz, E., Trunschke, A., Deutsch, J., Lieske, H. and Auroux, A. (2005). Application of calcined Mg–Al hydrotalcites for Michael additions: An investigation of catalytic activity and acid–base properties. *J. Catal.* 234: 119–130.

Prevot, V., Forano, C. and Besse, J.P. (1998). Synthesis and thermal and chemical behaviors of tartrate and succinate intercalated Zn_3Al and Zn_2Cr layered double hydroxides. *Inorg. Chem*. 37: 4293-4301.

Prevot, V., Forano, C. and Besse, J.P. (1999). Reactivity of oxalate with ZnAl layered double hydroxides through new materials. *J. Mater. Sci*. 9: 155-160.

Prinetto, F., Ghiotti, G., Graffin, P. and Tichit, D. (2000). Synthesis and characterization of sol-gel Mg/Al and Ni/Al layered double hydroxides and comparison with co-precipitated samples. *Microporous and Mesoporous Mater.* 39: 229-247.

Pungor, E. (1995). *A Practical Guide to Instrumental Analysis*. USA: CRC Press, p 384.

Rajamathi, M., Thomas, G.S. and Kamath, P.V. (2001).The many ways of making anionic clays. *Proc. Indian Acad. Sci. (Chem. Sci.)* 113: 671-680.

Ramos, E., Lopez, T., Bosch, P., Asomoza, M. and Gomez, R. (1997). Thermal stability of sol-gel hydrotalcites. *J Sol-Gel Sci. Technol.* 8: 437–442.

Rao, M.M., Reddy, B.R., Jayalakshmi, M., Jaya, V.S. and Sridhar, B. (2005). Hydrothermal synthesis of Mg-Al hydrotalcites by urea hydrolysis. *Mater. Res. Bull.* 40: 347-259.

Reichle, W.T. (1985). Catalytic reactions by thermally activated, synthetic, anionic clay minerals. *J. Catal.* 94: 547-557.

Reichle, W.T. (1986a). Synthesis of anionic clay minerals (mixed metal hydroxides, hydrotalcite). *Solid State Ionics.* 22: 135-141.

Reichle, W.T. (1986b). Anionic clay minerals. *Chemtech.* 58-63.

Reis, M.J., Silvério, F., Tronto, J. and Valim, J.B. (2004). Effects of pH, temperature, and ionic strength on adsorption of sodium dodecyl benzene sulfonate into Mg–Al–CO3 layered double hydroxides. *J. Phys. Chem. Solids* 65: 487–492.

Rey, F., Fornés, V. and Rojo, J.M. (1992). Thermal decomposition of hydrotalcites. An infrared and nuclear magnetic resonance spectroscopic study. *J. Chem. Soc. Faraday Trans*. 88: 2233-2238.

Rocha, J., del Arco, M., Rives, V. and Ulibarri, M. A. (1999). Reconstruction of layered double hydroxides from calcined precursors: A powder XRD and ^{27}Al MAS NMR study. *J. Mater. Chem.* 9: 2499-2503.

Saber, O. and Tagaya, H. (2003a). New layered double hydroxide, Zn–Ti LDH: Preparation and intercalation reactions. *J. Inclusion Phenomena and Macrocyclic Chem.* 45: 109–116.

Saber, O. and Tagaya, H. (2003b). Preparation and intercalation reactions of Zn-Sn LDH and Zn-Al-Sn LDH. *J. Porous Mater.* 10: 83–91.

Saber, O. and Tagaya, H. (2007). Preparation of new nano-layered materials and organic–inorganic nano-hybrid materials, Zn–Si LDH. *J. Porous Mater.* (10.1007/s10934-007-9171-x).

Sako, T. and Okuwaki, A. (1991). Intercalation of benzenecarboxylate ions into the interlayer of hydrotalcite. *Solid State Ionics* 45: 43-48.

Sibilia, J. P. (1988). *A Guide to Materials Characterization and Chemical Analysis*. USA: VCH Publishers, p 318.

Skoog, D.A., West, D.M. and Holler, F.A. (1996). *Fundamentals of Analytical Chemistry.* Seventh edition, USA: Saunders College Publishing.

Socrates, G. (1980). *Infrared Characteristic Group Frequencies*. New York: John Wiley and Sons.

Takagi, K., Sichi, T., Usami, H. and Sawaki, Y. (1993). Controlled photocycloaddition of unsaturated carboxylates intercalated in hydrotalcite clay interlayers. *J. Am. Chem. Soc.* 115: 4339.

Trikeriotis, M. And Chanotakis, D.F. (2007). Intercalation of hydrophilic and hydrophobic antibiotics in layered double hydroxides. *Inter. J. Pharmaceutics* 332: 176–184.

Trujillano, R., Holgado, M.J., Pigazo, F. and Rives, V. (2006). Preparation, physicochemical characterisation and magnetic properties of Cu–Al layered double hydroxides with CO_3^{2-} and anionic surfactants with different alkyl chains in the interlayer. *Physica B* 373: 267–273.

Vaccari, A. (1998). Preparation and catalytic properties of cationic and anionic clays. *Catal. Today.* 41: 53-71.

Vaccari, A. (1999). Clays and catalysis: A promising future. *Appl. Clay Sci*. 14:.161–198.

Van der Pol, A., Mojet, B.L., Van der Ven, E. and De Boer, E. (1994). Ordering of intercalated water and carbonate anions in hydrotalcite. An NMR study. *J. Phys. Chem*. 98: 4050-4054.

Vold, R.D. and Hattiangdi, G.S. (1949). Characterization of heavy metal soaps by X-ray diffraction. *Ind. Eng. Chem*. 41: 2311-2320.

Williams, G.R. and O'Hare. D. (2006). Towards understanding, control and application of layered double hydroxide chemistry. *J. Mater. Chem.* 16: 3065-3074.

Wydro, P. (2007). The influence of the size of the hydrophilic group on the miscibility of zwitterionic and nonionic surfactants in mixed monolayers and micelles. *J. Colloid Interface Sci.* 316: 107–113.

You, Y., Zhao, H. and Vance, G.F. (2002). Surfactant-enhanced adsorption of organic compounds by layered double hydroxides. *Colloids Surfaces A: Physicochem. Eng. Aspects* 205: 161-172.

Yun, S.K. and Pinnavaia, T.J. (1995). Water content and particle texture of synthetic hydrotalcite-like layered double hydroxides. *Chem. Mater*. 7: 348-354.

Zammarano, M., Bellayer, S., Gilman, J.W., Franceschi, M., Beyer, F.L., Harris, R.H. and Meriani, S. (2006). Delamination of organo-modified layered double hydroxides in polyamide 6 by melt processing. *Polymer.* 47: 652-662.

Zhang, J., Zhang, F., Ren, L., Evans, D.G. and Duan, X. (2004). Synthesis of layered double hydroxide anionic clays intercalated by carboxylate anions, *Mater. Chem. Phys.* 85: 207-214.

Zhao, Y., Li, F., Zhang, R., Evans, D.G. and Duan, X. (2002). Preparation of layered double hydroxide nanomaterials with a uniform crystallite size using a new

method involving separate nucleation and aging steps. *Chem. Mater.* 14: 4286-4291.

APPENDIX A: EXPERIMENTAL METHODS

A.1 Synthesis procedure for monocarboxylate intercalated LDH

Table A.1 below gives the detailed procedure followed to synthesise monocarboxylate intercalated LDH. All the mixtures were heated for 9 hours per day and allowed to cool down overnight at room temperature. This was repeated four times. In some instances the heating was done from high temperature for one cycle and then to the melting point of the acid in the three remaining cycles.

Table A.1: Synthetic procedure followed for intercalation of fatty acids in LDH

LDH-acetate (C2)	40 g SDS, 4.12AEC acetic acid (21.02 g), 20 g LDH-CO_3 stirred in 1 500 ml of distilled water for 2 days. pH of the mixture was 10.01. Final pH = 10.01 Experimental yield (acetate-LDH) = 24.61 g Expected yield (calculated from acetic acid and LDH-CO_3) = 41.02 g 60% product yield was recovered.
LDH-butyrate (C4)	1) 40 g SDS, 4.12AEC butyric acid (30.84 g), 20 g LDH-CO_3 stirred in 1 500 ml of distilled water at room temperature for 2 days. pH of the mixture was 10.01 Experimental yield (LDH-butyrate) = 14.74 g Expected yield (calculated from LDH-CO_3 and butyric acid) = 50.84 g 29% product yield was recovered. 2) The experiment was repeated at 80 °C using 4.5AEC, which amounted to 33.83 g butyric acid. 29% product yield was recovered
LDH-hexanoate (C6)	40 g SDS, 4.12AEC hexanoic acid (40.66 g), 20 g LDH-CO_3 dissolved in 1 500 ml distilled water at room temperature and allowed to stir for 2 days. Final pH = 10.03 Experimental yield (LDH-hexanoate) = 4.46 g Expected yield (calculated from LDH-CO_3 and hexanoic acid) = 60.66 g 7.35% product yield was recovered.
Octanoate-	1) 40 g SDS, 4.12AEC octanoic acid (50.6 g), 20 g LDH-CO_3 stirred in

LDH (C8)	1 500 ml of distilled water at room temperature for 2 days. Final pH = 10.01 Experimental yield (LDH-octanoate) = 7.77 g Expected yield (calculated from LDH-CO_3 and octanoic acid) = 70.60 g 11% product yield was recovered. 2) The experiment was repeated using 4.5AEC amounting to 55.38 g of octanoic acid. 35% product yield was recovered. 3) The experiment was repeated at 80 °C and 33% product yield was recovered.
LDH-decanoate (C10)	1) 40 g SDS, 4.12 AEC decanoic acid (60.29 g), 20 g LDH-CO_3 stirred in 1 500 ml of distilled water at 50 °C for 3 days, with partial addition of decanoic acid and 1 day without acid addition. Final pH = 10.00 Experimental yield (LDH-decanoate) = 10.92 g Expected yield (calculated from LDH-CO_3 and decanoic acid) = 80.29 g 13.6% product yield was recovered. 2). The experiment was repeated using 4.5AEC (66.14 g) of decanoic acid and heating was from 37 to 32°C. 21% product yield was recovered.
LDH-laurate (C12)	1) 40 g SDS, 4.12AEC lauric acid (70.4 g), 20 g LDH-CO_3 stirred in 1 500 ml of distilled water at 60 °C for 3 days, with partial addition of lauric acid and 1 day without acid addition. Final pH = 10.01 Experimental yield (LDH laurate) = 28.93 g Expected yield (calculated from HT and lauric acid) = 90.40 g 32% product yield was recovered. 2) A similar procedure was followed with heating from 53 to 48 °C and 37% product yield was recovered. 3) The experiment was repeated using 4.5AEC (76.92 g) lauric acid at 65, 70 and 80°C. Product yields of 35, 45 and 39% respectively were recovered.

LDH-myristate (C14)	1) 40 g SDS, 4.12 AEC myristic acid (80.63 g), 20 g LDH-CO_3 stirred in 1 500 ml of distilled water at 60 °C for 3 days, with partial addition of myristic acid and 1 day without acid addition. Final pH = 10.05 Experimental yield (LDH-myristate) = 15.63 g Expected yield (calculated from LDH-CO_3 and myristic acid) = 100.63 g 15.5% product yield was recovered. 2) The experiment was repeated using 4.5AEC (87.67g) myristic acid with heating from 59 to 54 °C. 32% product yield was recovered.
LDH-stearate (C18)	1) 40 g SDS, 4.12AEC stearic acid (100 g), 20 g LDH-CO_3 stirred in 1 500 ml of distilled water at 80 °C for 3 days, with partial addition of stearic acid and 1 day without acid addition. Final pH = 10.00 Experimental yield (LDH-stearate) = 57.60 g Expected yield (calculated from LDH-CO_3 and stearic acid) = 120 g 48% product yield was recovered. 2) The experiment was repeated with the mixture being heated from 75 to 70 °C. 20% product yield was recovered. 3) The experiment was also repeated at 50, 60, 65, 70, 75 and 85 °C using 4.5AEC (109.24 g stearic acid) and at 80 °C using SDS. Product yields of 40, 22, 40, 43, 71 and 64% respectively were recovered.
LDH-LDH-behenate (C22)	1) 40 g SDS, 4.12AEC behenic acid (119.21 g), 20 g LDH-CO_3 stirred in 1 500 ml of distilled water at 90 °C for 3 days, with partial addition of behenic acid and 1 day without acid addition. Final pH = 10.02 Experimental yield (LDH-LDH-behenate) = 41.76g Expected yield (calculated from LDH-CO_3 and behenic acid) = 139.21 g 37% product yield was recovered. 2) The experiment was repeated using 4.5AEC (130.78 g) behenic acid. The mixture was heated from 85 to 80 °C. 93% product yield was recovered.

APPENDIX B: THERMAL ANALYSIS

B.1: Expected TG mass loss after the first and last thermal events

Thermal decomposition steps: $[Mg_{1-x}Al_{x(}OH)_2]$ $(CO_3)_{x/2}.0.5\ H_2O$, where x = 0.3114

Molecular mass = 248.88 g/mol

After the first thermal event: dehydrated LDH: $[Mg_{1-x}Al_x(OH)_2]$ $(CO_3)_{x/2}$

Molecular mass = 219.95 g/mol

$$\text{Expected \%residual mass (LDH dehydrated)} = 100 \times \frac{\text{MM(dehydrated LDH)}}{\text{MM(LDH)}}$$

$$= 100 \times \frac{219.95\ \text{g/mol}}{248.48\ \text{g/mol}}$$

$$= 88.38\%$$

Last thermal event: MgO and Al_2O_3

Molecular mass = 140.10g/mol (LDO, based on the assumption that the residue contains only MgO and Al_2O_3)

$$\text{Expected \%residual mass (at 700°C)} = 100 \times \frac{\text{MM(dehydrated LDH)}}{\text{MM(LDH)}}$$

$$= 100 \times \frac{140.10\ \text{g/mol}}{248.48\ \text{g/mol}}$$

$$= 56.26\%$$

B.2: Thermogravimetric curves and the derivative fatty acid intercalated LDH

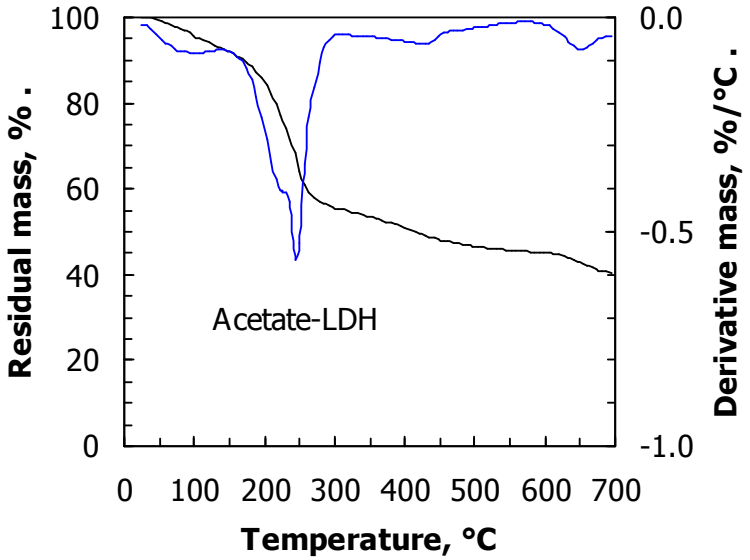

Figure B1: TG/DTG curves of acetate intercalated LDH synthesised at room temperature

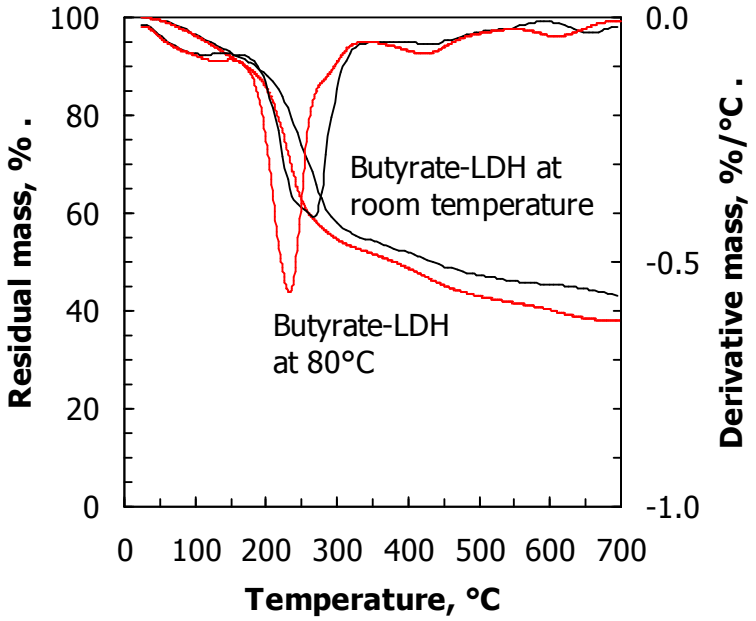

Figure B2: TG/DTG curves of butyrate intercalated LDH synthesised at room temperature and at 80 °C

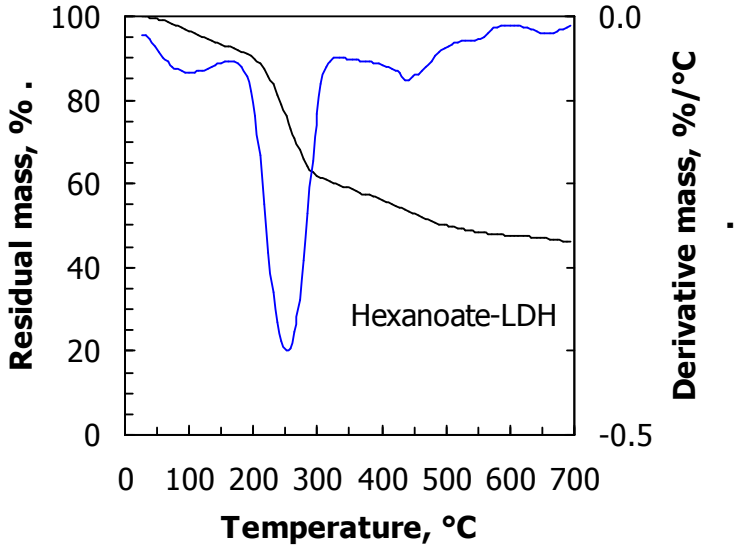

Figure B3: TG/DTG curves for hexanoate intercalated LDH at room temperature

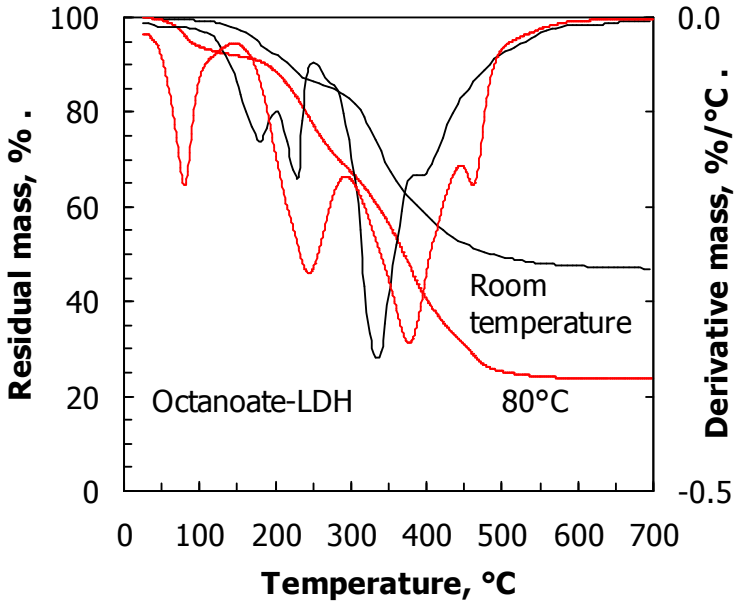

Figure B4: TG/DTG curves of octanoate intercalated LDH synthesised at room temperature and at 80 °C

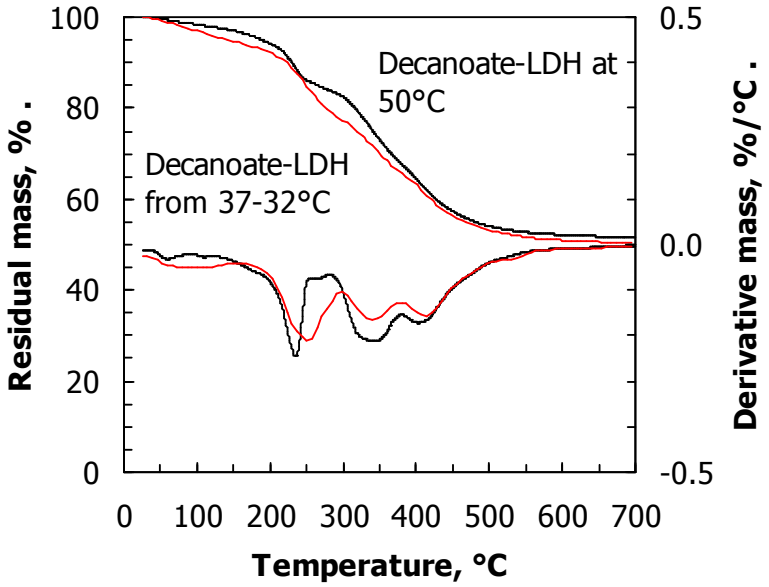

Figure B5: TG/DTG curves of decanoate intercalated LDH synthesised at 50 °C and from 37 to 32 °C

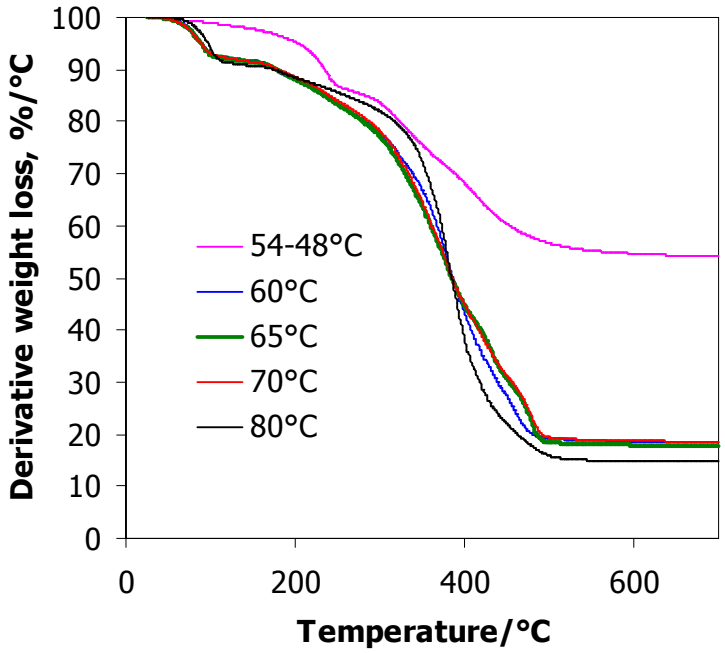

Figure B6: TG curves of LDH-laurate prepared at 54–48, 60, 65, 70 and 80 °C

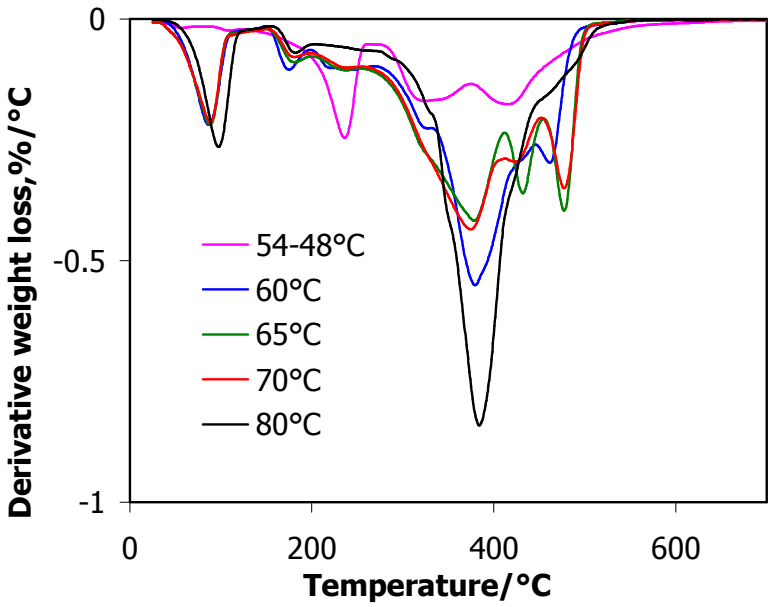

Figure B7: Derivative of weight loss curves of LDH-laurate obtained at 54-48, 60, 65, 70 and 80 °C

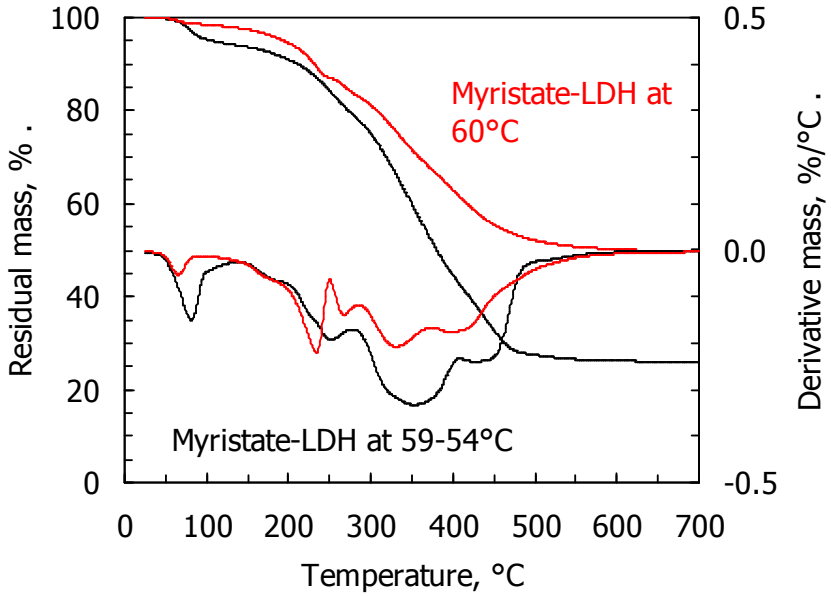

Figure B8: TG/DTG curves of LDH-myristate prepared at 59–54 and at 60 °C

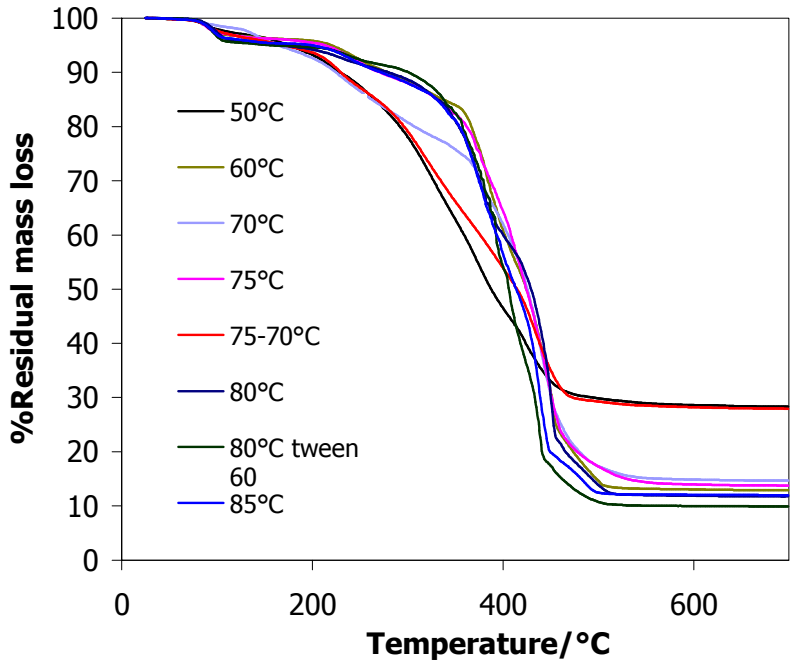

Figure B9: TG curves of LDH-stearate prepared at 50, 60, 70, 75, 75–70, 80 and 85°C using SDS and at 80 °C using Tween 60

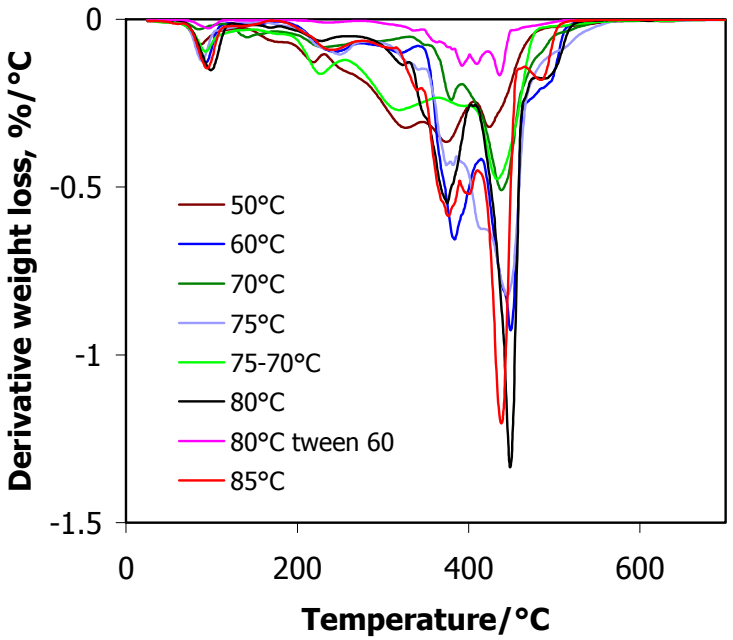

Figure B10: Derivative of weight loss curves of LDH-stearate prepared at 50, 60, 70, 75, 80 and 85 °C

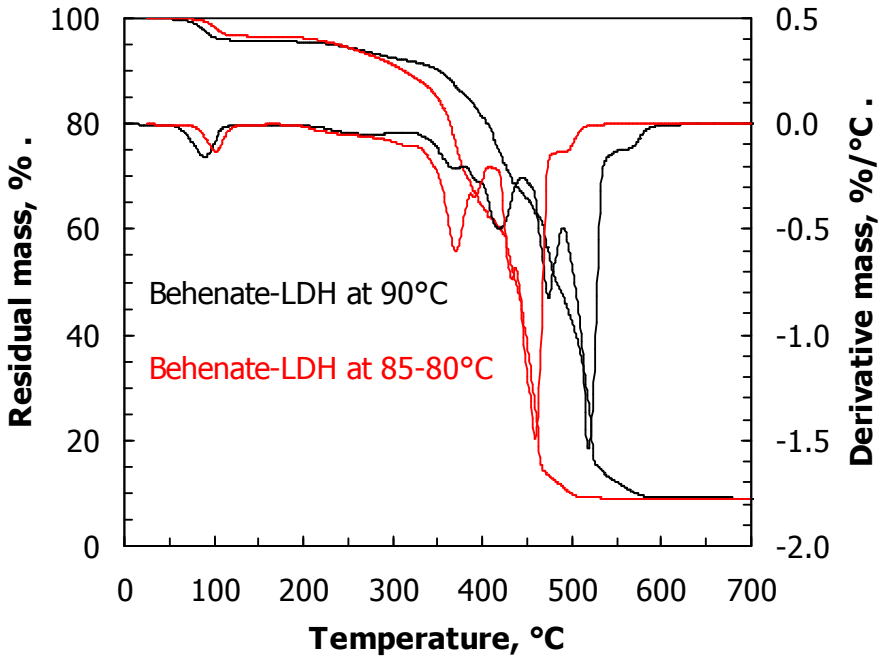

Figure B11: TG/DTG curves of LDH-behenate prepared at 90 and 85–80 °C

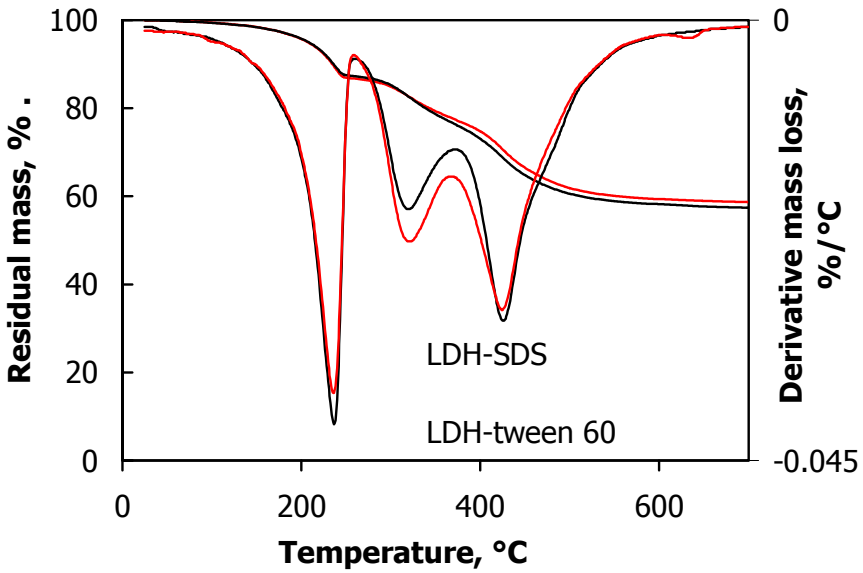

Figure B12: TG/DTG curves of the product obtained by dispersing the LDH in distilled water in the presence of the surfactants SDS (LDH-SDS) and Tween 60 (LDH-Tween 60) at 80 °C

APPENDIX C: FT-IR

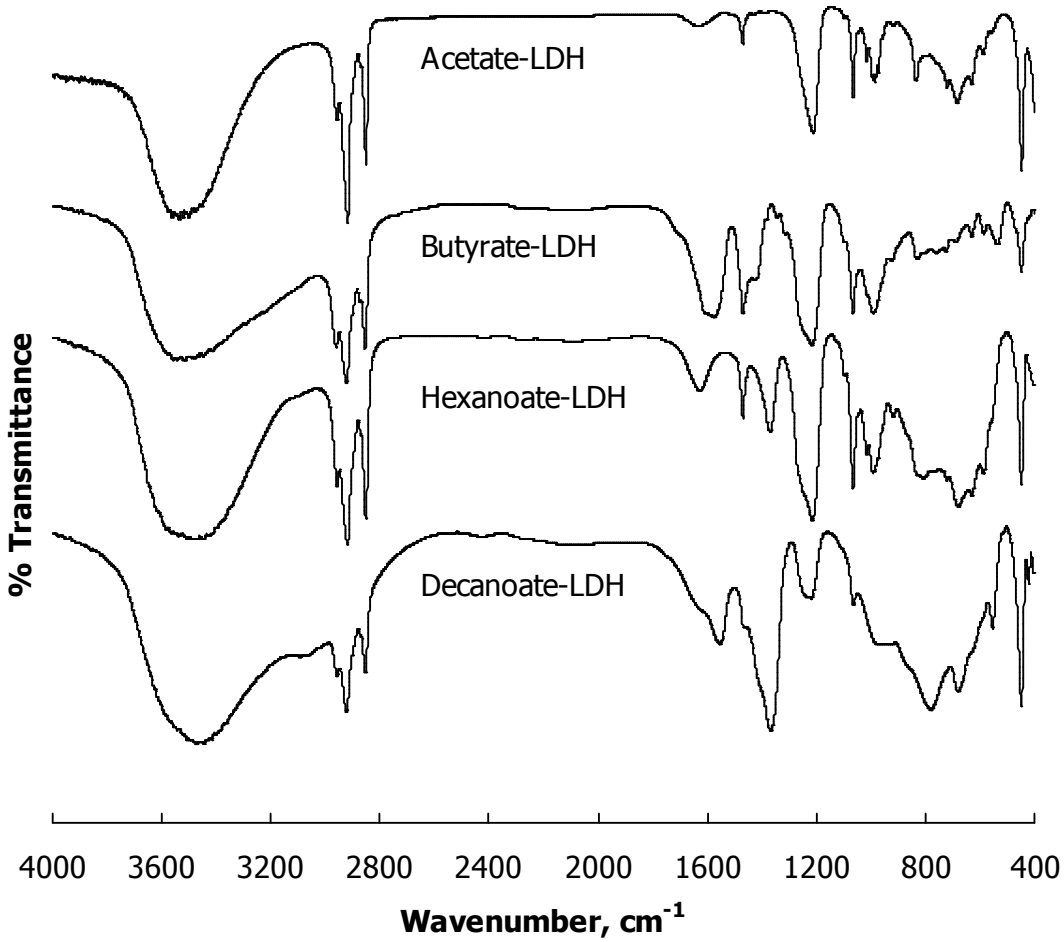

Figure C1: FT-IR spectra of short-chain carboxylates: acetate, butyrate, hexanoate and decanoate acid intercalated LDH, obtained at room temperature and at 50 °C for decanoate

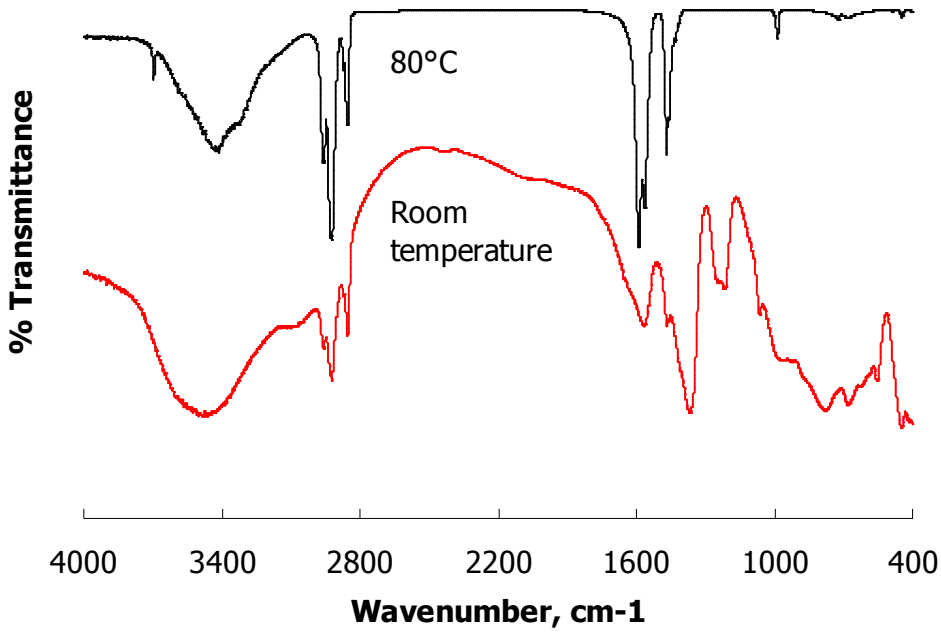

Figure C2: FT-IR spectra of LDH-octanoate prepared at room temperature and at 80 °C

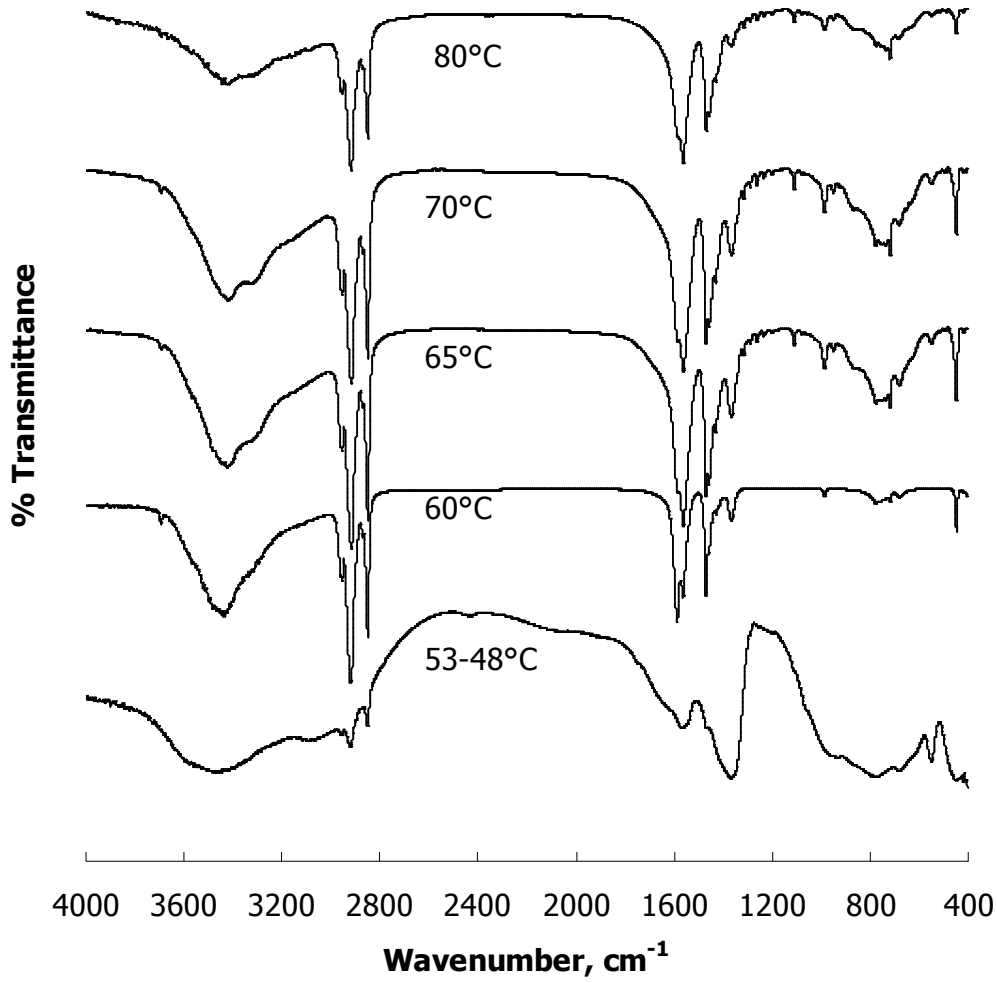

Figure C3: FT-IR spectra of LDH-laurate prepared at 80, 70, 65 and 60 °C and from 53–58 °C

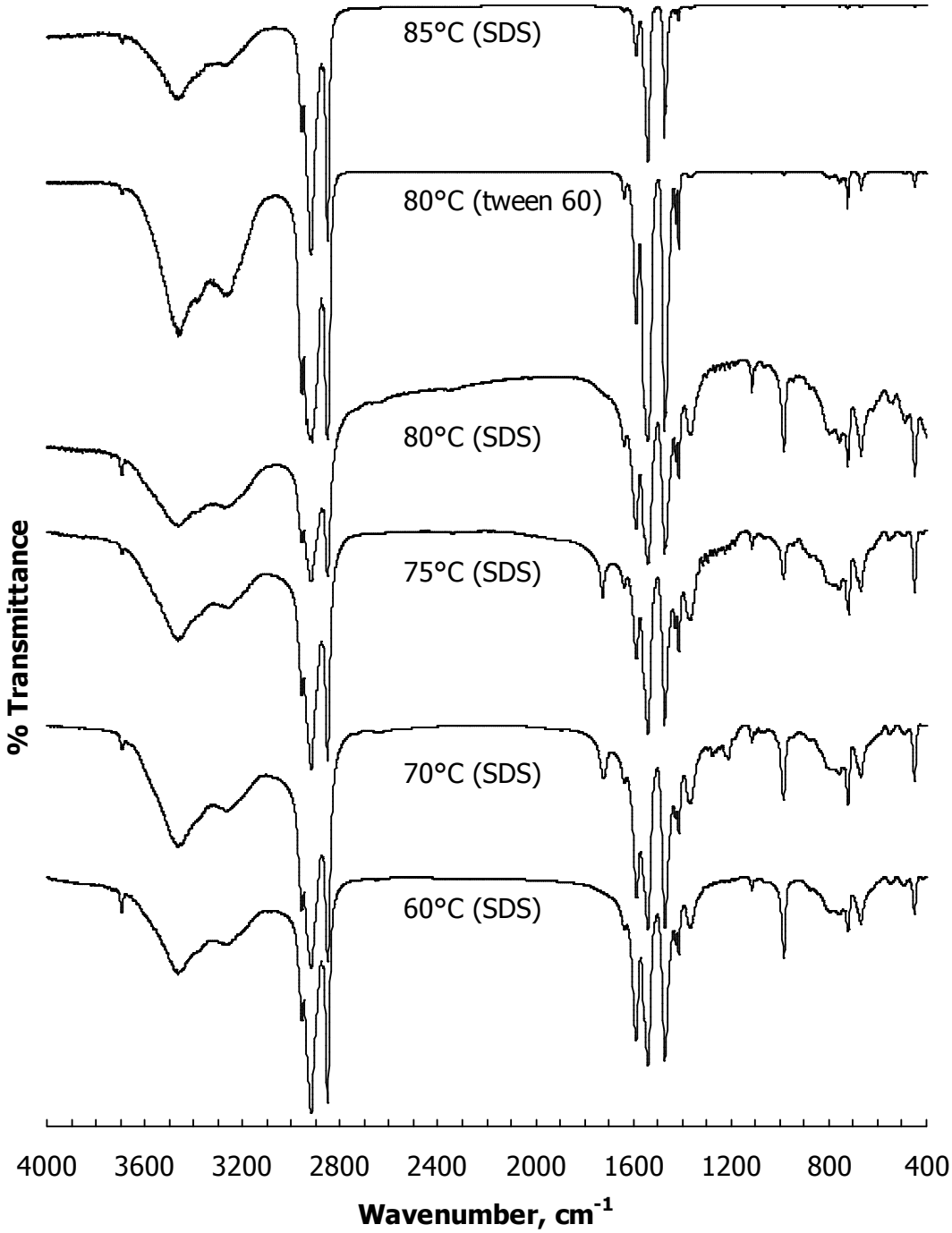

Figure C4: FT-IR spectra of LDH-stearate prepared at 60, 70, 75, 80 and 85 °C using SDS and at 80 °C using Tween 60

APPENDIX D: XRD RESULTS

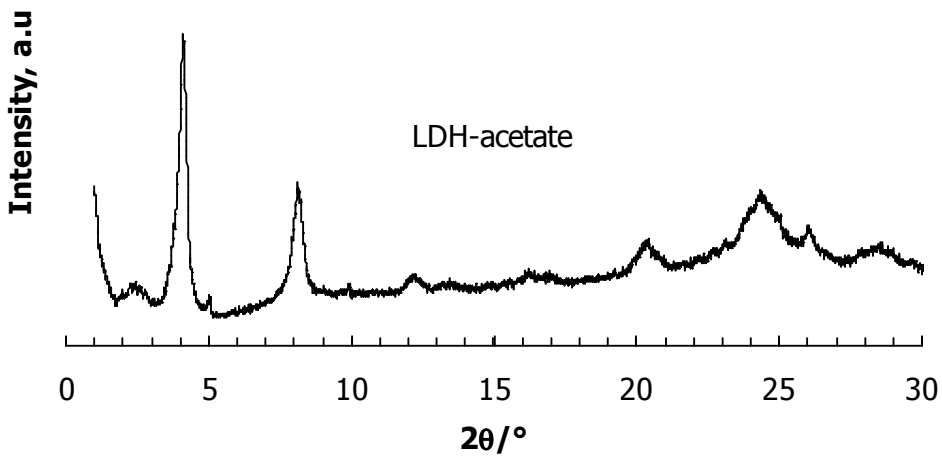

Figure D1: XRD pattern of LDH-acetate prepared at room temperature

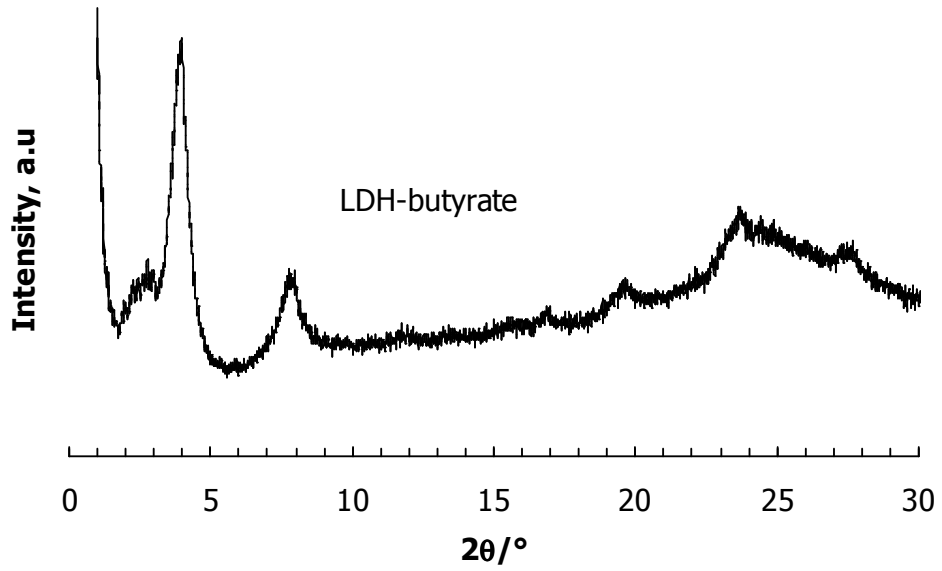

Figure D2: XRD pattern of LDH-butyrate prepared at 80 °C

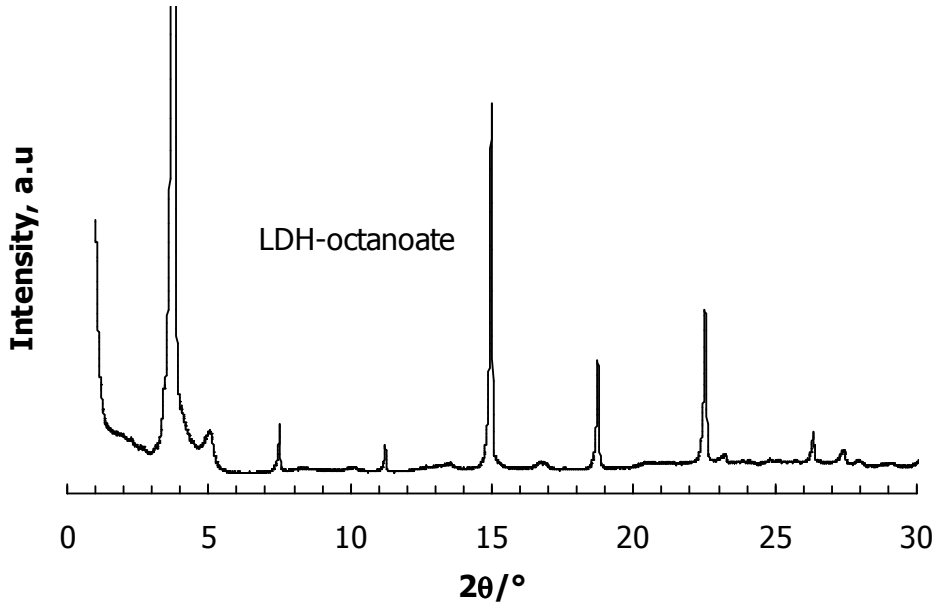

Figure D3: XRD pattern of LDH-octanoate prepared at 80 °C

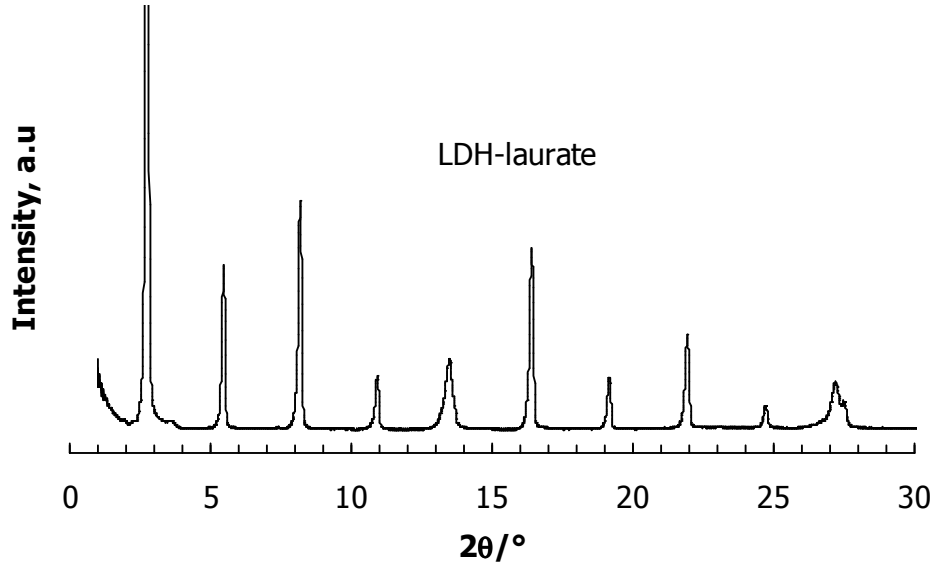

Figure D4: XRD pattern of LDH-laurate prepared at 80 °C

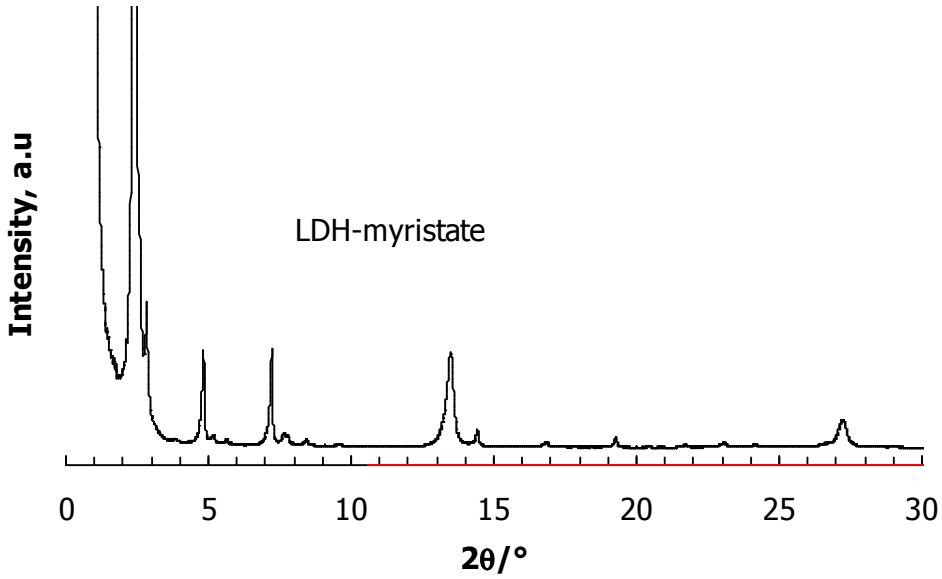

Figure D5: XRD pattern of LDH-myristate prepared at 60 °C

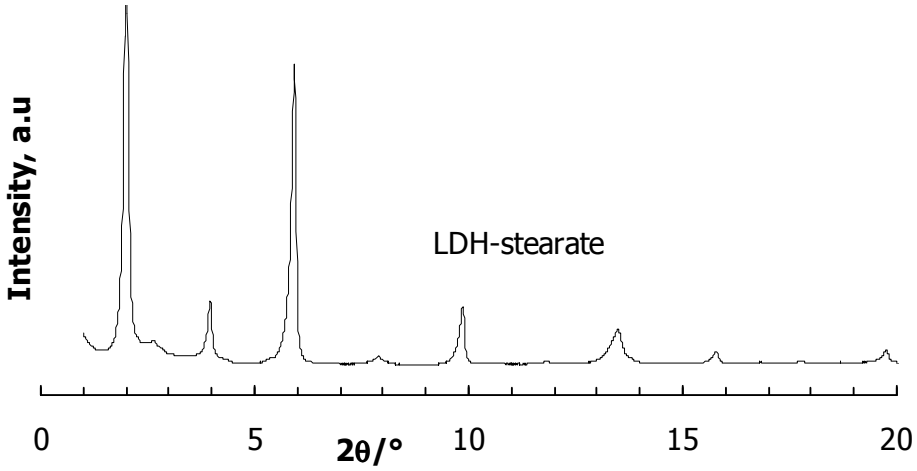

Figure D6: XRD pattern of LDH stearate prepared at 80 °C using SDS

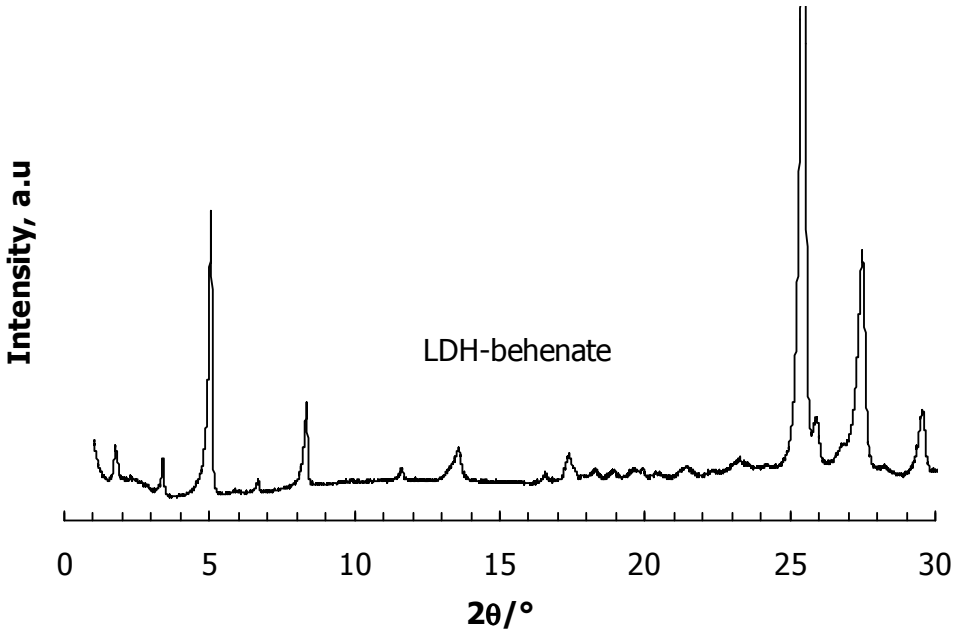

Figure D7: XRD pattern of LDH-behenate prepared at 90 °C

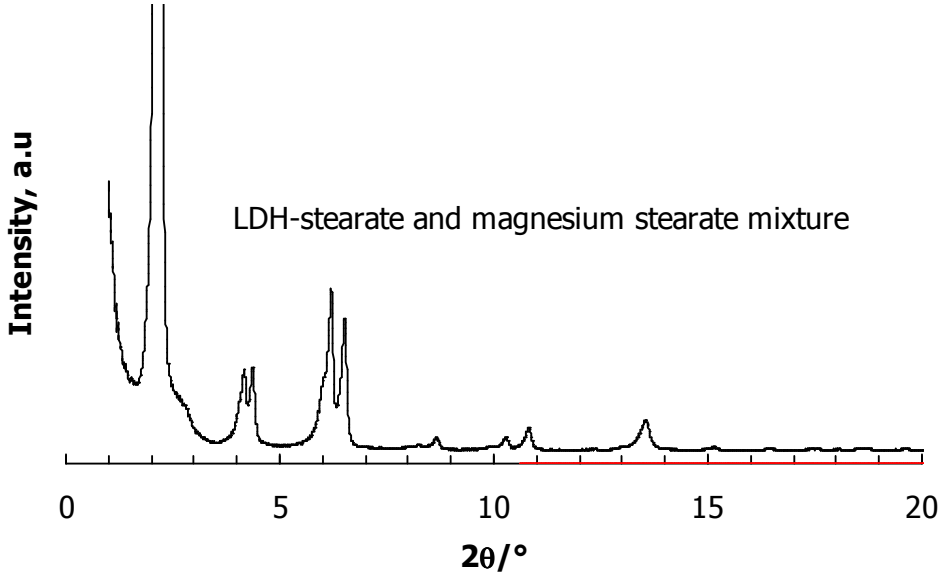

Figure D8: XRD pattern of a mixture of LDH-stearate and magnesium stearate prepared at 80 °C

APPENDIX E: SEM RESULTS

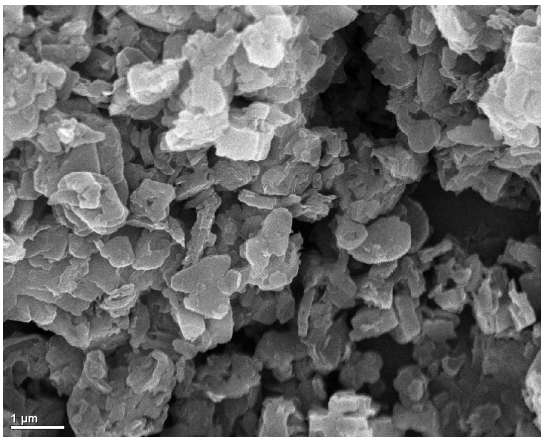

Figure E1: SEM image of LDH-acetate

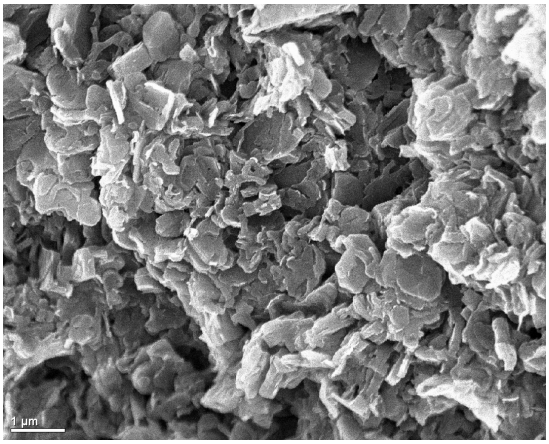

Figure E2: SEM image of LDH-butyrate

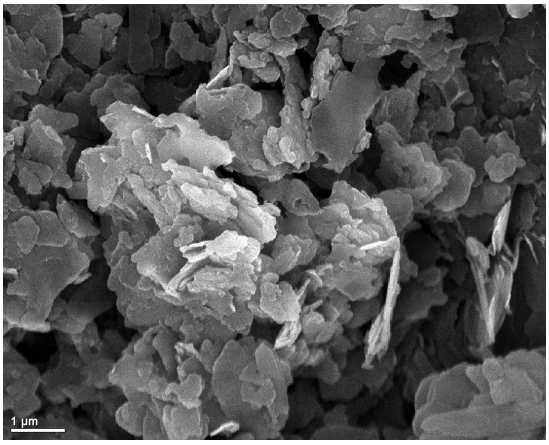

Figure E3: SEM image of LDH-octanoate

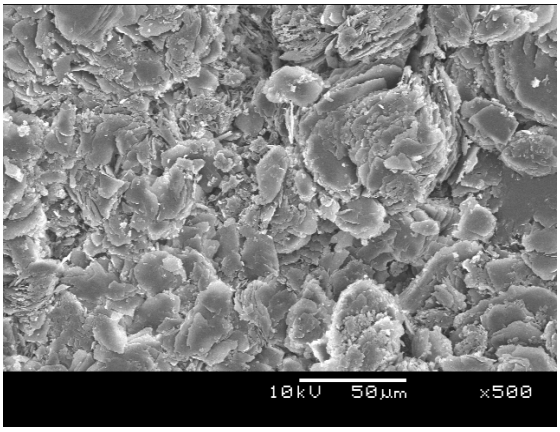

Figure E4: SEM image of LDH-behenate